ANTIBACTERIAL, ANTIOXIDANT AND CYTOTOXICITY EVALUATION OF SELECTED SCHIFF BASE LIGANDS AND THEIR CORRESPONDING METAL COMPLEXES

A DISSERTATION SUBMITTED IN FULFILMENT

OF THE REQUIREMENT FOR THE DEGREE OF

DOCTOR OF PHILOSOPHY IN SCIENCE

(BIOCHEMISTRY)

OF

THE UNIVERSITY OF NAMIBIA

BY

TEOPOLINA N NAWINDA

201148757

OCTOBER 2025

MAIN SUPERVISOR: PROF PETRINA KAPEWANGOLO (UNIVERSITY OF NAMIBIA)

CO-SUPERVISOR: PROF VEIKKO UAHENGO (UNIVERSITY OF NAMIBIA)

List of conference proceedings

T. Nawinda, P. Kapewangolo, V. Uahengo. Antioxidant, antibacterial and cytotoxicity evaluation of selected hydrazone-based ligands and their corresponding metal complexes. National Commission for Research Science and Technology annual conference. Students' Research Symposium. 6th – 10th November 2023, Windhoek, Namibia. (Presentation).

Abstract

Schiff bases are compounds that possess an azomethine group and are considered as aldehyde and ketone derivatives. Schiff bases have diverse pharmacological properties and constitute an important class of compounds for new drug development hence researchers are investigating these compounds for different biological activities. The present study was designed to synthesize Schiff base ligands and their metal complexes which were then screened for antibacterial and antioxidant activity as well as cytotoxicity against a cervical cancer cell line. Schiff base ligands were synthesized by means of the Schiff's base reaction, and for each ligand, metal complexes of copper II (Cu^{2+}) and nickel II (Ni^{2+}) were synthesized. The structural confirmation of the synthesized compounds was done by Proton Nuclear Magnetic Resonance (^{1}H NMR) and Fourier Transform Infrared (FTIR) spectroscopies. The antibacterial activity of the ligands and metal complexes was assayed by means of the agar disc diffusion method while the antioxidant activity was determined using the 2,2-diphenyl-1-picrylhydrazyl (DPPH) and reducing power assays. Cytotoxicity studies were conducted against Henrietta Lacks (HeLa) cells using the 3-(4,5-dimethylthiazol-2-yl)-2,5-diphenyltetrazolium bromide (MTT) assay. Both ligands and metal complexes displayed antibacterial activity against strains of *Staphylococcus aureus*, *Streptococcus mutans*, *Neisseria gonorrhoea*, *and Escherichia coli* with minimum inhibitory concentration (MIC) values ranging from 2.5 – 10 mg/mL. All tested compounds demonstrated a concentration-dependent antioxidant activity, with half maximal inhibitory concentration (IC_{50}) values in the range of 1.33 – 85.81 µg/mL. Selected ligands and metal complexes exhibited cytotoxic activity against HeLa cells, having IC_{50} values in the range of 4.12 – 16.80 µg/mL. Copper metal complexes exhibited the best antibacterial activity with

recorded MIC of 2.5 mg/mL against most tested bacteria species. On the other hand, nickel metal complexes had the best antioxidant activity with IC_{50} values of 1.33 – 33.92 µg/mL. Most ligands and metal complexes exhibited moderate cytotoxicity against HeLa cells. However, L6 was the most toxic to HeLa cells as indicated by a lower IC_{50} (4.12 ± 0.6 µg/mL), compared to other compounds tested for cytotoxicity in the present study. There are no literature reports on the antibacterial, antioxidant and cytotoxic activities of the compounds analysed in this study. The results generated from this study showed that the biologically active ligands and metal complexes could be used as compounds of interest in the drug discovery process.

Table of Contents

LIST OF TABLES

LIST OF FIGURES

LIST OF ABBREVIATIONS

ABTS	2,2'-azino-bis (3-ethylbenzothiazoline-6-sulfonic acid))
AMR	Antimicrobial Resistance
ATCC	American Type Culture Collection
BHA	Butylated Hydroxy Anisole
BHT	Butylated Hydroxy Toluene
cGMP	Guanosine 3',5'-cyclic monophosphate
Co	Cobalt
Cu	Copper
CVE	Crystal Violet Elution
DMEM	Dulbecco's Modified Eagle Medium
DMPD	N, N-dimethyl-para-phenylenediamine
DMSO	Dimethyl sulfoxide
DNA	Deoxyribonucleic Acid
DPPH	2, 2, -diphenyl-1-picrylhydrazyl
ET	Electron Transfer
FT-IR	Fourier Transform Infrared Spectroscopy
GOX	Glutathione Oxidase
GPX	Glutathione Peroxidase
GR	Glutathione Reductase
^{1}HNMR	Proton Nuclear Magnetic Resonance
HAT	Hydrogen Atom Transfer
HIV	Human Immunodeficiency Virus
HPV	Human Papilloma Virus
IC_{50}	Half-maximal Inhibitory Concentration
IE	Infective Endocarditis
MIC	Minimum Inhibitory Concentration

MRSA	Methicillin-Resistant *Staphylococcus aureus*
MSSA	Methicillin-Sensitive *Staphylococcus aureus*
MTT	3-(4,5-dimethylthiazol-2-yl)-2,5-diphenyltetrazolium bromide
Ni	Nickel
NO^-	Nitric Oxide
O^-_2	Super Oxide
OH	Hydroxyl
RDDN	Research Discovery Development of New antibiotics
RO^-	Alkoxyl
ROO^-	Peroxyl
ROS	Reactive Oxygen Species
SOD	Superoxide Dismutase
SRB	Sulforhodamine B
STI	Sexually Transmitted Infections
TBHQ	Tert-Butylated Hydroquinone
TLC	Thin Layer Chromatography
VRE	Vancomycin Resistant Enterococci
VRSA	Vancomycin Resistant *Staphylococcus aureus*
WHO	World Health Organization
Zn	Zinc

ACKNOWLEDGEMENTS

First and foremost, I would like to extend my sincere appreciation and gratitude to the Almighty God, without belief there is no hope.

- I am grateful to the University of Namibia for providing me with financial support and the platform to conduct this research.
- To my supervisor (Prof Petrina Kapewangolo), you are a rare breed. Thank you for the guidance, support and mentorship throughout this project.
- My co-supervisor, Prof Veikko Uahengo, thank you for all the chemistry knowledge you have instilled in me, and for always taking time out of your busy schedule to attend to my queries.
- Dr Jaco Brandt of the Central Analytical Facility of Stellenbosch University, thank you for your assistance in performing the NMR experiments.
- Dr Simeon Hamukoshi and Mr Johannes Naimhwaka – I appreciate your guidance on the chemistry aspect.
- My family, friends and colleagues, you have always had my back and for that I owe you one.
- To my dearest parents, I am because you were, and I aspire to forever make you proud.

DEDICATION

This thesis is dedicated to my late parents, my family at large, and the almighty God who has been my source of strength that I needed to complete this academic pursuit. To my husband, Lazarus Unandapo and my children, Jack and Gracelynn, this is for us.

DECLARATIONS

I, NAWINDA TEOPOLINA N, declare hereby that this study is a true reflection of my own research, and that this work, or part thereof has not been submitted for a degree at any other institution.

No part of this thesis/dissertation may be reproduced, stored in any retrieval system, or transmitted in any form, or by any means (e.g. electronic, mechanical, photocopying, recording or otherwise) without the prior permission of the author, or The University of Namibia in that behalf.

I, NAWINDA TEOPOLINA N, grant The University of Namibia the right to reproduce this thesis in whole or in part, in any manner or format, which The University of Namibia may deem fit.

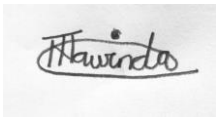

Teopolina Ndagwedhapo Nawinda

……. ….…… ……

Name of student Signature Date

CHAPTER 1

INTRODUCTION

1.1 Background

Antimicrobial resistance (AMR), has been declared among the top ten global health threats by the World Health Organization (WHO) in 2019 (1). In addition, antibiotic resistance remains one of the main challenges in the treatment of infectious diseases, and it is currently linked to high mortality hence a need to examine various compounds as effective antimicrobial agents (1,2). Microbial infections are known to trigger the production of reactive oxygen species (ROS) and reactive nitrogen (RNS) species (3).

Excessive reactive oxygen species lead to cellular oxidative stress, which could result in degenerative diseases such as cancer and cardiovascular disease (4). Antioxidants are molecules that have the ability to inhibit or delay undesired oxidation reactions (5). Antioxidants significantly delay or prevent oxidation by donating their electrons to ROS and thereby neutralizing the adverse effects of the latter (6). Despite synthetic antioxidants being successfully used due to their high efficacy, low cost and stability in products such as foods, pharmaceuticals or cosmetics, there is a need for better and safer antioxidants as most of the existing ones have safety concerns (7). Antioxidants are crucial in the prevention of many diseases, as high levels of ROS cause changes in physiological processes resulting in the emergence of illnesses such as cancer (8).

Cancer is a disease in which abnormal cells grow uncontrollably and spread to other parts of the body (9,10). With almost 10 million cancer deaths recorded in 2020 globally, the World Health Organization recognizes cancer as a second leading cause

of death internationally after cardiovascular disease (11,12). Although most cancers arise from carcinogens in the environment (13), oxidative stress remains the leading cause of the initiation and progression of cancer (14,15). The incidence of various cancers is on the rise globally and is predicted to rise to 20 million new cases by 2025 (11). A study by Hassanpour and Dehghani revealed that more than 277 different types of cancers are in existence (16). In men, lung, prostate, colorectal, stomach, and liver cancers are the most common types whereas breast, colorectal, lung, thyroid, and cervical cancers are the most common amongst women (17). Globally, cervical cancer is regarded as one of the leading causes of cancer morbidity and mortality (18). More than half a million women are diagnosed with cervical cancer each year globally, and over 300 000 deaths from cervical cancer are recorded worldwide annually due to a lack of effective cures (19,20).

The conventional methods for cancer treatment and management are surgery, radiation, immunotherapy and chemotherapy (21,22). Chemotherapy is regarded as the most effective treatment in most types of cancers, which has led to its extensive use in cancer therapy (21). Chemotherapy is however associated with side effects that could be life-threatening such as fever, unusual bleeding, diarrhoea and impaired kidney function (23,24) hence a need for better cytotoxic agents.

The side effects of chemotherapy are induced by ROS that are generated during treatment (14,15). In addition, chemotherapy causes immunosuppression which is risky to patients as their weakened immune systems result in fungal and bacterial infections (25–27). In view of the above facts, there is a need to discover new cancer treatment options with a combination of antioxidant, antibacterial and cytotoxic effects (28–30). It is on these grounds that the present study sought to carry out in

vitro cytotoxicity screening of compounds that exhibited significant antioxidant and antibacterial activity.

Cytotoxicity is the ability of a compound to damage or kill live cells (31). Although cytotoxicity screening is usually carried out during preclinical studies of compounds or drug leads, cytotoxicity assays are also used in determining chemotherapeutical potential of compounds (32). In the present study, in vitro cytotoxicity of selected Schiff base ligands and metal complexes was assessed by examining cell viability of HeLa cells by using the 3-(4,5-dimethylthiazolyl-2)-2,5-diphenyltetrazolium bromide (MTT) assay. HeLa is a cervical cancer cell line that was derived from cancer cells of the late Henrietta Lacks in 1951 (33,34). This cell line has since been used in cancer research and developing new treatments, making it the oldest and most commonly used human cell line (34).

Schiff base ligands are defined as compounds that possess an azomethine group, and are considered as aldehyde and ketone derivatives (35). Schiff bases and their metal complexes have gained significant recognition in novel drug development and are widely studied molecules due to their ease of preparation and diverse pharmacological potential (36–38). Schiff bases, particularly hydrazone base ligands as well as their sulphur and nitrogen derivatives, are reported to exhibit antibacterial, antifungal, antioxidant, anticancer, anti-inflammatory, antidiabetic, and anti-HIV activities amongst other biological activities (38,39).

Schiff base ligands such as those derived from salicylaldehyde and 2-hydroxy-1-naphthaldehyde are considered as “privileged ligands” due to their ability to coordinate different metals (40,41). Furthermore, Schiff bases with metal complexes in most cases have demonstrated better biological activity compared to free imines,

and they also serve as intermediates in the synthesis of natural products (42,43). Salicylaldehyde (2-hydroxybenzaldehyde) is a common carbonyl precursor for the synthesis of Schiff bases (41). Amongst other pharmacological properties, Schiff bases of substituted salicylaldehyde and 2-hydroxy-1-naphthaldehyde are notable antioxidant, anticancer and antimicrobial agents in the form of both ligands or ligand metal complexes (44,45). It is on this basis that the present study evaluated selected salicylaldehyde and 2-hydroxy-1-naphthaldehyde Schiff base ligands as well as their copper (II) and nickel (II) metal complexes for antibacterial, antioxidant and cytotoxic activity.

1.2 Problem statement

Most pathogenic bacteria species have developed resistance against the existing antibiotics hence a need for new antimicrobial agents. There is a need for safer and better antioxidants since most available antioxidant drugs are associated with safety concerns such as kidney and digestive issues, disruption to the endocrine system etc. Some commercial drugs derived from Schiff bases such as the platinum (Pt) metal-based anticancer drug cisplatin are reported to have severe side effects (46) hence a need to explore more Schiff base compounds for cytotoxicity. Furthermore, chemotherapy, which is the commonly used method for cancer treatment and management produces free radicals and suppresses immune systems of patients, which often results in more damage and bacterial infections. This has led to a need for treatment methods with a combination of antibacterial, antioxidant and cytotoxic activity. Schiff bases derived from 2-hydroxy-1-naphthaldehyde and salicylaldehyde have gained recognition due to their astonishing array of biological properties such as antidiabetic, antimicrobial, anticancer and anti-inflammatory activity but their antibacterial and antioxidant potential is not extensively studied (47,48). There is no

literature documentation on the antibacterial, antioxidant, and cytotoxicity studies done on the ligands and metal complexes employed in this study.

1.3 Objectives of the study

The objectives of this study were to:

- **a)** Synthesize Schiff base ligands based on 2-hydroxy-1-naphthaldehyde and salicylaldehyde.
- **b)** Synthesize Cu^{2+} and Ni^{2+} metal complexes of the Schiff base ligands in **a)**.
- **c)** Confirm the formation of the synthesized ligands and metal complexes by means of ^{1}H NMR and FTIR.
- **d)** Determine the antibacterial activity of the synthesized ligands and their metal complexes against bacterial strains of *Escherichia coli* (ATCC 9637), *Neisseria gonorrhoeae* (ATCC 19424), *Staphylococcus aureus* (ATCC 25923), and *Streptococcus mutans* (ATCC 25175) by means of the Kirby-Bauer disc agar diffusion method.
- **e)** Evaluate the antioxidant activity of the Schiff base ligands and their metal complexes using 2,2-diphenyl-1-picrylhydrazyl (DPPH) and reducing power assays.
- **f)** Determine the cytotoxicity of selected Schiff base ligands and their metal complexes against the HeLa cell line using the MTT assay.

1.4 Significance of the study

The study of Schiff base ligands and their metal complexes as antibacterial agents is important since most bacteria species have developed resistance against existing agents. Evaluating different compounds for antioxidant activity could lead to the

discovery of safer and better antioxidants which could be administered as dietary supplements. Cytotoxicity analysis of the synthesized ligands and metal complexes will aid in determining their cytotoxic effects against the HeLa cell line. The findings of this study will shed light on the use of Schiff base ligands based on 2-hydroxy-1-naphthaldehyde and salicylaldehyde as well as their copper (II) and nickel (II) metal complexes in novel drug development.

1.5 Limitations of the study

The Schiff base ligands synthesized in the present study could have been chelated to many metal ions, but this was impossible due to limited reagents. Various antibacterial and antioxidant assays exist as described in literature. However, due to limited resources not all of them could be employed in the present study. Many different types of commercial cell lines could have been explored but have not been screened in this study. Due to limited resources, non-cancerous cell lines were not included in the study to represent the cytotoxicity of ligands and metal complexes in healthy cells.

1.6 Delimitations of the study

In the present study, metal complexes of copper (II) and nickel (II) were synthesized. This study investigated bacterial susceptibility using the Kirby-Bauer disc agar diffusion method. The antioxidant activity of the ligands and metal complexes was determined using DPPH and reducing power assays. Furthermore, the cytotoxicity of selected ligands and metal complexes was investigated against the cervical cancer (HeLa) cell line model.

CHAPTER 2

LITERATURE REVIEW

2.1 Antibacterial agents and antibiotic resistance

Infectious diseases resulting from bacterial infections have increased dramatically in recent years (49). For over 70 years, antibacterial agents have been used in the management of infections caused by pathogenic microorganisms (50). Additionally, there have been many significant advances in antimicrobial therapy, however the widespread use and misuse of antibiotics has caused the emergence of bacteria resistance to antibiotics, posing a serious threat to human health (51). Particularly, the emergence of multidrug-resistant gram-positive bacteria, including vancomycin-resistant *S. aureus* (VRSA), methicillin-resistant *S. aureus* (MRSA), and vancomycin-resistant *Enterococci* (VRE), has become a serious problem in the treatment of bacterial diseases (52).

Antimicrobial resistance (AMR) is defined as the ability of microorganisms to survive and be viable in the presence of antimicrobial agents (53). Various factors determine antimicrobial resistance and they include a lack of the target site for a specific antibiotic, absence of a cell wall, the inability of an antibiotic to enter the bacterial cells due to the presence of an outer membrane , presence of an export system or the ability to produce enzymes that can inactivate the antibiotics (54). Antibacterial agents are molecules that act against bacterial infections (55). Antibacterial agents display various mechanisms of action, which are categorised based on the structure of bacteria or the function that is affected by the agents and these include inhibition of cell wall synthesis, cell membrane function, nucleic acid synthesis, folate metabolism, and ribosome function (56). Globally, nearly 700,000 deaths occur every year as a result of antibiotic-resistant microorganisms (57),

justifying the need to develop new compounds that can act against resistant bacteria (49). Schiff bases and their metal complexes are known to be promising antimicrobial agents, bringing hope to the discovery of antimicrobial agents that are effective against resistant microbes (58).

2.2 A brief overview of bacteria species targeted in the present study

2.2.1 *Escherichia coli*

Escherichia coli is a gram-negative bacteria, and it is the most common facultative anaerobe found in the intestinal tract of humans (59). *E. coli* lives in a mutually beneficial association with hosts and rarely causes diseases (60). It is, however, also one of the most common human and animal pathogens as it is responsible for a broad spectrum of infections like enteritis, urinary tract infection, bloodstream infections and neonatal meningitis (60,61). Most infections from *E. coli* are linked to contaminated food, and this poses a health concern as the microbe has developed antimicrobial resistance against several different classes of antibiotics with distinct mechanisms of action, which include beta-lactams and quinolones (62,63).

2.2.2 *Neisseria gonorrhoea*

Neisseria gonorrhoea, a gram-negative bacteria commonly known as *gonococcus* is the causative agent of gonorrhoea, a sexually transmitted infection (STI) that remains a major global public health problem (64). Infections by this pathogenic microbe spread to the bloodstream in both males and females, and symptoms may be acute but could be life-threatening if left untreated (65). Although gonorrhoea has been successfully treated by means of antimicrobials for the past 70 to 80 years, most *N. gonorrhoea* strains have developed resistance to most antimicrobials some of which are penicillins, tetracyclines, macrolides, sulfonamides, cephalosporins, and

fluoroquinolones (66). Gonorrhoea has a high morbidity burden, with more than 106 million new infections every year globally (67). Furthermore, the World Health Organization (WHO) has classified *N. gonorrhoea* as a "Priority 2" microorganism in the WHO Global Priority List of Antibiotic-Resistant Bacteria in order to provide guidance to Research, Discovery, and Development of New antibiotics (RDDN) (68). The continuous rise in the number of antibiotic resistant *gonococci* could result in gonorrhoea being untreatable, and this is the driving force for research in hopes of finding new treatment options to control the disease (69).

2.2.3 *Staphylococcus aureus*

Staphylococcus aureus is a gram-positive bacteria commonly associated with human bacterial infections, including those of the skin and other soft tissues, respiratory tract, bones and bloodstream (70). Infection by *S. aureus* appears as skin lesions (boils), but could develop into serious conditions such as leucocytosis, endocarditis, meningitis and pneumonia if left untreated (71). Over the years, *S. aureus* clinical isolates, which are the main cause of nosocomial infections, have developed a continuous antimicrobial resistance (72). In terms of sensitivity to antibiotics, *S. aureus* is classified into methicillin-sensitive *Staphylococcus aureus* (MSSA) and methicillin-resistant *Staphylococcus aureus* (MRSA) and treatment of the latter is a health challenge worldwide due to a gradual increase in the number of drug-resistant species (73). Antibiotic-resistance of *S. aureus* arises mainly by the acquisition of antibiotic-resistance genes from other *S. aureus* strains or from other genera (74). Vancomycin, linezolid, and daptomycin are antibiotics that effectively treat *S. aureus* infections. However, resistance to these drugs calls for the development of better antibacterial agents against this pathogen (75).

2.2.4 *Streptococcus mutans*

Streptococcus mutans is a gram-positive bacteria that is a primary causative agent of dental caries in humans (76). This microbe has an ability to form biofilms (dental plaques) on tooth surfaces by synthesizing adhesive glucan from sucrose, and glucan then mediates firm adherence of bacterial cells to tooth surfaces (76,77). Anti-caries such as fluoride and chlorhexidine are used to get rid of dental plaques but they are associated with side-effects and drug resistance (78). Although *S. mutans* is a natural inhabitant of the oral cavity, it can cause other infections such as infective endocarditis (IE), intra-amniotic infections and peritoneal abscesses (79). *Streptococcus mutans* has developed resistance against penicillin and ampicillin, resulting in a health hazard as the two antibiotics are used as antimicrobial prophylaxis for high-risk cardiovascular patients prior to dental procedures, hence the need to develop alternative inhibitors against *S. mutans* (78,80).

2.3 Oxidative stress and the importance of antioxidants

Oxidation is a chemical reaction that produces free radicals, thereby leading to chain reactions that could damage the cells of organisms (81). Free radicals are derived from atoms of oxygen, nitrogen and sulphur elements. In addition, free radicals are highly unstable due to their unpaired electron and hence they react with biomolecules such as DNA and lipids, thereby causing oxidative stress (82). Free radicals based on oxygen are known as reactive oxygen species (ROS) and include hydroxyl (HO·), superoxide (O_2·), nitric oxide (NO·), peroxyl (ROO·), and alkoxyl (RO·) radicals (83,84). Reactive oxygen species occur as by-products of cellular metabolism or as a result of stress on cells that coexist with a range of diseases (85). However, external sources such as medication, radiation, pollution and cigarette smoke could generate free radicals (86).

The production of reactive species can overpower the body's ability to eliminate or contain them, resulting in a redox imbalance/oxidative stress (81,87). Oxidative stress plays a significant role in diverse diseases such as cancer, arthritis, asthma, autoimmune diseases, neurodegenerative diseases, Alzheimer's disease, Parkinson's dementia, cardiovascular dysfunction, cataracts, and diabetes (88). In order to regulate redox imbalances, organisms have developed antioxidant mechanisms including the production of antioxidants and enzymes in response to excess ROS production and oxidative stress during metabolism (89).

Antioxidants are substances that significantly delay or inhibit the oxidation of a molecule (lipids, carbohydrates, proteins, and nucleic acids), by preventing the initiation and/or termination of chain reactions by free radicals (82,90,91). Enzymatic antioxidants include catalase, superoxide dismutase (SOD), glutathione reductase (GR), glutathione oxidase (GOX), and glutathione peroxidase (GPX) (92). Amongst the enzymatic antioxidants, SOD, catalase, and GPX are the most common and vital in removing harmful oxygen products (92). Despite the existence of endogenous antioxidant mechanisms, dietary micronutrients namely vitamins E, C, and beta carotene are a great source of exogenous antioxidants (93). The main sources of natural dietary antioxidants are fruits, vegetables, whole grains, green and black tea, beer, wine, coffee and spices (94). The human body cannot solely depend on endogenous antioxidants to counteract free radical, hence there is a need for supplementation with synthetic antioxidants (95). Additionally, synthetic antioxidants have gained major recognition because they are cheaper and effective as compared to natural antioxidants (96). However, most synthetic antioxidants such as butylated hydroxyanisole (BHA), butylated hydroxytoluene (BHT), and tert-

butylhydroquinone (TBHQ) have exhibited harmful effects, therefore there is a need for better and safer synthetic antioxidants (97).

2.4 Cervical cancer and HeLa cell line

Cervical cancer comes about when cancer develops in the cervix (98). Cervical cancer is regarded as the leading cause of cancer-related deaths amongst women in western, eastern, middle, and southern Africa (99). Nearly all cases of cervical cancer result from persistent infection with high risk subtype human papillomavirus (HPV) (100,101). Cervical infections with HPV trigger changes in cellular mechanisms, leading to the slow accumulation of microscopic lesions that eventually develop into cervical cancer (20,102). Cervical cancer remains a global threat, as most infections with high risk HPV result in cancer due to a limited treatment options (20). Cervical cancer is a largely preventable disease and early-stage detection improves survival rates (103). Nevertheless, the disease remains a killer for women in low and middle-income countries due to limited resources such as vaccinations and screening programs, and often presents with advanced and untreatable health complications (103).

For the last three decades, cervical cancer has been effectively treated with a platinum-based agent cisplatin and related drugs, in combination with radiotherapy (104,105). Despite that, the use of cisplatin in cervical cancer treatment is hampered by major side effects of this drug such as nausea and vomiting, kidney damage, neuropathy, hearing loss and bone marrow suppression (105,106). Besides, treatment of cervical cancer with cisplatin is sometimes regarded ineffective owing to the development of drug resistance (107,108). Consequently, there is a need to explore more compounds for cytotoxicity. Analysing compounds for cytotoxicity aid in determining the chemotherapeutic potential of those compounds (109). This is based

on the fact that cytotoxic compounds reportedly disrupt the activities of cancerous cells by hindering the process of protein and nucleic acid production (110). Cytotoxicity screening is usually carried out during preclinical studies of compounds or drug leads but these assays are also used in determining anticancer potential of compounds (32). Furthermore, modern pharmaceutical development regard cytotoxicity experiments crucial in providing vital information about a new molecule's biological attributes based on its basic tolerability (32). The present study analysed the cytotoxicity of selected Schiff base ligands and metal complexes using HeLa cells.

HeLa is an immortal human cell line that is commonly used in scientific research (111). This famous cell line was derived from the cervical cancer tumour tissue of the late Henrietta Lacks in 1951 (112,113), and holds a significant value in many medical breakthroughs, such as the development of the polio vaccine and cancer research (114). Cytotoxicity studies involving HeLa cells aid in determining the anticancer potential of a compound by means of in vitro experiments (115). In addition, cytotoxicity analysis of HeLa cells help in the establishment of safety profiles of drug candidates (116,117).

2.5 Schiff base ligands and metal complexes

The term Schiff's base is derived from the name of the German chemist Hugo Schiff, the first person to describe the end products from the reaction of primary amines with carbonyl compounds in 1864 (118). Schiff bases are therefore defined as compounds that contain an azomethine/imine group (C=N), as they are synthesized by condensation of a carbonyl compound (aldehyde or ketone) with a primary amine under distillation (119), to form compounds with a molecular formula of $R_1R_2C=NR_3$ where R_3 is a phenyl or alkyl group (120), via a reaction driven by an

acid or base catalyst or heat (121). A ligand is an ion or a neutral molecule that binds to a central metal atom via coordinate bonds formed through the donation of one or more of the electron pairs present in the ligand (122). Schiff base ligands containing nitrogen and oxygen donor atoms are the most frequently used in chemistry and biochemistry owing to their ease of synthesis, chelating ability, and potential catalytic and pharmacological applications (123). Additionally, these ligands are considered as building blocks for various organic substrates due to their ability to form stable metal complexes with high coordination number as they exhibit keto-enol tautomerism (124,125).

Schiff bases act as multidentate ligands with transition metals and they have a wide range of applications (126), including their use as organic constituents in pharmaceutical formulations (127). The biological activities of Schiff base complexes can be manipulated by changing functional groups and metal ions on the Schiff base ligands, and this provides flexibility in designing complexes with special characteristics (128). In addition, the biological activity of Schiff base ligands gets enhanced when chelated to transition metal ions via substitution reactions, and bivalent forms of zinc, copper, cobalt, and nickel are particularly favoured as these metal ions play an important role in biological processes (123). However, substitutions of groups such as OH or NH on Schiff base ligands have an effect on the coordination behaviour and the biological activity of these compounds (129). In the present study, Schiff base ligands were chelated to $Copper^{2+}$ and $Nickel^{2+}$ metal ions.

2.6 Biological roles and medical applications of copper and nickel

Copper (Cu) is an essential micronutrient that is involved in several metabolic processes including the elimination of free radicals, synthesis of hormones, proper

iron metabolism, neurotransmission and the stabilization of extracellular matrix (130,131). Adequate dietary amounts of Cu are needed as a Cu deficiency affects the activity of copper-dependent enzymes such as superoxide dismutases, cytochome C oxidase, lysal oxidase, tyrosinase, amine oxidases, vascular adhesion protein-1, dopamine β-monoxygenase, monoamine and diamine oxidases (132,133). The biological functions and benefits of copper has led to its application in designing biomaterials with unique properties such as promoting bone fracture and wound healing, protecting the cardiovascular system and killing of bacterial and cancer cells (131).

Nickel (Ni) is essential for the proper functioning of the human body, as this micronutrient is involved in lipid metabolism and boosts hormonal activity (134). Additionally, Ni is necessary for the action or formation of Guanosine 3',5'-cyclic monophosphate (cGMP), a signalling molecule that is responsible for the regulation of various processes such as blood pressure control, cardiovascular health as well as sodium metabolism (135). In medicine, nickel complexes are used as precursor molecules to efficiently produce synthetic amino acids (136). These synthetic amino acids are vital in biotechnology as they are used in the production of medicinal drugs and probiotics to combat a host of diseases and are also incorporated in food for improved nutritional content (136,137). In addition, the strong reducing power of nickel in comparison to other metal ions such as those of copper and cobalt has prompted research on nickel metal complexes as novel synthetic antioxidants (138).

2.7 Biological activity and medical applications of Schiff base ligands

Studies on the use of Schiff base ligands and their derivatives in drug development attracted attention after the discovery of chemotherapeutic actions of cisplatin, a drug used globally for cancer treatment (139,140). Literature reveals that Schiff

bases are known to exhibit various pharmacological and biological activities including antibacterial, anticancer, antifungal, anti-inflammatory, antioxidant, and antimalarial activity (141,142). In fact, the presence of other groups in the structures of Schiff base ligands, such as sulfonic acid, enhances the biological activities of these compounds (143,144). Currently, aromatic Schiff base ligands derived from hydrazides of phenolic acids and aromatic aldehydes, have gained recognition in the design of novel chemical compounds due to their array of medicinal properties, including antiviral, anticancer, antifungal, antioxidant, anti-inflammatory and antibacterial activities (145). The present study synthesized Schiff base ligands with aromatic ring systems, to form various molecular hybrids with versatile biological properties.

2.8 Methods employed in the present study

In the present study, selected Schiff base ligands and their corresponding metal complexes were synthesized and subjected to antibacterial, antioxidant, and cytotoxicity screening. Antibacterial activity was evaluated using the disc agar diffusion method and agar dilution method was used to determine minimum inhibitory concentration (MIC) values while antioxidant activity was determined by means of DPPH and reducing power assays. Cytotoxicity studies were conducted against the HeLa cell line using the MTT method.

2.8.1 Synthesis of Schiff base ligands

Schiff bases are considered as aldehydes or ketones bearing an azomethine group (N=CH) instead of the carbonyl group (C=O) (146,147) and they are formed as condensation products from primary amines and aldehydes or ketones (148,149). Schiff base ligands have received great attention from researchers because of their ease of synthesis and their ability to form complexes with almost all metals (149).

The synthesis of Schiff bases entails a nucleophilic addition of the NH_2 group to the C=O of the aldehyde or ketone, with the concurrent elimination of water to acquire maximum yield of the Schiff bases (150–152). Schiff base synthesis is a reversible reaction and is frequently carried out by refluxing a mixture containing equimolar of primary amines and aldehyde or ketone within non-aqueous organic solvents (153,154).

Confirmation of Schiff base formation is conducted by mean of various methods such as proton Nuclear Magnetic Resonance (^{1}H NMR) spectroscopy, ultraviolet visible (UV-Vis) spectroscopy and Fourier Transform Infrared (FTIR) spectroscopy (155). The formation of Schiff bases and metal complexes in the present study was confirmed using ^{1}H NMR and FTIR techniques. ^{1}H NMR spectroscopy is a technique that makes use of the magnetic properties of protons in order to provide information about the structure of a molecule as well as its identity (156). On the other hand, FTIR spectroscopy is applicable in identifying and analysing chemical compounds by measuring how they absorb infrared radiation at different wavelengths (157).

2.8.2 Kirby-Bauer agar disc diffusion antimicrobial activity screening method

The agar disc diffusion method is the most commonly used method to test for the susceptibility of bacteria to an antibacterial agent (158). Additionally, the agar disc diffusion method is preferable owing to its versatility, does not require any special equipment and it applies to a wide range of bacteria and agents (159). A filter paper disc is placed onto the inoculated agar and impregnated with the test compound, which will diffuse into the agar around the disc (160). The solubility of the chemical and its molecular size determine the size of the area of chemical infiltration around the disc (160). An organism that is susceptible to the test compound will not grow in

the area around the disc, and this area of no growth is known as a "Zone of inhibition" or "Clear zone" and is measured in mm (161). A quantitative antibacterial method is used to determine MIC, defined as the lowest concentration of an antimicrobial that inhibits the visible growth of a microorganism after overnight incubation (162). MIC values determine in vitro levels of susceptibility or resistance of specific bacterial strains to an antibiotic, and for this reason, MIC is a determinant in the choice of an infection therapy (163).

2.8.3 Assays for antioxidant activity screening

Antioxidant reactions take place by means of two reaction mechanisms, namely hydrogen atom transfer (HAT) and electron transfer (ET) (164). HAT applies to antioxidants with an ability to quench free radicals by donating a hydrogen atom, whereas ET applies to antioxidants that transfer one electron to reduce any compound including metals, radicals and carbonyls to gain stability (165). According to Abramovič *et al* (166), the reactivity of antioxidants is influenced by the structure of the antioxidant molecule, pH of the assay solution and also the type of solvent used. Radical scavenging-based methods include DPPH, N,N-dimethyl-para-phenylenediamine ($DMPD^+$), 2-2'-azino-bis(3-ethylbenzothiazoline-6-sulfonic acid ($ABTS^+$), and O_2^- assays (167). In the present study, antioxidant activity was evaluated by means of DPPH and reducing power assays.

a) DPPH free radical scavenging assay

Despite various experimental methods available for antioxidant studies, DPPH is the most commonly used because this assay is simple, fast, inexpensive and sensitive (168,169). DPPH is a free-radical molecule that is dark violet in colour, and is soluble in methanol or ethanol due to its hydrophobic nature (91,170). In addition,

DPPH has the best absorption maximum at a wavelength around 515 nm attributable to the presence of an unpaired electron (171). In the presence of an antioxidant, the violet-coloured DPPH molecule is reduced and hence changes colour to pale yellow, and the colour intensity is indirectly proportional to the antioxidant activity of test samples (169). **Figure 1** illustrates how DPPH is reduced to a more stable molecule in the presence of an antioxidant, whereby the antioxidant donates a proton to the unpaired electron on one of the nitrogen atoms of DPPH.

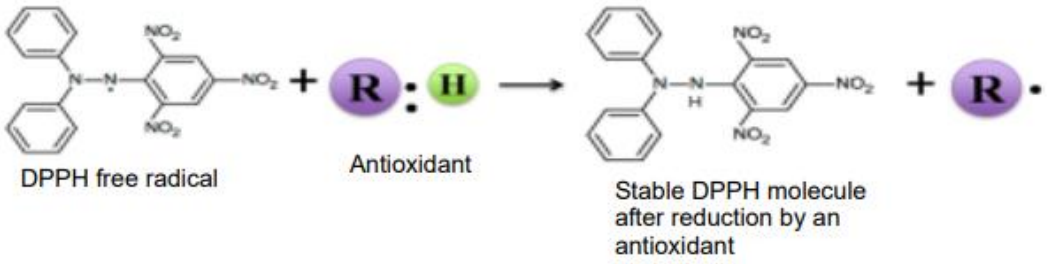

Figure 1. An illustration of a general DPPH reaction, as reported by Liang & Kitts (172) and Shalaby & Shanab (173).

b) Reducing power assay

Ferric reduction is often used as an indicator of a substance's ability to donate electrons (174). Substances with reduction potential are reactive with potassium ferricyanide (Fe^{3+}) to form potassium ferrocyanide (Fe^{2+}), and the latter reacts with ferric chloride to form a blue-green ferric ferrous complex that has an absorption maximum at 700 nm (175). The reducing power of test samples increases with concentration, and the absorbance measurements are taken as directly related to the total reducing capacity of an electron-donating antioxidant (174).

2.8.4 Cytotoxicity screening

Cytotoxicity assays are essential and are categorized based on various markers that are used to measure metabolically active cells such as enzyme activity, cell adherence and cell membrane permeability (176). Cytotoxicity assays include dye exclusion assays, colorimetric assays, colony formation assays, and live–cell imaging (177). Calorimetric cytotoxicity assays include (3-(4,5-dimethylthiazol-2-yl)-2,5-diphenyl tetrazolium bromide (MTT), sulforhodamine B (SRB) and crystal violet elution (CVE) assays (178). In the present study, the MTT assay was used to measure the cytotoxicity of the synthesized ligands and metal complexes against a HeLa cell line model.

MTT is one of the commonly used methods of measuring cell viability in cytotoxicity studies (179). This method is based on the principle of measuring the cell's viability and metabolic activity (180). The reduction reaction of MTT is illustrated in **Figure 2**. In the presence of viable cells, mitochondrial dehydrogenase enzymes convert the yellow-coloured MTT compounds into dark-blue insoluble formazan crystals (181). Coenzymes such as NADH facilitate the transfer of electrons to MTT, thereby reducing it to its formazan product (180). Solvents such as Dimethyl sulfoxide (DMSO) and acidified propanol are commonly used to solubilize the formazan crystals before taking absorbance readings (182).

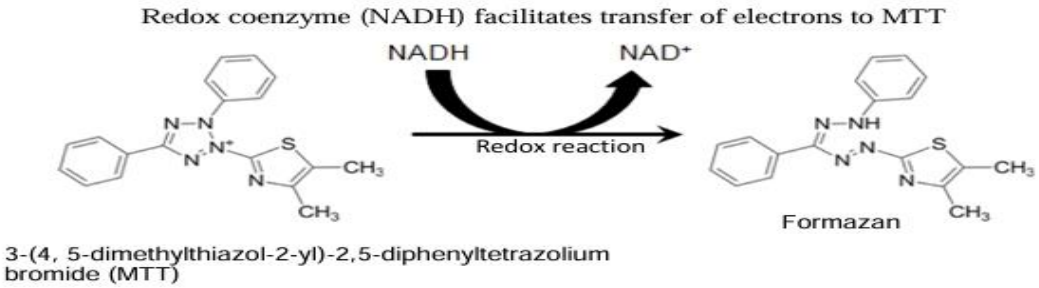

Figure 2. The conversion of MTT dye to formazan by reduction. The reaction is facilitated by the co-factor NADH which is an electron donor. Image was obtained from Riss *et al* (183).

CHAPTER 3

RESEARCH METHODS

3.1 Research ethics

An ethical clearance certificate, Reference Number: SOS-0015 for this study was obtained from the University of Namibia (UNAM) Research and Ethics Committee **(Appendix 1)**. Research permission to conduct the study was granted by the UNAM Centre for Postgraduate Studies. The HeLa cells that were used in the study are a commercial cell line model, commonly used in basic research and are non-hazardous. No animal or human subjects were utilized in this study. All laboratory work was carried out in accordance with outlined safety rules, and all waste generated was discarded according to UNAM safety protocols.

3.2 Research design

Schiff base ligands and metal complexes of Cu^{2+} and Ni^{2+} were synthesized by means of Schiff's base reaction. Structural confirmation of the synthesized Schiff base ligands was carried out by using proton NMR spectroscopy (^{1}H NMR). Fourier-Transform infrared (FTIR) spectroscopy was employed to confirm the presence of azomethine moiety in ligands as well as the chelation of the synthesized Schiff base ligands to metal ions of Cu^{2+} and Ni^{2+}.

Quantitative data was obtained from the antioxidant assays and the half – maximal inhibitory concentration (IC_{50}) was calculated using GraphPad prism software (Version 6). Antibacterial activity studies produced quantitative data by means of MIC values. The cytotoxicity experiments were conducted in a Biosafety Level (BSL) II laboratory. For cytotoxicity data, percent cell viability was calculated from

which the cytotoxic concentration of compound required to cause death to 50% of viable cells (IC_{50}) was calculated using GraphPad prism software (Version 6).

Statistical analysis was carried out in order to determine the significance of the data. Statistical analysis was done using the R software for statistical computing. An independent sample t – test was carried out at 95% confidence interval and threshold of 0.05. The threshold determines if the p – value is small enough to reject the null hypothesis. The p-value measures the probability of obtaining observed results, based on the null and alternative hypothesis.

3.3 Experimental procedures

3.3.1 Materials and instrumentation

All solvents were purchased from commercial sources. ^{1}H NMR for ligands was carried out by means of a BRUKER X400 (400MHz) spectrophotometer, using deuterated dimethyl sulfoxide-6 (DMSO-d_6). FTIR spectra of the metal complexes were obtained on a PerkinElmer spectrophotometer (spectrum 65) in the range of 4000−700 cm^{-1}. Absorbance readings for antioxidant assays were measured using Spectra Max M2 spectrophotometer (molecular devices, USA), and the half-maximal inhibitory concentration (IC_{50}) values were calculated using GraphPad prism software (Version 6). A minimum of three trials was conducted in triplicates for all biological assays.

3.3.2 Synthesis of Schiff's base ligands

Schiff base ligands and metal complexes (**33 compounds**) were synthesized using a friendly and cost-effective method, the Schiff's base reaction, a condensation reaction of aldehyde or ketone and primary amine derivatives in ethanol or methanol. Synthesis was carried out by means of the reaction illustrated in **Figure 3**.

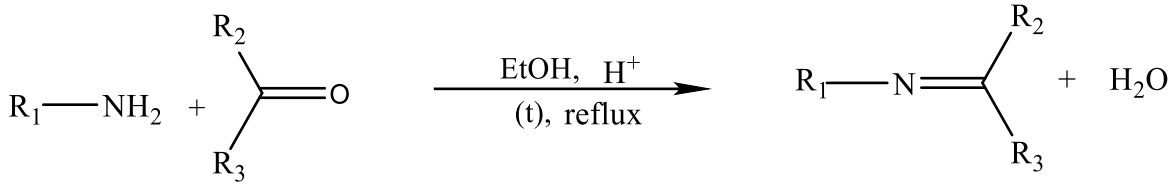

Figure 3. General reaction for Schiff base synthesis where R_1, R_2 and R_3 are different functional components ranging from single atom, aromatic rings and metal complex-based compounds. Illustration by Kanwal *et al* (184).

Synthesis of Schiff base ligands and their metal complexes was carried out following modified procedures as outlined by Santiago *et al* (185). For the ligands, at least 1 g of the limiting reagent was used and ethanol was used as a solvent. Each reactant was dissolved in 15.00 mL of ethanol and the resultant solutions were mixed accordingly, in a1:1 ratio. The synthesis reactions were monitored by means of Thin Layer Chromatography (TLC). All precipitates were left to completely dry, after filtration and washing several times, in a desiccator containing silica beads. Eleven (11) Schiff base ligands were synthesized and labeled **L1-L11**, respectively. Each of the synthesized ligands were complexed with either copper (II) or nickel (II), yielding 22 metal complexes. The chemical structures of the ligands and metal complexes were obtained using the Chemdraw professional 15 software. Structural confirmation of both the ligands and metal complexes was carried out using ^{1}H NMR and FTIR spectroscopy. The detailed preparation of each ligand is as follow:

a) (L1 (1-((E)-((4-((E)- phenyldiazenyl)phenyl)imino)methyl)naphthalen-2-ol**)**

A 15.00 mL ethanolic solution of 2-hydroxy-1-naphthaldehyde (0.8607 g) was added to a 15.00 mL ethanolic solution of para-phenylazoaniline (1.0004 g). The mixture was stirred at room temperature for 1 h, and an orange precipitate that formed was filtered out of the reaction mixture and rinsed

with cool ethanol. Yield: 61%, ^{1}H NMR (400 MHz, DMSO-d_6): δ ppm: 8.55 (1 H, C=N), 7.03 (1 H, OH), 8.04-7.8 (H $_{Ar\ (benzene)}$) (Figure 11).

b) (L2 (2-((E)-((4-((E)-phenyldiazenyl)phenyl)imino)methyl)phenol**)**

A 15.00 mL ethanolic solution of Salicylaldehyde (0.62 g, 0.53 mL) was added to a 15.00 mL ethanolic solution of para-phenylazoaniline (1.0008 g). A coral precipitate slowly formed at room temperature hence the mixture was further stirred under reflux for 4 h. The reaction product was filtered out of the reaction mixture and rinsed with warm ethanol. Yield: 58%, ^{1}H NMR (400 MHz, DMSO-d_6): δ ppm: 8.59 (1 H, C=N), 6.98 (1 H, OH), 7.93-6.88 (H $_{Ar\ (benzene)}$) (Figure 12).

c) (L3 ((E)-1-((2-phenylhydrazono)methyl)naphthalen-2-ol**)**

A 30.00 mL ethanolic solution of 2-hydroxy-1-naphthaldehyde (1.0028 g) was added to a 15.00 mL ethanolic solution of Phenylhydrazine (0.68 g, 0.57 mL) and stirred for 4 h under reflux. A yellow product that started forming slowly at room temperature was filtered out of the reaction mixture and rinsed with warm ethanol. Yield: 56%, ^{1}H NMR (400 MHz, DMSO-d_6): δ ppm: 8.95 (1 H, C=N), 7.58 (1 H, OH), 8.37-6.81 (H $_{Ar\ (benzene)}$), 10.53 (1 H, NH) (Figure 13).

d) (L4 ((E)-2-((2-phenylhydrazono)methyl)phenol**)**

A 15.00 mL ethanolic solution of Salicylaldehyde (1.12 g, 0.96 mL) was added to a 15.00 mL ethanolic solution of phenylhydrazine (1.00 g, 0.91 mL). The mixture was refluxed for 4 hours while stirring and the mother liquor was

kept in the freezer to allow for precipitation. A cream precipitate was obtained after 24 h and it was rinsed with cold ethanol. Yield: 57%, ^{1}H NMR (400 MHz, DMSO-d_6): δ ppm: 8.15 (1 H, C=N), 7.53 (1 H, OH), 7.27-6.78 (H $_{Ar\ (benzene)}$), 10.40 (1 H, NH) (Figure 14).

e) (L5 ((E)-1-((2-methylhydrazono)methyl)naphthalen-2-ol**)**

A 15.00 mL ethanolic solution of 2-hydroxy-1-naphthaldehyde (1.0083 g) was added to a 15.00 ethanolic solution of methylhydrazine (0.27 g, 0.31 mL). The mixture was stirred under reflux for 4 h and kept in the freezer until a dark brown powder formed. The powder was rinsed with cool ethanol. Yield: 45%, ^{1}H NMR (400 MHz, DMSO-d_6): δ ppm: (1 H, C=N), (1 H, OH), (H $_{Ar\ (benzene)}$), 12.86 (1 H, NH) (Figure 15).

f) (L6 ((E)-2-((2-methylhydrazono)methyl)phenol**)**

A 15.00 mL ethanolic solution of methylhydrazine (1.00 g, 1.15 mL) was added to a 15.00 mL ethanolic solution of salicylaldehyde (2.65 g, 2.26 mL). After stirring under reflux, the mixture was left in the freezer and the light brown precipitate that formed was rinsed with cold ethanol. Yield: 67%, ^{1}H NMR (400 MHz, DMSO-d_6): δ ppm: 7.68 (1 H, C=N), 7.29 (1 H, OH), 7.64-6.80 (H $_{Ar\ (benzene)}$), 11.42 (1 H, NH) (Figure 16).

g) (L7((E)-4-((2-hydroxynaphthalen-1-yl)methylene)amino)naphthalene-1-sulfonic acid**)**

A 15.00 mL ethanolic solution of naphthionic acid (1.0038 g) was added to a 15.00 mL ethanolic solution of 2-hydroxy-1-naphthaldehyde (0.7765 g). The

mixture was then refluxed while stirring for 3 h. A yellow powder formed, and was rinsed with warm ethanol. Yield: 54%, ^{1}H NMR (400 MHz, DMSO-d_6): δ ppm: 8.62 (1 H, C=N), 7.16 (1 H, OH), 8.26-7.39 (H $_{Ar\ (benzene)}$), 9.85 (1 H, OH $_{(SO3H)}$) (Figure 17).

h) (L8 ((E)-4-((2-hydroxybenzylidene)amino)naphthalene-1-sulfonic acid**)**

A 15.00 mL ethanolic solution of naphthionic acid (1.0056 g) was added to a 15.00 mL ethanolic solution of salicylaldehyde (0.55 g, 0.47 mL). A small amount of a yellow powder formed within 10 min of heating, and the mixture was further refluxed and stirred for 3 h. The final product was filtered from the reaction mixture then rinsed with warm ethanol. Yield: 52%, ^{1}H NMR (400 MHz, DMSO-d_6): δ ppm: 8.91 (1 H, C=N), 7.04 (1 H, OH), 8.16-7.02 (H $_{Ar\ (benzene)}$), 9.04 (1 H, OH $_{(SO3H)}$) (Figure 18).

i) (L9 ((E)-4-(((2-hydroxynaphthalen-1-yl)methylene)amino)benzenesulfonic acid**)**

A 15.00 mL solution of Sulphanilic acid (1.0059 g) was added to a 15.00 mL ethanolic solution of 2-hydroxy-1-naphthaldehyde (1.0041 g). The resultant solutions were mixed and refluxed with stirring for 4 h. After filtration, the product (a mustard yellow powder) was rinsed with warm ethanol. Yield: 65%, ^{1}H NMR (400 MHz, DMSO-d_6): δ ppm: 8.52 (1 H, C=N), 7.04 (1 H, OH), 7.95-7.30 (H $_{Ar\ (benzene)}$), 9.67 (1 H, OH $_{(SO3H)}$) (Figure 19).

j) (L10 ((E)-4-((2-hydroxybenzylidene)amino)benzenesulfonic acid**)**

A 15.00 mL ethanolic solution of sulphanilic acid (1.0009 g) was added to a 15.00 mL ethanolic solution of salicylaldehyde (0.71 g, 0.61 mL). The mixture was stirred under reflux for 3.5 h. A white powder was filtered out of the mixture and rinsed with warm ethanol. Yield: 86%, ^{1}H NMR (400 MHz, DMSO-d_6): δ ppm: 8.64 (1 H, C=N), 7.26 (1 H, OH), 8.35-7.82 ($H_{Ar\ (benzene)}$), 8.65 (1 H, $OH_{(SO3H)}$) (Figure 20).

k) (L11 ((E)-((2-hydroxynaphthalen-1-yl)methylene)sulfamic acid**)**

A 15.00 mL ethanolic solution of amidosulfonic (1.0098 g) was added to a 15.00 mL solution of 2-hydroxy-1-naphthaldehyde (1.7772 g). After refluxing with stirring for 4 h, the reaction mixture was left in the freezer and the brown crystals that formed were filtered out and rinsed with cold ethanol. Yield: 82%, ^{1}H NMR (400 MHz, DMSO-d_6): δ ppm: 8.10 (1 H, C=N), 7.23 (1 H, OH), 7.86-7.37 ($H_{Ar\ (benzene)}$), 8.94 (1 H, $OH_{(SO3H)}$) (Figure 21).

3.3.3 Synthesis of Cu (II) and Ni (II) complexes

Metal complexes were synthesized by reacting each of the ligands with $CuCl_2$ and $NiCl_2$, whereby the ligands were the limiting reagent. Synthesis was done using a mole ratio of metal salt to ligand of 1:2, using 0.5 mmol of ligands. Methanol (5.00 mL) was used as a solvent for all reactants and all products were allowed to completely dry in a desiccator. Metal complexation of the ligands was confirmed by using FTIR spectroscopy.

a) Copper (II) complex with L1

A 5.00 mL methanolic solution of L1 (0.0877 g) was mixed with 0.0213 g of $CuCl_2$ (in 5.00 mL methanol). The mixture was stirred at room temperature and after 1 h an orange product formed, then it was filtered using vacuum filtration. The orange precipitate was rinsed with methanol and collected. The product was recrystallized in cold methanol, filtered and allowed to dry in a desiccator.

b) Nickel (II) complex with L1

A solution of L1 (0.0879 g dissolved in 5.00 mL methanol) was added to a methanolic solution of $NiCl_2$ (0.0163 g). The mixture was stirred at room temperature and after 1 h a dark orange precipitate formed. The product was recrystallized in cold methanol, filtered and allowed to dry in a desiccator.

c) Copper (II) complex with L2

A 5.00 mL methanolic solution of L2 (0.0752 g) was added to a 5.00 mL methanolic solution of $CuCl_2$ (0.0213 g) to yield a brown powder after refluxing with stirring for 4 h. The product was recrystallized in warm methanol, filtered and allowed to dry in a desiccator.

d) Nickel (II) complex with L2

A 5.00 mL methanolic solution of $NiCl_2$ (0.0162 g) was added to a 5.00 mL methanolic solution of L2 (0.0753 g) After 4 h of refluxing and stirring, the mixture was placed in the freezer and a dark coral powder yield was rinsed with cold methanol, filtered and allowed to dry in a desiccator.

e) Copper (II) complex with L3

A 5.00 mL methanolic solution of 0.0655 g of L3 was added to a 5.00 mL methanolic solution of $CuCl_2$ (0.0213 g). The resultant mixture was stirred for 4 h under reflux, and a dark green solution with little to no precipitate was left in the freezer to yield an emerald green powder. The product was recrystallized in warm methanol, filtered and allowed to dry in a desiccator.

f) Nickel (II) complex with L3

A 5.00 mL methanolic solution of 0.0655 g of L3 was added to a 5.00 mL methanolic solution of $NiCl_2$ (0.0163 g). The resultant mixture was stirred for 4 h under reflux, and a yellow powder was collected. The product was recrystallized in warm methanol, filtered and allowed to dry in a desiccator.

g) Copper (II) complex with L4

A 5.00 ml methanolic solution of L4 (0.1062 g) was added to a 5.00 mL methanolic solution of $CuCl_2$ (0.0426 g) and the mixture was stirred under reflux for 4 h. At the end of the reaction the mixture was placed in a freezer to yield a dark brown powder. The product was recrystallized in warm methanol, filtered and allowed to dry in a desiccator.

h) Nickel (II) complex with L4

A 5.00 methanolic solution of $NiCl_2$ (0.0324g) was added to a 5.00 methanolic solution of L4 (0.1062 g). The mixture was refluxed while stirring. After 4 h there was no precipitation and the mixture left in the freezer

until an off-white powder formed. The product was rinsed with cold methanol after filtration and left to further dry in a desiccator.

i) Copper (II) complex with L5

A 5.00 mL methanolic solution of $CuCl_2$ (0.0428 g) was added to a 5.00 mL methanolic solution of L5 (0.1002 g). The mixture was stirred under reflux for 4 h. At the end of the reaction the mixture was placed in a freezer to yield a dark brown powder. The product was recrystallized in cold methanol, filtered and allowed to dry in a desiccator.

j) Nickel (II) complex with L5

A 5.00 methanolic solution of L5 (0.0506 g) was mixed with $NiCl_2$ (0.0165 g in methanol). The resultant mixture was stirred for 4 h under reflux, and a dark brown powder was collected after freezing. The product was recrystallized in cold methanol, filtered and allowed to dry in a desiccator.

k) Copper (II) complex with L6

A 5.00 mL methanolic solution of L6 (0.0381 g) was mixed with 0.0212 g of $CuCl_2$ (in 5.00 mL methanol). The mixture was stirred under reflux and after freezing a dark green powder was collected and rinsed with warm methanol. The product was left to dry in a desiccator.

l) Nickel (II) complex with L6

A 5.00 mL methanolic solution of L6 (0.0380 g) was added to a 5.00 mL methanolic solution of $NiCl_2$ (0.0160 g). The mixture was stirred under reflux

and after freezing a cream powder was collected and rinsed with cold methanol, then left to dry in a desiccator.

m) Copper (II) complex with L7

A 5.00 mL methanolic solution of L7 (0.0944 g) was mixed with a 5.00 mL solution of $CuCl_2$ (0.0214 g) to yield a yellow powder after refluxing with stirring for 4 h. The product was recrystallized in warm methanol, filtered and allowed to dry in a desiccator.

n) Nickel (II) complex with L7

A 5.00 mL solution of $NiCl_2$ (0.0163 g) was added to a 5.00 mL methanolic solution of L7 (0.0944 g). After 4 h of refluxing and stirring, the mixture was placed in the freezer and a bright orange powder yielded was rinsed with cold methanol. The product was left to dry in a desiccator.

o) Copper (II) complex with L8

A 5.00 mL methanolic solution of $CuCl_2$ (0.0214 g) was added to a 5.00 mL methanolic solution of L8 (0.0819 g). The mixture was stirred under reflux for 4 h. At the end of the reaction the mixture was placed in a freezer to yield a light grey powder. The product was recrystallized in cold methanol, filtered and allowed to dry in a desiccator.

p) Nickel (II) complex with L8

A 5.00 mL methanolic solution of L8 (0.0819 g) was mixed with $NiCl_2$ (0.0163 g in 5.00 mL methanol). The resultant mixture was stirred for 4 h

under reflux, and a light-yellow powder was collected. The product was recrystallized in warm methanol, filtered and allowed to dry in a desiccator.

q) Copper (II) complex with L9

A 5.00 ml methanolic solution of L9 (0.0818 g) was added to a 5.00 mL methanolic solution of $CuCl_2$ (0.0214 g). The mixture was stirred under reflux for 4 h. At the end of the reaction the mixture was placed in a freezer to yield a mustard yellow powder. The product was recrystallized in cold methanol, filtered and allowed to dry in a desiccator.

r) Nickel (II) complex with L9

A 5.00 mL methanolic solution of $NiCl_2$ (0.0163 g) was added to a 5.00 mL methanolic solution of L9 (0.0818 g). The mixture was refluxed while stirring. After 4 h there was no precipitation and the mixture left in the freezer until a mustard yellow powder formed. The product was rinsed with cold methanol after filtration and left to further dry in a desiccator.

s) Copper (II) complex with L10

A 5.00 mL methanolic solution of $CuCl_2$ (0.0426 g) was added to a 5.00 mL methanolic solution of L10 (0.0426 g). The mixture was stirred under reflux for 4 h. At the end of the reaction the mixture was placed in a freezer to yield a white powder. The product was recrystallized in cold methanol, filtered and allowed to dry in a desiccator.

t) Nickel (II) complex with L10

A 5.00 mL methanolic solution of L10 (0.1386 g) was mixed with $NiCl_2$ (0.0324 g in 5.00 mL methanol). The resultant mixture was stirred for 4 h under reflux, and a white powder was collected after freezing. The product was recrystallized in cold methanol, filtered and allowed to dry in a desiccator.

u) Copper (II) complex with L11

A 5.00 mL methanolic solution of L11 (1.1256 g) was added to a 5.00 mL methanolic solution of $CuCl_2$ (0.0428 g). The mixture was refluxed with stirring for 4 h. After freezing, a brown powder was collected. The product was recrystallized in warm cold methanol, filtered and allowed to dry in a desiccator.

v) Nickel (II) complex with L11

A 5.00 mL methanolic solution of $NiCl_2$ (0.0324 g) was added to a 5.00 mL methanolic solution of L11 (0.1258 g). After 4 h of refluxing and stirring, the mixture was placed in the freezer and a dark brown powder yielded was rinsed with cold methanol and left to dry in a desiccator.

3.3.4 Antibacterial activity screening

The determination of the antibacterial activity of the ligands and their metal complexes was conducted by means of Kirby Bauer disc agar diffusion method, using modified methods previously described by Philip *et al* (186) and Yousif *et al* (187). All apparatus used for antibacterial activity assays were sterilized in an autoclave at 121ºC for 30 min, to rule out any form of contamination. Furthermore, the assays were carried out using aseptic techniques and all apparatus were sterilized

after use in order to fulfil the safety measure requirements. Bacteria samples were disposed of according to the regulations of the University of Namibia.

a) Test microorganisms

A total of four commercial bacterial species were tested, namely: *Escherichia coli* (ATCC 9637), *Neisseria gonorrhoeae* (ATCC 19424), *Staphylococcus aureus* (ATCC 25923) and *Streptococcus mutans* (ATCC 25175). Bacterial cultures were prepared by dissolving a few crystals in sterile nutrient broth, followed by incubation for 36 h at 37ºC to allow for bacterial growth. The grown cultures were kept at 5ºC until further usage.

b) Antibacterial activity screen test

An antibacterial activity screen test was conducted to determine whether the extracts were active against the test bacteria at a given concentration prior to testing activity at lower concentrations. Ligands and metal complexes dissolved in 5% Dimethyl-Sulfoxide (DMSO) were screened at a concentration of 10 mg/mL. Each bacterium sample (200 µL) was inoculated onto the surface of nutrient agar. Sterile paper discs were placed onto the inoculated agar using flame sterilized biceps and paper discs were impregnated with 10 µL of the test samples. Vancomycin (30 µg) and Rifampicin (5 µg) served as the positive controls for gram-negative and gram-positive bacteria, respectively and 5% DMSO as a negative control. The plates were inverted and allowed to dry for an hour in a fridge then incubated for 24 h at 37ºC. The clear zones around the discs were an indication of antibacterial activity and microorganisms that were inhibited by the samples were used for the agar disc diffusion antibacterial test.

c) Kirby Bauer disc agar diffusion method

Test samples (ligands/metal complexes) were dissolved in 5% DMSO, to prepare solutions of 0.63, 1.25, 2.50, 5.00, and 10.00 mg/mL. A 24 h bacterial suspension (200 µL) was aseptically inoculated on nutrient agar plates. Paper discs were placed onto the inoculated plates and impregnated with 10 µL of prepared samples of varying concentrations. DMSO (5%) served as a negative control and the antibiotics Vancomycin (30 µg) and Rifampicin (5 µg) served as the positive controls for gram-negative and gram-positive bacteria, respectively. The plates were inverted, and the discs were allowed to dry for an hour in a fridge to allow for pre-diffusion of the samples then incubated for 24 h at 37°C. Positive results were indicated by the presence of clear zones of inhibition around discs impregnated with ligands or metal complexes suggesting that they inhibited bacterial growth. Inhibition zones were measured with a meter ruler and the diameters were recorded in mm.

d) Determination of MIC values

The least ligand/metal complex concentration that inhibited visible bacterial growth was determined using modified procedures as outlined by Veiga *et al* (188). MIC values were deduced from concentrations that inhibited bacterial growth in the disc agar diffusion assay. Bacteria 16 h cultures were serially diluted with sterile nutrient broth to achieve bacteria sample with a dilution factor of 10^{-5}. To each labelled sterile tube, 100 µL of ligand/metal complex, 200 µL broth and 10 µL of a bacterium sample were aseptically added. The tubes were incubated for 16 h at 37ºC, and a loop full using an inoculating loop was obtained from each tube and aseptically streaked onto nutrient agar plates. The plates were incubated for 16 h at 37°C. The MIC value

was determined as the lowest concentration of the ligands/metal complexes in the broth medium that inhibited the visible growth of the test microorganism(s).

3.3.5 Determination of the antioxidant activity of the synthesized ligands and metal complexes

a) **DPPH free radical scavenging assay**

The 2,2-diphenyl-1-picrylhydrazyl (DPPH) free radical-scavenging ability of the ligands and metal complexes was measured according to a modified protocol previously described by Philip *et al* (186). Test samples (0.78, 1.56, 3.13, 6.25, 12.5, 25, 50, 100 µg/mL) dissolved in absolute ethanol were mixed with an ethanolic solution of DPPH (90 µM), and further incubated in the dark at room temperature for 30 min. The absorbance values were measured at 520 nm using a Spectra Max M2 spectrophotometer (Molecular devices, USA) and converted into percentage inhibition using the equation below. DPPH blank was used as a negative control and a known antioxidant ascorbic acid was used as a standard control.

% inhibition = {(Absorbance of control – absorbance of sample)/absorbance of control} x 100

Percentage inhibition values were used to calculate the concentration that would scavenge 50% or more of DPPH free radicals (IC_{50}), using Graphpad Prism 6 software, and values were reported as ± standard error of the mean (SEM).

b) **Ferric reducing power assay**

The ferric reducing power of the test samples was evaluated according to a protocol previously described by Jafari *et al* (189), with modifications. Samples were tested at

varying concentrations of 0.20, 0.39, 0.78, 1.56, 3.13, 6.25, 12.50 and 25µg/mL. Samples dissolved in absolute ethanol (2.5 mL) were mixed with 2.5 mL of 200 mmol/L sodium phosphate buffer (pH 6.6) and 2.5 mL of 1% potassium ferricyanide. The mixture was incubated at 50°C for 20 min, followed by an addition of 2.5 mL of 10% trichloroacetic acid (w/v), and subsequently centrifuged at 650 rpm for 10 min. The upper layer (5 mL) was mixed with 5 mL of deionised water and 1 mL of 0.1% of ferric chloride. Absorbance was measured at 700 nm using a Spectra Max M2 spectrophotometer (Molecular devices, USA). Gallic acid was used as a standard control.

3.3.6 Cytotoxicity screening

The cytotoxic effects of selected ligands and metal complexes in this study were evaluated against the HeLa cell line using the MTT assay as described by Liu *et al* (190) with minor modifications. This method is based on the conversion of yellow MTT to blue formazan crystals by mitochondrial succinate dehydrogenase in the presence of viable cells (191).

The cell line used for this study was purchased from Cellonex (SA). To validate the use of the synthesized ligands and metal complexes for anticancer applications, toxicity assessment against the HeLa cell line was performed. The assay was done in triplicates. The cells were maintained in 10% Dulbecco's Modified Eagle Medium (DMEM) at 37 °C, 5% CO_2, 95% air and 100% relative humidity. One hundred microlitres of the cell suspension at a concentration of 10,000 cells was placed in every well of a 96-well plate and incubated for 24 hours. After incubation, the medium seeded with HeLa cells was treated with different concentrations of the ligand / metal complexes (0.78 - 100 µg/mL). After 48 h of treatment, 100 µL of spent media was removed then 10 µL of MTT (5mg/mL) was added per well. After a

further incubation for 3 h, 50 µL of acidified propanol was added per well of the 96 well plate before incubating for another 40 min. Absorbance readings were taken at 570 nm using a Spectra Max M2 spectrophotometer (Molecular devices, USA). Auranofin (0.3 - 20 mg/mL) was used as a standard control in this study.

The percentage of viable cells was calculated using the following formula:

% cell viability = 100 - Abs (Test)/Abs (Control) x 100

Cell viability was plotted in relation to logarithmic concentrations of hydrazone ligands / metal complexes and IC_{50} was determined using GraphPad Prism software (Version 6.01).

CHAPTER 4

RESULTS

4.1 Yields of the synthesized ligands and metal complexes

The quantities (in grams) of the ligands that were synthesized in this study are provided in **Table 1**, whereby % yield = (actual yield/theoretical yield) x 100. The synthesized compounds were of varying colours, although some of the compounds had similar colours. Quantities and colours of metal complexes are provided in **Table 2**. Images of the synthesized compounds are included as supplementary material under **Appendix 3**.

Table 1. Yields and colours of the synthesized ligands.

Ligand(L)	**Theoretical yield (g)**	**Actual yield (g)**	**% Yield**	**Colour**
L1	2.0008	1.2267	61	Orange
L2	2.0016	1.1644	58	Coral
L3	0.5014	0.2832	56	Yellow
L4	2.000	1.1460	57	Cream
L5	0.5042	0.2255	45	Dark brown
L6	0.2500	0.1667	67	Light brown
L7	2.0076	1.0849	54	Bright yellow
L8	2.0112	1.0358	52	Light yellow
L9	2.0082	1.3142	65	Mustard yellow
L10	1.0009	0.8559	86	White
L11	2.0196	1.6582	82	Brown

Table 2. Yields and colours of Cu (II) and Ni (II) metal complexes.

Ligand	Cu (II) metal complex				Ni (II) metal complex			
	Actual yield (g)	**Theoretical yield (g)**	**%yield**	**Colour**	**Actual Yield (g)**	**Theoretical yield (g)**	**%yield**	**Colour**
L1	0.0494	0.0878	56	Orange	0.0763	0.0880	87	Dark orange
L2	0.0379	0.0752	46	Brown	0.0493	0.0752	66	Dark coral
L3	0.2365	0.3328	71	Emerald green	0.0345	0.0656	53	Yellow
L4	0.0365	0.0531	69	Dark brown	0.0471	0.0531	89	Off-white
L5	0.1025	0.1503	68	Dark brown	0.0179	0.0253	71	Dark brown
L6	0.0592	0.0764	77	Dark green	0.0123	0.0190	64	Cream
L7	0.0364	0.0472	77	Yellow	0.0923	0.0944	98	Bright orange
L8	0.0198	0.0410	48	Light grey	0.0300	0.0410	73	Light yellow
L9	0.0245	0.0409	60	Mustard yellow	0.0247	0.0409	60	Mustard yellow
L10	0.0687	0.0852	81	White	0.0592	0.0693	85	White
L11	0.1503	0.1884	80	Brown	0.1484	0.1887	79	Dark brown

4.2 Chemical structures of the synthesized ligands and metal complexes.

In the present study, a total of 33 compounds were synthesized. The chemical names, chemical structures and molecular masses of the ligands presented in **Table 3** were generated by capturing names and molecular weights of compounds into the Chemdraw software. Structures of both Ni(II) and Cu(II) metal complexes in **Table 4** and **Table 5** respectively, were drawn by using the same software.

Table 3. Chemical structures of the synthesized Schiff base ligands.

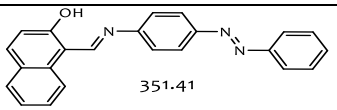 351.41 1-((*E*)-((4-((*E*)-phenyldiazenyl)phenyl)imino) methyl)naphthalen-2-ol **L1**	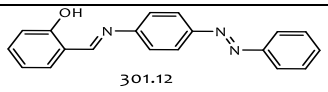 301.12 2-((*E*)-((4-((*E*)-phenyldiazenyl)phenyl)imino)methyl)phenol **L2**
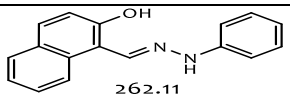 262.11 (*E*)-1-((2-phenylhydrazono)methyl) naphthalen-2-ol **L3**	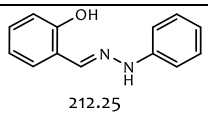 212.25 (*E*)-2-((2-phenylhydrazono)methyl)phenol **L4**
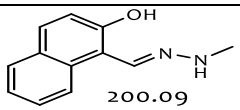 200.09 (*E*)-1-((2-methylhydrazono)methyl) naphthalen-2-ol **L5**	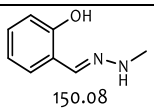 150.08 (*E*)-2-((2-methylhydrazono)methyl)phenol **L6**
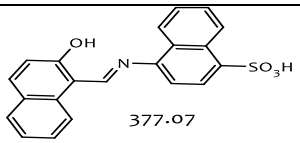 377.07 (*E*)-4-(((2-hydroxynaphthalen-1-yl)methylene) amino)naphthalene-1-sulfonic acid **L7**	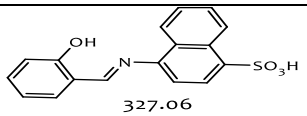 327.06 (*E*)-4-((2-hydroxybenzylidene)amino) naphthalene-1-sulfonic acid **L8**
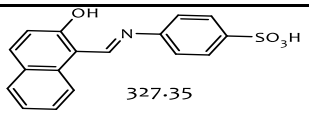 327.35 (*E*)-4-(((2-hydroxynaphthalen-1-yl)methylene)amino)benzenesulfonic acid **L9**	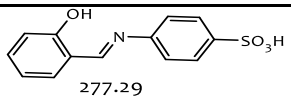 277.29 (*E*)-4-((2-hydroxybenzylidene)amino) benzenesulfonic acid **L10**
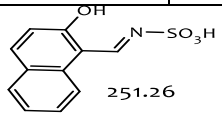 251.26 (*E*)-((2-hydroxynaphthalen-1-yl) methylene)sulfamic acid **L11**	

The structures of nickel (II) metal complexes that were synthesized in the present study are shown in **Table 4**. The reactant ratio of ligand to metal ion (2:1) is also evident. The structures also show the atoms of the ligands that bind to metal ions to form metal complexes.

Table 4. Chemical structures of nickel (II) metal complexes.

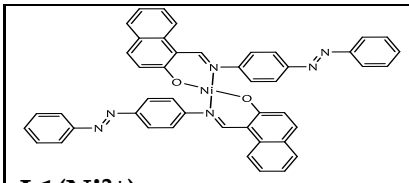 **L1(Ni^{2+})**	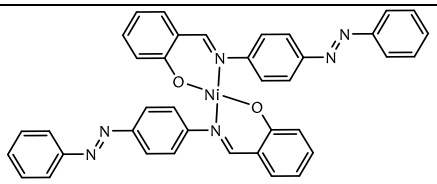 **L2(Ni^{2+})**
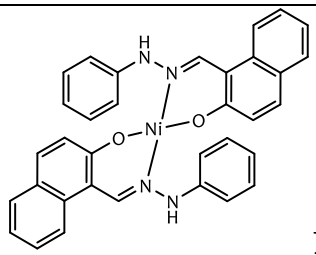 **L3(Ni^{2+})**	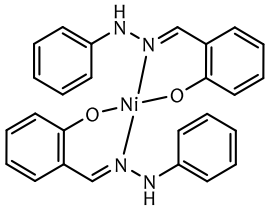 **L4(Ni^{2+})**
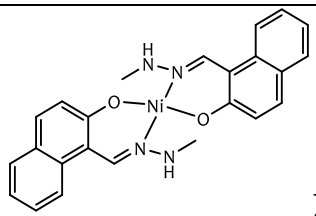 **L5(Ni^{2+})**	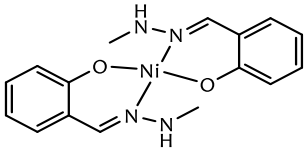 **L6(Ni^{2+})**
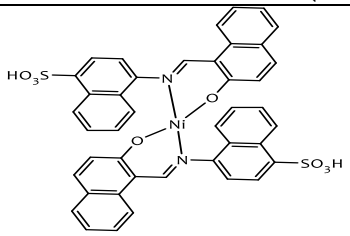 **L7(Ni^{2+})**	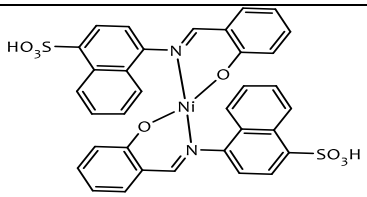 **L8(Ni^{2+})**
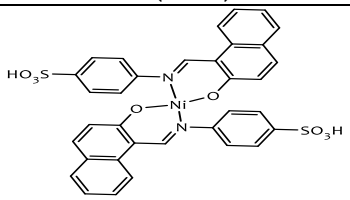 **L9(Ni^{2+})**	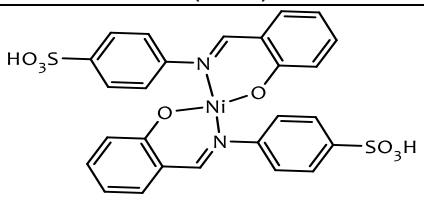 **L10(Ni^{2+})**
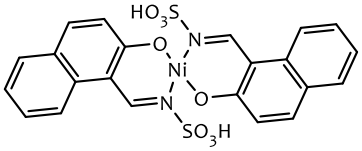 **L11(Ni^{2+})**	

The structures of copper (II) metal complexes that were synthesized in the present study are displayed in **Table 5**. Ligands and metal cations reacted in a 2:1 ratio and atoms involved in complexation are also shown.

Table 5. Chemical structures of copper (II) metal complexes.

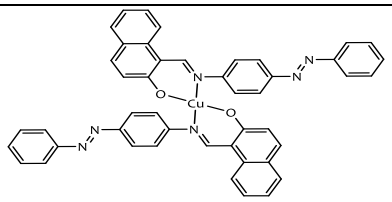 **L1(Cu^{2+})**	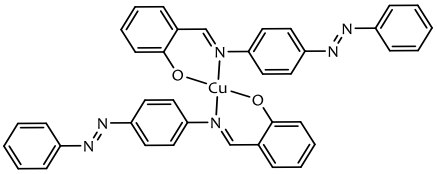 **L2(Cu^{2+})**
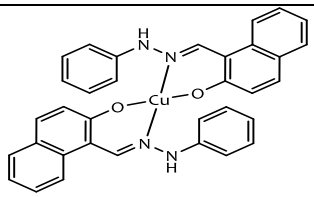 **L3(Cu^{2+})**	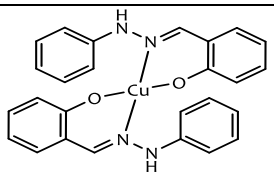 **L4(Cu^{2+})**
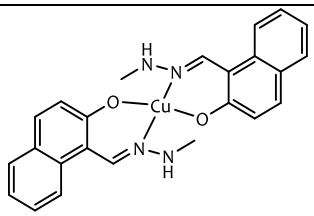 **L5(Cu^{2+})**	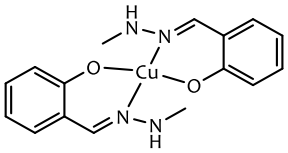 **L6(Cu^{2+})**
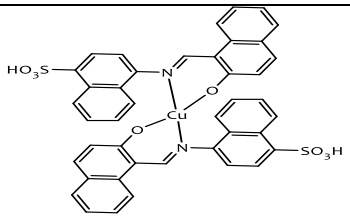 **L7(Cu^{2+})**	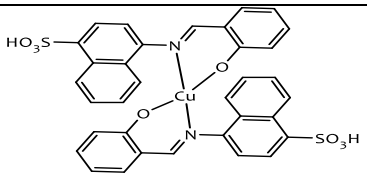 **L8(Cu^{2+})**
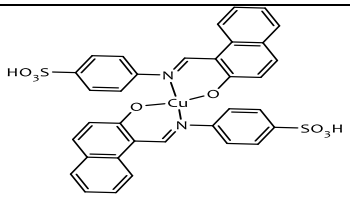 **L9(Cu^{2+})**	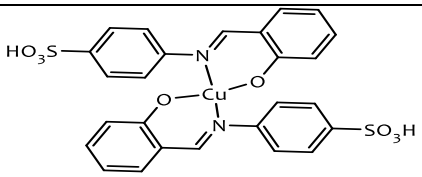 **L10(Cu^{2+})**
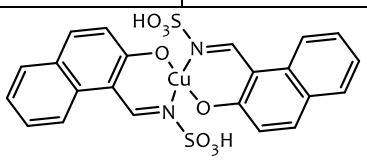 **L11(Cu^{2+})**	

4.3 ^{1}H NMR data of the ligands

The ^{1}H NMR spectra of the ligands were recorded in DMSO-d_6 solution. The spectra show that the different non-equivalent protons resonate at different values of the applied field. Chemical shifts are summarized in **Table 6** and the generated spectra are listed in **Appendix 2**. The spectra of all the Schiff base ligands exhibit singlet peaks in the δ 8.95 – 7.68 ppm and δ 7.58 – 6.98 ppm range, which are assigned to the azomethine (–CH=N–) and phenolic (OH) protons, respectively. The multiplet peaks observed in the δ 8.37 - 6.78 ppm range are assigned to protons of the aromatic rings. The sulfonic acid (-SO_3H) protons for L7, L8, L9, L10, and L11 appeared as a singlet peak in the δ 9.85-8.65 ppm range. The chemical shifts for singlet peaks of –NH protons of L3, L4, L5, and L6 resonate at 10.5, 10.40, 12.86, and 11.42 δ ppm, respectively. The chemical shift values obtained for different non-equivalent protons are, in agreement with literature and therefore the ^{1}H NMR results support the assigned geometry of the synthesized ligands.

Table 6. ^{1}H NMR data for Schiff base ligands using DMSO-d_6 as a solvent.

Compound	Chemical shifts (ppm)				
	C=N	**OH**	**SO_3H**	**Aromatic protons**	**NH**
L1	8.55	7.03	-	8.04 - 7.8	-
L2	8.59	6.98	-	7.93 -6.88	-
L3	8.95	7.58	-	8.37 – 6.81	10.53
L4	8.15	7.53	-	7.27 - 6.78	10.40
L5	8.49	7.13	-	8.24 – 7.34	12.86
L6	7.68	7.29	-	7.64 – 6.80	11.42
L7	8.62	7.16	9.85	8.26 – 7.39	-
L8	8.91	7.04	9.04	8.16 – 7.02	-
L9	8.52	7.04	9.67	7.95 – 7.30	-
L10	8.64	7.26	8.65	8.35 -7.82	-
L11	8.10	7.23	8.94	7.86 – 7.37	-

(-) denotes, functional group not present in that particular compound.

4.4 FTIR data of ligands and metal complexes

FTIR was used to confirm the presence of the azomethine group as well as chelation of metal ions with the synthesized ligands. Noteworthy characteristic bands of the FTIR spectra for the Schiff base ligands and metal complexes that were analysed in the present study are given in **Table 7** and the spectra are listed in **Appendix 2**. The FTIR spectra of the ligands show bands in the 1635-1609 cm^{-1} range, corresponding to C=N (azomethine) stretching vibrations, indicating that the desired Schiff base ligands were indeed formed. On complexation, the C=N vibrations shifted to a lower frequency, and new bands appeared in the 1633-1578 cm^{-1} range, which confirms the coordination of the azomethine nitrogen atom to the central metal of either Ni^{2+} or Cu^{2+}. A band for the phenolic (OH) group appeared in the 3382-3053 cm^{-1} range in the spectra of free ligands. Bands for the OH group were absent in the spectra of metal complexes, which indicates proton substitution by metal cation coordination to oxygen (O-M) in this case M being either Ni^{2+} or Cu^{2+}. From the FTIR results, it may be concluded that the synthesized ligands are bidentate and coordinate with the metal ions through the azomethine nitrogen and the phenolic oxygen. Ultimately, the bands in the spectra are common for all the ligands and metal complexes, and data generated is consistent with literature documentations.

Table 7. Infrared spectral data of Schiff base ligands and metal complexes.

Compound	Frequency (cm^{-1})			
	Free ligand		Ni (II) metal complex	Cu (II) metal complex
	v(O-H)	v(C=N)	v(C=N)	
L1	3056	1623	1621	1622
L2	3054	1614	1613	1612
L3	3324	1621	1619	1618
L4	3290	1622	1602	1607
L5	3382	1623	1620	1621
L6	3258	1618	1606	1603
L7	3053	1622	1610	1606
L8	3089	1609	1607	1578
L9	3354	1635	1632	1633
L10	3081	1632	1628	1629
L11	3077	1630	1628	1628

4.5 Antibacterial activity of ligands and metal complexes

4.5.1 Antibacterial activity preliminary screening

Bacteria species used in this study were subjected to a preliminary screen, in order to determine the microorganisms that were susceptible to each ligand or metal complex. In addition, preliminary screening was necessary to determine the highest concentration at which the antibacterial activity of the ligands/metal complexes would be studied. Bacteria species whose growth was inhibited by the ligands/metal complexes in the screen test were then further used in the disc agar diffusion method for antibacterial activity studies. Antibacterial activity screening was done on both gram-positive (*S. aureus, S. mutans*) and gram-negative (*E. coli, N. gonorrhoea*) bacteria species.

The preliminary screen test results for the ligands (**Table 8**) show that all of the bacteria species used in this study were susceptible to L9, L10, and L11. However, L1, L2, and L3 did not inhibit the growth of any of the tested bacteria species. Both L5 and L8 only inhibited the growth of *S. aureus*. L4 inhibited the growth of both *N. gonorrhoea* and *S. aureus*, but did not inhibit the growth of *E. coli* or that of *S. mutans*. All tested bacteria with an exception of *E. coli* were susceptible to L6. On the other hand, only *N. gonorrhoea* and *S. aureus* were susceptible to L7.

Table 8. Antibacterial activity screen test results for ligands.

Ligand (L)	**Bacteria**			
at 10 mg/mL	***E. coli***	***N. gonorrhoea***	***S. aureus***	***S. mutans***
L1	×	×	×	×
L2	×	×	×	×
L3	×	×	×	×
L4	×	√	√	×
L5	×	×	√	×
L6	×	√	√	√
L7	×	√	√	×
L8	×	×	√	×
L9	√	√	√	√
L10	√	√	√	√
L11	√	√	√	√

√ Bacterial growth inhibition × No bacterial growth inhibition

The results in **Table 9** show that out of all nickel metal complexes tested in the present study, only L6(Ni^{2+}) inhibited the growth of all four (4) bacteria species. On the other hand, none of the tested bacteria showed susceptibility to nickel metal complexes of L1, L2, L3, L4, L7, L8, and L11.

Table 9. Antibacterial activity screen test results for nickel (II) metal complexes.

Metal complex	**Bacteria**			
	S. aureus	***S. mutans***	***N. gonorrhoea***	***E. coli***
(10 mg/mL)				
L1(Ni^{2+})	×	×	×	×
L2(Ni^{2+})	×	×	×	×
L3(Ni^{2+})	×	×	×	×
L4(Ni^{2+})	×	×	×	×
L5(Ni^{2+})	√	×	√	√
L6(Ni^{2+})	√	√	√	√
L7(Ni^{2+})	×	×	×	×
L8(Ni^{2+})	×	×	×	×
L9(Ni^{2+})	×	×	√	×
L10(Ni^{2+})	×	×	√	√
L11(Ni^{2+})	×	×	×	×

√ Bacterial growth inhibition × No bacterial growth inhibition

The results in **Table 10** show that copper (II) metal complexes of L4, L5, and L6 inhibited the growth of all four bacteria species. On the other hand, none of the bacteria tested showed susceptibility to copper (II) metal complexes of L1, L2, L7, L8, and L10.

Table 10. Antibacterial activity screen test results for copper (II) metal complexes.

Metal complex	**Bacteria**			
	S. aureus	***S. mutans***	***N. gonorrhoea***	***E. coli***
(10 mg/mL)				
L1(Cu^{2+})	×	×	×	×
L2(Cu^{2+})	×	×	×	×
L3(Cu^{2+})	×	×	×	×
L4(Cu^{2+})	√	√	√	√
L5(Cu^{2+})	√	√	√	√
L6(Cu^{2+})	√	√	√	√
L7(Cu^{2+})	×	×	×	×
L8(Cu^{2+})	×	×	×	×
L9(Cu^{2+})	×	×	√	√
L10(Cu^{2+})	×	×	×	×
L11(Cu^{2+})	√	√	×	√

√ Bacterial growth inhibition × No bacterial growth inhibition

4.5.2 Disc diffusion antibacterial activity of ligands and metal complexes

The antibacterial activity of the ligands and metal complexes was determined by means of the agar disc diffusion method. Antibacterial activity testing of the ligands and metal complexes was conducted using concentrations in the range of 0.63 – 10 mg/mL. The clear zones of inhibition were measured in mm. The bacteria demonstrated a concentration-dependent susceptibility to both the ligands and metal complexes. DMSO (5%) served as a negative control and the antibiotics Vancomycin

(30 µg) and Rifampicin (5 µg) served as the positive controls for gram-negative and gram-positive bacteria, respectively. Also, as expected, no inhibition zones were noted for the negative control (5% DMSO).

Table 11 shows that all the ligands that inhibited the growth *S. aureus* had activity even at the lowest concentration tested (0.63 mg/mL), with clear zones in the range of 7.0 – 9.0 mm. This further suggests that *S. aureus* was highly susceptible to the ligands. L9 and L10 had the highest inhibition zones of 9.0 ± 0.6 and 9.0 ± 0.0 mm at the lowest concentration tested, which indicates significant antibacterial activity.

Table 11. Antibacterial activity of ligands against *S. aureus.*

Concentration (mg/mL)	**Zone of inhibition (mm)**						
	L4	**L6**	**L7**	**L8**	**L9**	**L10**	**L11**
0.63	7.0 ± 0.0	7.0 ± 0.0	8.0 ± 1.0	8.0 ± 1.2	9.0 ± 0.6	9.0 ± 0.0	8.0 ± 0.6
1.25	8.0 ± 0.6	7.0 ± 0.6	10.0 ± 0.6	8.0 ± 0.6	9.0 ± 0.6	9.0 ± 0.0	9.0 ± 1.0
2.5	9.0 ± 0.6	8.0 ± 0.0	10.0 ± 0.0	8.0 ± 0.6	9.0 ± 0.0	9.0 ± 0.0	9.0 ± 0.6
5	10.0 ± 0.0	10.0 ± 1.2	11.0 ± 0.6	9.0 ± 0.6	9.0 ± 0.6	10.0 ± 0.6	10.0 ± 0.6
10	10.0 ± 0.6	10.0 ± 0.6	11.0 ± 0.0	10.0 ± 0.6	9.0 ± 0.6	10.0 ± 0.6	10.0 ± 0.6

The data is presented as ± standard deviation where n = 3. Inhibition zone of the standard Rifampicin = 24 mm.

Based on the results in **Table 12**, the greatest zone of inhibition displayed by the ligands in this study recorded for *N. gonorrhoea* was 12.0 ± 1.2 mm, which was exhibited by L5 at a concentration of 10 mg/mL. However, L7 and L11 displayed the greatest zone of inhibition (8.00 mm) at the lowest concentration tested. On the other hand, *N. gonorrhoea* was not susceptible to L4, L5, and L6 at the lowest concentration (0.63 mg/mL), nor was it inhibited by L4 and L6 at 1.25 mg/mL.

Table 12. Antibacterial activity of ligands against *N. gonorrhoea*.

Concentration	**Zone of inhibition (mm)**						
(mg/mL)	**L4**	**L5**	**L6**	**L7**	**L9**	**L10**	**L11**
0.63	-	-	-	8.0 ± 0.0	7.0 ± 0.6	7.0 ± 0.6	8.0 ± 0.0
1.25	-	7.0 ± 0.6	-	8.0 ± 1.0	8.0 ± 0.6	9.0 ± 0.0	8.0 ± 0.0
2.5	7.0 ± 0.6	8.0 ± 1.2	7.0 ± 0.0	9.0 ± 1.2	10.0 ± 0.0	9.0 ± 0.6	9.0 ± 0.0
5	8.0 ± 0.00	10.0 ± 1.0	7.0 ± 0.0	9.0 ± 0.6	10.0 ± 0.6	10.0 ± 0.6	9.0 ± 1.0
10	11.0 ± 0.6	12.0 ± 1.2	8.0 ± 0.0	10.0 ± 0.6	11.0 ± 0.6	11.0 ± 1.0	10.0 ± 0.0

(-) denotes no inhibition zone. The data is presented as ± standard deviation where n = 3. Inhibition zone of the standard Vancomycin = 23 mm.

A summary of the antibacterial activity of the ligands tested against *S. mutans* is provided in **Table 13**. The greatest bacterial growth inhibition was recorded for L6, with inhibition zones of 10.0 ± 0.0 and 14.0 ± 0.3 mm at the lowest (0.63 mg/mL) and highest (10.0 mg/mL) concentrations tested, respectively. The results also show that only L6 inhibited the bacterial growth of *S. mutans* at lower concentrations of 0.63 and 1.25 mg/mL. This is an indication that L6 demonstrated the best antibacterial activity against *S. mutans* in comparison to the other ligands tested in this study.

Table 13. Antibacterial activity of ligands against *S. mutans*.

Concentration (mg/mL)	**Zone of inhibition (mm)**			
	L6	**L9**	**L10**	**L11**
0.63	10.0 ± 0.0	-	-	-
1.25	11.0 ± 0.1	-	-	-
2.5	11.0 ± 0.0	-	7.0 ± 0.6	8.0 ± 0.0
5	12.0 ± 0.0	7.0 ± 0.6	9.0 ± 0.0	9.0 ± 0.0
10	14.0 ± 0.3	9.0 ± 0.6	9.0 ± 0.6	10.0 ± 0.6

(-) denotes no inhibition zone. The data is presented as ± standard deviation where n = 3. Inhibition zone of the standard Rifampicin = 18 mm.

As shown in **Table 14**, the greatest zone of inhibition recorded for ligands tested against *E. coli* in this study was 10.0 ± 0.6 mm, which was exhibited by L9 and L11 at a concentration of 10 mg/mL. However, the results show that L9, L10, and L11 had no antibacterial activity against *E. coli* at concentrations ≤ 1.25 mg/mL. Furthermore, L10 and L11 did not display antibacterial activity at a concentration of 2.5 mg/mL either.

Table 14. Antibacterial activity of ligands against *E. coli.*

Concentration	**Zone of inhibition (mm)**		
(mg/mL)	**L9**	**L10**	**L11**
0.63	-	-	-
1.25	-	-	-
2.5	8.0 ± 0.6	-	-
5	9.0 ± 1.0	7.0 ± 0.0	8.0 ± 0.0
10	10.0 ± 0.6	9.0 ± 0.0	10.0 ± 0.6

(-) denotes no inhibition zone. The data is presented as ± standard deviation where n = 3. Inhibition zone of the standard Vancomycin = 11 mm.

To sum up the antibacterial activity of the ligands, it was noted that all of the bacteria species tested in the present study were susceptible to L9, L10, and L11. However, amongst all of the tested bacteria species, *S. aureus* was highly susceptible to the ligands. This is justifiable by the fact that all of the ligands that displayed antibacterial activity against *S. aureus* inhibited the growth of this bacterium even at the lowest concentration tested (0.63 mg/mL). Besides, even L8 that did not prove to have any antibacterial activity against *E. coli, S. mutans,* and *N. gonorrhoea* did inhibit the growth of *S. aureus*. The greatest recorded zone of inhibition by ligands was that of L6 against *S. mutans,* with inhibition zones of 10.0 ± 0.0 and 14.0 ± 0.3 mm at the lowest (0.63 mg/mL) and highest (10.0 mg/mL) concentrations tested,

respectively. Minimum inhibitory concentrations for all ligands that demonstrated antibacterial activity were found to be > 10 mg/mL, which was the highest concentration at which the ligands tested.

4.5.3 Antibacterial activity of nickel (II) metal complexes

The antibacterial activity of the ligands was enhanced upon chelation of ligands with Cu^{2+} and Ni^{2+} metal ions. The metal complexes displayed a concentration-dependent antibacterial activity.

It was observed that only nickel metal complexes of L5 and L6 displayed antibacterial activity against *S. aureus*. Based on the zones of inhibition displayed in **Table 15**, L6(Ni^{2+}) inhibited the growth of *S. aureus* better than L5(Ni^{2+}), which signifies that the antibacterial activity of L6(Ni^{2+}) against *S. aureus* was greater than that of L5(Ni^{2+}).

Table 15. Antibacterial activity of nickel (II) metal complexes against *S. aureus*.

Concentration (mg/mL)	**Zone of inhibition (mm)**	
	L5(Ni^{2+})	**L6(Ni^{2+})**
0.63	-	-
1.25	-	10.0 ± 0.6
2.5	8.0 ± 0.0	13.0 ± 0.3
5	8.0 ± 0.3	13.0 ± 0.6
10	9.0 ± 0.6	14.0 ± 1.0

(-) denotes no inhibition zone. The data is presented as ± standard deviation where n = 3. Inhibition zone of the standard Rifampicin = 24 mm.

As indicated in **Table 16**, the nickel metal complex that exhibited the best antibacterial activity against *N. gonorrhoea* in this study was L9(Ni^{2+}). The least antibacterial activity was observed for L6(Ni^{2+}), which only inhibited the growth of *N. gonorrhoea* at the highest concentration tested (10 mg/mL).

Table 16. Antibacterial activity of nickel (II) metal complexes against *N. gonorrhoea*.

Concentration	**Zone of inhibition (mm)**			
(mg/mL)	**L5(Ni^{2+})**	**L6(Ni^{2+})**	**L9(Ni^{2+})**	**L10(Ni^{2+})**
0.63	-	-	8.0 ± 0.0	-
1.25	-	-	9.0 ± 0.7	8.0 ± 0.7
2.5	8.0 ± 0.6	-	9.0 ± 0.7	8.0 ± 0.0
5	8.0 ± 0.3	-	9.0 ± 0.0	8.0 ± 0.0
10	9.0 ± 0.6	9.0 ± 0.6	9.0 ± 0.6	8.0 ± 0.6

(-) denotes no inhibition zone. The data is presented as ± standard deviation where n = 3. Inhibition zone of the standard Vancomycin = 23 mm.

The bacterium strain of *S. mutans* used in this study was only susceptible to one of nickel (II) metal complexes, namely L6(Ni^{2+}). The zones of inhibition recorded in **Table 17** indicate that L6(Ni^{2+}) was able to inhibit the visible growth of *S. mutans* with inhibition zones ranging up to 16 ± 0.1 mm at a concentration of 10 mg/mL.

Table 17. Antibacterial activity of L6(Ni^{2+}) against *S. mutans*.

Concentration (mg/mL)	**Zone of inhibition (mm)**
0.63	-
1.25	9.0 ± 0.6
2.5	13.0 ± 0.0
5	14.0 ± 0.3
10	16.0 ± 0.1

(-) denotes no inhibition zone. The data is presented as ± standard deviation where n = 3. Inhibition zone of the standard Rifampicin = 18 mm.

The results in **Table 18** show that only nickel metal complexes of L5, L6, and L10 demonstrated antibacterial activity against *E. coli*. The greatest zone of inhibition measured 9.0 mm, which was recorded for L6(Ni^{2+}). However, none of the aforementioned metal complexes inhibited the growth of *E. coli* at concentrations ≤ 1.25 mg/mL.

Table 18. Antibacterial activity of nickel (II) metal complexes against *E. coli*.

Concentration	**Zone of inhibition (mm)**		
(mg/mL)	**L5(Ni^{2+})**	**L6(Ni^{2+})**	**L10(Ni^{2+})**
0.63	-	-	-
1.25	-	-	-
2.5	-	-	7.0 ± 0.0
5	8.0 ± 0.0	9.0 ± 0.6	8.0 ± 1.0
10	8.0 ± 0.3	9.0 ± 1.0	8.0 ± 0.0

(-) denotes no inhibition zone. The data is presented as ± standard deviation where n = 3. Inhibition zone of the standard Vancomycin = 11 mm.

The antibacterial activity results of nickel (II) metal complexes generated in this study indicate that L6(Ni^{2+}) was active against all of the bacteria strains. *N. gonorrhoea* was more susceptible to the nickel metal complexes as compared to other bacteria used in this study. This is attributed to the fact that the growth of this bacterium was inhibited by four of the tested nickel metal complexes, with zones of inhibition observed even at the lowest concentration tested (0.63 mg/mL). In contrast, *S. mutans* demonstrated the least sensitivity to the nickel (II) metal complexes as compared to other bacteria species, as the growth of *S. mutans* was only inhibited by L6(Ni^{2+}).

4.5.4 Antibacterial activity of copper (II) metal complexes

The following results were generated from the antibacterial activity evaluation of copper (II) metal complexes in the present study. The antibacterial activity was noted to be concentration-dependent.

As indicated in **Table 19**, only copper (II) metal complexes of L4, L5, L6, and L11 exhibited antibacterial activity against *S. aureus*. The greatest bacterial growth inhibition by copper (II) metal complexes recorded for *S. aureus* was 11.0 mm, which was displayed by both L4(Cu^{2+}) and L5(Cu^{2+}) at a concentration of 10 mg/mL. Besides, all of the nickel metal complexes tested against *S. aureus* showed antibacterial activity even at the lowest concentration tested (0.63 mg/mL), with the exception of L6(Cu^{2+}).

Table 19. Antibacterial activity of copper (II) metal complexes against *S. aureus*.

Concentration	**Zone of inhibition (mm)**			
(mg/mL)	**L4(Cu^{2+})**	**L5(Cu^{2+})**	**L6(Cu^{2+})**	**L11(Cu^{2+})**
0.63	8.0 ± 0.7	10.0 ± 0.5	-	8.0 ± 0.7
1.25	9.0 ± 1.4	10.0 ± 0.5	8.0 ± 0.6	8.0 ± 0.0
2.5	9.0 ± 0.7	10.0 ± 0.6	8.0 ± 0.3	8.0 ± 0.4
5	10.0 ± 0.7	10.0 ± 0.3	9.0 ± 0.0	9.0 ± 0.7
10	11.0 ± 1.4	11.0 ± 0.7	9.0 ± 0.6	9.0 ± 0.0

(-) denotes no inhibition zone. The data is presented as ± standard deviation where n = 3. Inhibition zone of the standard Rifampicin = 24 mm.

The results in **Table 20** are an indication that copper (II) metal complexes demonstrated good antibacterial activity against *N. gonorrhoea* which is evident from zones of inhibitions that ranged up to 9.0 mm at the lowest concentration tested (0.6 mg/mL). In addition, it is only L6(Cu^{2+}) that did not demonstrate antibacterial activity against *N. gonorrhoea* at the lowest concentration tested. The greatest zone of inhibition by copper (II) metal complexes recorded for *N. gonorrhoea* was 10.0 mm which was exhibited by L4(Cu^{2+}), L5(Cu^{2+}), and L9(Cu^{2+}) at a concentration of 10 mg/mL.

Table 20. Antibacterial activity of copper (II) metal complexes against *N. gonorrhoea*.

Concentration (mg/mL)	**Zone of inhibition (mm)**				
	L4(Cu^{2+})	**L5(Cu^{2+})**	**L6(Cu^{2+})**	**L9(Cu^{2+})**	**L11(Cu^{2+})**
0.63	8.0 ± 0.0	9.0 ± 0.3	-	8.0 ± 0.7	8.0 ± 0.0
1.25	8.0 ± 0.7	9.0 ± 0.5	-	8.0 ± 0.0	8.0 ± 1.1
2.5	9.0 ± 0.7	10.0 ± 0.0	8.0 ± 0.3	8.0 ± 0.0	8.0 ± 0.0
5	9.0 ± 0.3	10.0 ± 0.3	8.0 ± 0.0	9.0 ± 1.1	8.0 ± 0.0
10	10.0 ± 0.3	10.0 ± 0.6	8.0 ± 0.0	10.0 ± 0.7	9.0 ± 1.4

(-) denotes no inhibition zone. The data is presented as ± standard deviation where n = 3. Inhibition zone of the standard Vancomycin = 23 mm.

The copper (II) metal complexes tested against *S. mutans* exhibited significant antibacterial activity against this bacterium. This is evident from zones of inhibitions that ranged up to 9.0 mm at the lowest concentration tested, as indicated in **Table 21**. However, L4(Cu^{2+}) and L11(Cu^{2+}) did not show antibacterial activity against *S. mutans* at the lowest concentration tested. The greatest zone of inhibition recorded for copper (II) metal complexes was 13.0 mm, which was exhibited by L6(Cu^{2+}) at a concentration of 10 mg/mL.

Table 21. Antibacterial activity of copper (II) metal complexes against *S. mutans*.

Concentration (mg/mL)	**Zone of inhibition (mm)**			
	L4(Cu^{2+})	**L5(Cu^{2+})**	**L6(Cu^{2+})**	**L11(Cu^{2+})**
0.63	-	9.0 ± 0.7	9.0 ± 1.0	-
1.25	8.0 ± 0.7	9.0 ± 0.3	10.0 ± 0.3	8.0 ± 0.4
2.5	8.0 ± 1.0	10.0 ± 0.6	10.0 ± 0.6	8.0 ± 0.4
5	9.0 ± 0.7	10.0 ± 0.0	11.0 ± 0.6	9.0 ± 1.1
10	10.0 ± 0.7	11.0 ± 1.0	13.0 ± 0.3	10.0 ± 0.7

(-) denotes no inhibition zone. The data is presented as ± standard deviation where n = 3. Inhibition zone of the standard Rifampicin = 18 mm.

As indicated in **Table 22**, the antibacterial activity of copper (II) metal complexes against *E. coli* was significant. This is evident from zones of inhibitions that ranged up to 10.0 mm at the lowest concentration tested (0.63 mg/mL), although L9(Cu^{2+}) did not display any antibacterial activity against *E. coli* at concentrations ≤ 2.5 mg/mL. The greatest zone of inhibition by copper (II) metal complexes recorded for *E. coli* was 14.0 mm which was exhibited by L6(Cu^{2+}) at a concentration of 10 mg/mL.

Table 22. Antibacterial activity of copper (II) metal complexes against *E. coli*.

Concentration (mg/mL)	**Zone of inhibition (mm)**				
	L4(Cu^{2+})	**L5(Cu^{2+})**	**L6(Cu^{2+})**	**L9(Cu^{2+})**	**L11(Cu^{2+})**
0.63	8.0 ± 0.7	10.0 ± 0.0	10.0 ± 0.3	-	8.0 ± 0.0
1.25	8.0 ± 0.0	10.0 ± 0.6	10.0 ± 0.6	-	9.0 ± 0.7
2.5	8.0 ± 0.7	11.0 ± 0.6	10 ± 0.0	-	9.0 ± 0.7
5	9.0 ± 0.7	11.0 ± 0.0	11.0 ± 0.0	8.0 ± 0.0	9.0 ± 0.4
10	10.0 ± 0.3	12.0 ± 0.0	14.0 ± 0.6	9.0 ± 0.7	9.0 ± 0.4

(-) denotes no inhibition zone. The data is presented as ± standard deviation where n = 3. Inhibition zone of the standard Vancomycin = 11 mm.

The antibacterial activity results of copper (II) metal complexes generated in this study indicate that all the bacteria strains were susceptible to copper (II) metal complexes of L4, L5, L6, and L11. The greatest recorded zone of inhibition by copper (II) metal complexes was 14.0 mm, exhibited by L6(Cu^{2+}) against *E. coli* at a concentration of 10 mg/mL.

4.5.5 Minimum inhibitory concentrations

The minimum concentrations required to inhibit the visible growth of the bacteria that were susceptible to the different metal complexes are given in **Table 23**. MIC values of metal complexes varied based on the bacteria, as well as the type of metal complex. Based on the MIC values as summarized in **Table 23**, copper (II) metal complexes exhibited the best antibacterial activity in this study, as compared to the ligands and nickel (II) metal complexes. However, the ligands demonstrated the least antibacterial activity, with MIC values greater than 10 mg/mL, which was the highest concentration at which antibacterial activity was tested.

Table 23. MIC values for antibacterial activity of metal complexes.

	Minimum inhibitory concentration (mg/mL)			
Metal complex	***N. gonorrhoea***	***E. coli***	***S. aureus***	***S. mutans***
L4(Cu^{2+})	5	2.5	10	2.5
L5(Cu^{2+})	5	>10	>10	2.5
L5(Ni^{2+})	>10	N/A	>10	N/A
L6(Cu^{2+})	10	10	10	5
L6(Ni^{2+})	>10	10	2.5	>10
L9(Cu^{2+})	>10	>10	N/A	N/A
L9(Ni^{2+})	>10	N/A	N/A	N/A
L10(Ni^{2+})	>10	10	N/A	N/A
L11(Cu^{2+})	N/A	2.5	5	2.5

N/A: Implies that a bacterium was not susceptible to the metal complex

4.6 Antioxidant activity of ligands and metal complexes

The antioxidant activity of the ligands and their metal complexes was determined using the DPPH free radical scavenging and ferric reducing power assays. For both assays, the ligands and metal complexes showed varying concentration-dependent antioxidant activity. IC_{50} values were calculated to determine the concentration of the ligands/metal complexes required to inhibit 50% of the DPPH free radical, whereby the lower the IC_{50} value, the higher the antioxidant activity of the ligand/metal complex.

4.6.1 DPPH free radical scavenging activity of ligands

The results of the antioxidant activity of the ligands tested in this study are given in **Figure 4A and B**. The ligands demonstrated a concentration-dependent DPPH free radical scavenging activity. The IC_{50} values for the ligands as displayed in **Table 24** indicate that L4 and L5 exhibited the lowest IC_{50} values of 2.11 ± 0.3 and 2.55 ± 0.3 µg/mL respectively, signifying better antioxidant activity as compared to the other ligands analysed in this study. The standard vitamin C (Vit C) had an IC_{50} value of 1.96 ± 0.6 µg/mL.

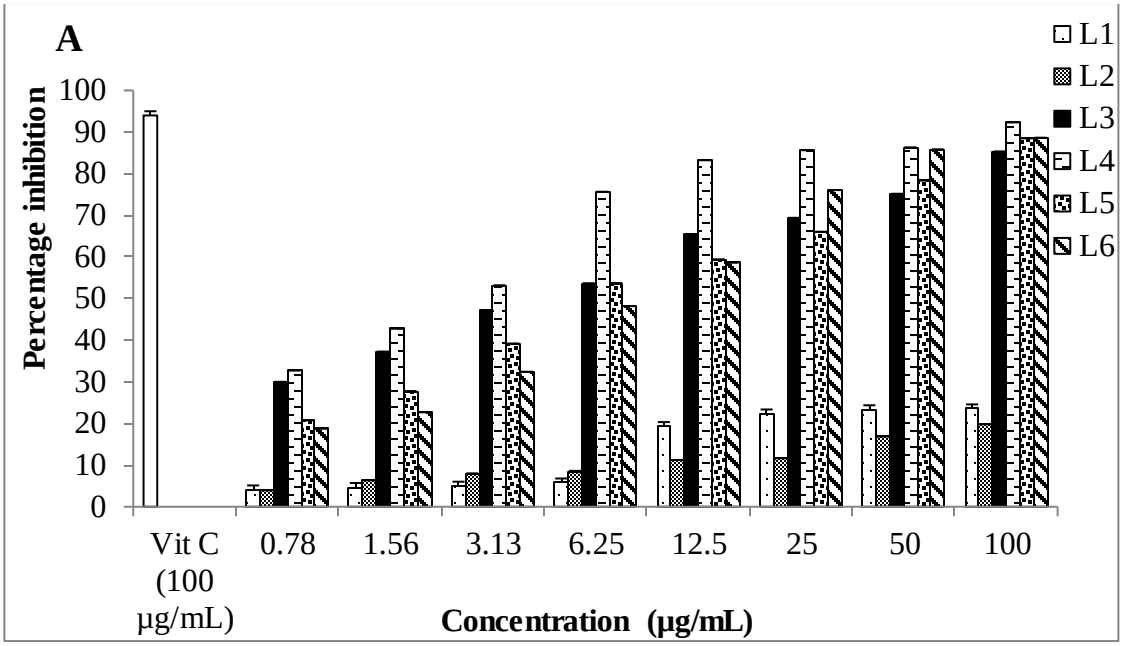

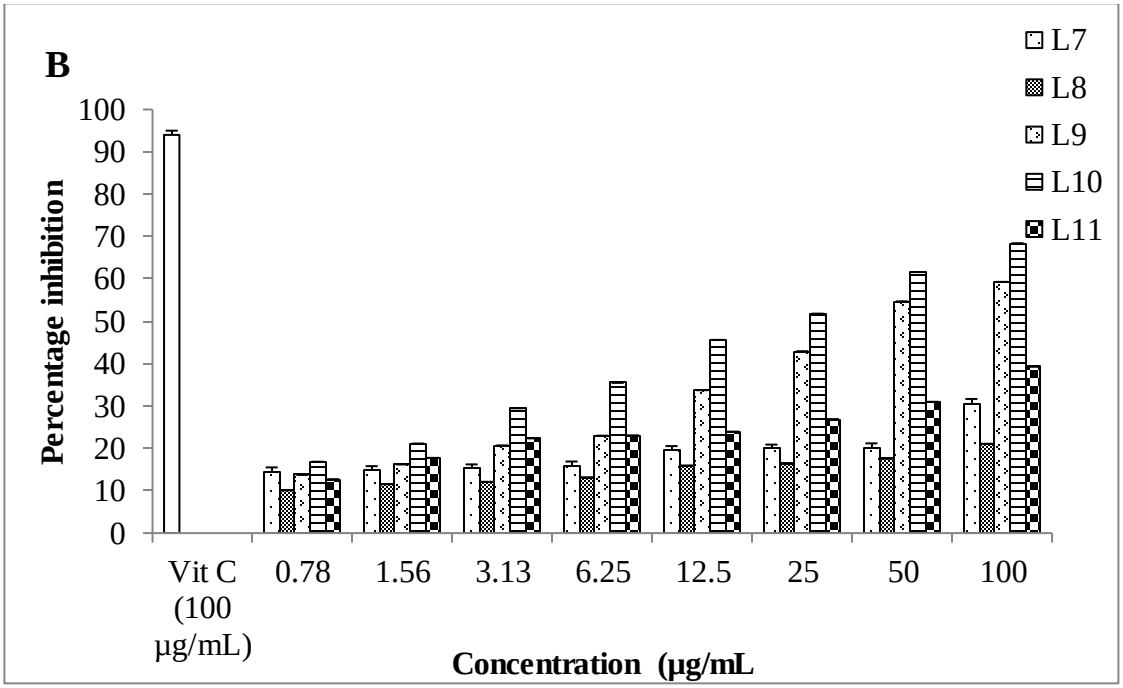

Figure 4. DPPH free radical scavenging activity of L1-L6 (A) and L7-L11 (B). The data represents the mean of replicas where n=3. Vitamin C was used as a standard control and error bars are based on SEM.

The IC_{50} values for the ligands analysed for antioxidant activity in the present study are presented in **Table 24**. A comparable free radical scavenging activity was observed between the ligands and the standard, Vitamin C. IC_{50} values of ligands ranged between 2.11 - 22.93 µg/mL. However, the IC_{50} values for L1, L2, L7, L8, and L11 was found to be greater than 100 µg/mL, which was the highest concentration tested in this study.

Table 24. The least concentration of ligands required to scavenge 50% of DPPH free radicals.

Ligand	**IC_{50} (µg/mL) ± SEM**
L1	> 100
L2	> 100
L3	4.26 ± 1.80
L4	2.11 ± 0.30
L5	2.55 ± 0.30
L6	7.00 ± 1.20
L7	> 100
L8	> 100
L9	22.93 ± 2.70
L10	19.86 ± 3.30
L11	> 100
Vitamin C	1.96 ± 0.60

4.6.2 DPPH free radical scavenging activity of metal complexes

Figure 5A and B show the DPPH free radical scavenging activity of the nickel (II) metal complexes presented as percentage inhibition. The IC_{50} values presented in **Table 25** indicate that, L4(Ni^{2+}) and L3(Ni^{2+}) exhibited the lowest IC_{50} values of 1.33 ± 0.30 and 1.64 ± 0.40 µg/mL, respectively, even lower than that of the standard vitamin C (IC_{50} = 1.96 ± 0.60 µg/mL).

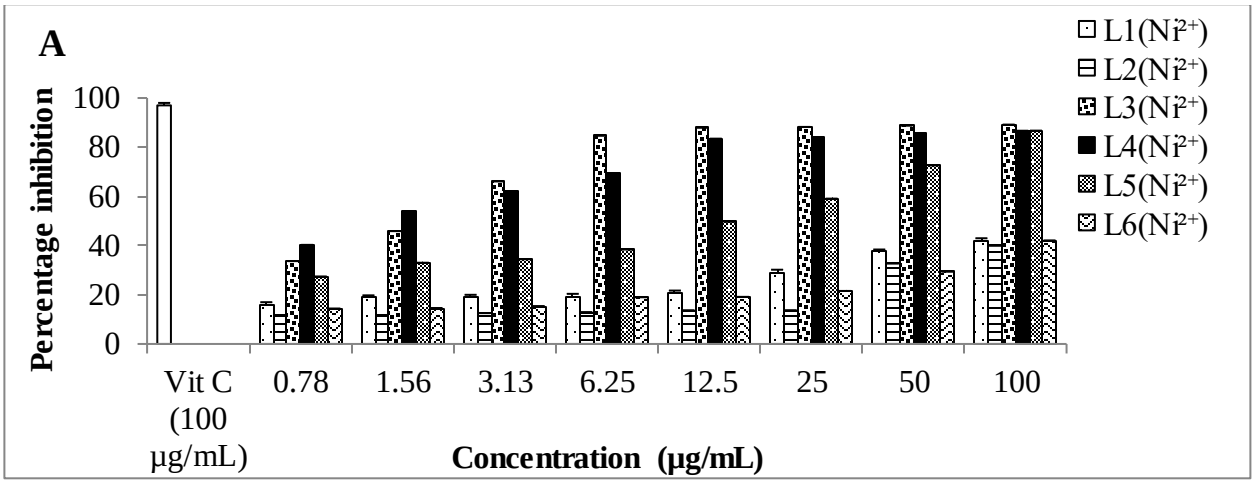

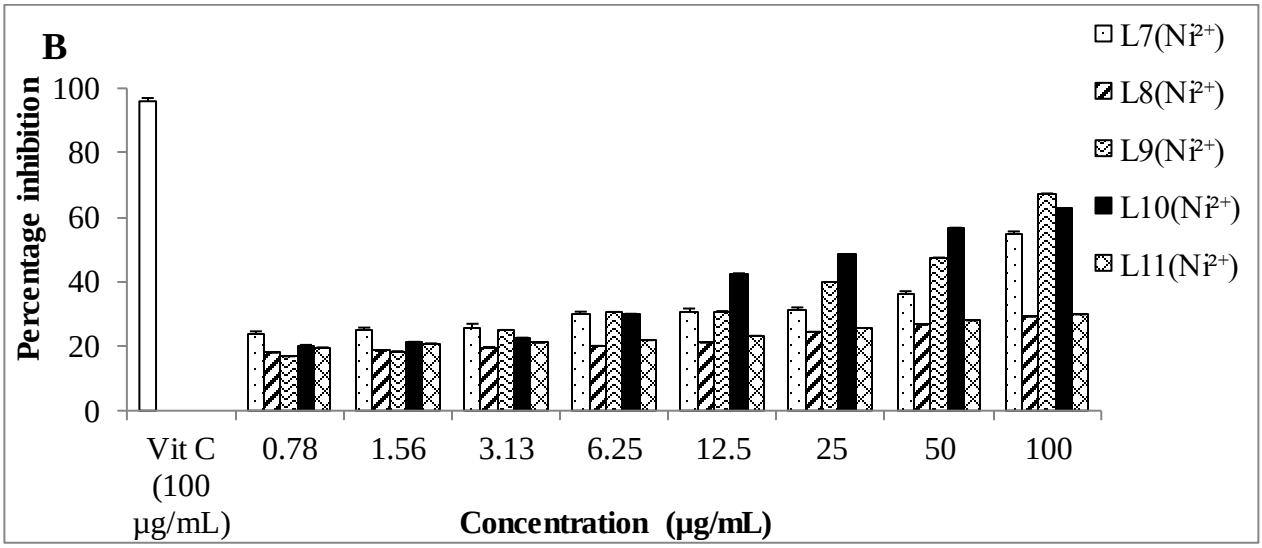

Figure 5. DPPH free radical scavenging activity of nickel (II) metal complexes for L1-L6 (A) and L7-L11 (B) presented as a mean of replicas where n=3. Vitamin C was used as a standard control and error bars are based on SEM.

The IC_{50} values for nickel (II) metal complexes are specified in **Table 25**. IC_{50} values ranged between 1.33 - 33.92 µg/mL. On the contrary, nickel (II) metal complexes of L1, L2, L6, L7, L8, and L11 displayed IC_{50} values greater than 100 µg/mL, which is the highest concentration at which nickel metal complexes in this study were tested.

Table 25. The least concentration of nickel (II) metal complexes required to scavenge 50% of DPPH free radicals.

Metal complex	**IC_{50} (µg/mL) ± SEM**
L1(Ni^{2+})	> 100
L2(Ni^{2+})	> 100
L3(Ni^{2+})	1.64 ± 0.40
L4(Ni^{2+})	1.33 ± 0.30
L5 (Ni^{2+})	9.37 ± 2.10
L6(Ni^{2+})	> 100
L7(Ni^{2+})	> 100
L8(Ni^{2+})	> 100
L9 (Ni^{2+})	33.92 ± 3.70
L10 (Ni^{2+})	28.56 ± 4.10
L11(Ni^{2+})	> 100
Vitamin C	1.96 ± 0.60

The DPPH free radical scavenging activity of copper (II) metal complexes is presented in **Figure 6A and B** whereby $L3Cu^{2+}$ significantly exhibited the highest % inhibition against DPPH free radicals ($p > 0.05$). In addition, it is evident from the IC_{50} values of copper (II) complexes in **Table 26** that $L3(Cu^{2+})$ exhibited the lowest IC_{50} value (1.36 ± 0.40 µg/mL), even lower than that of the standard vitamin C which is reported as 1.96 ± 0.60 µg/mL.

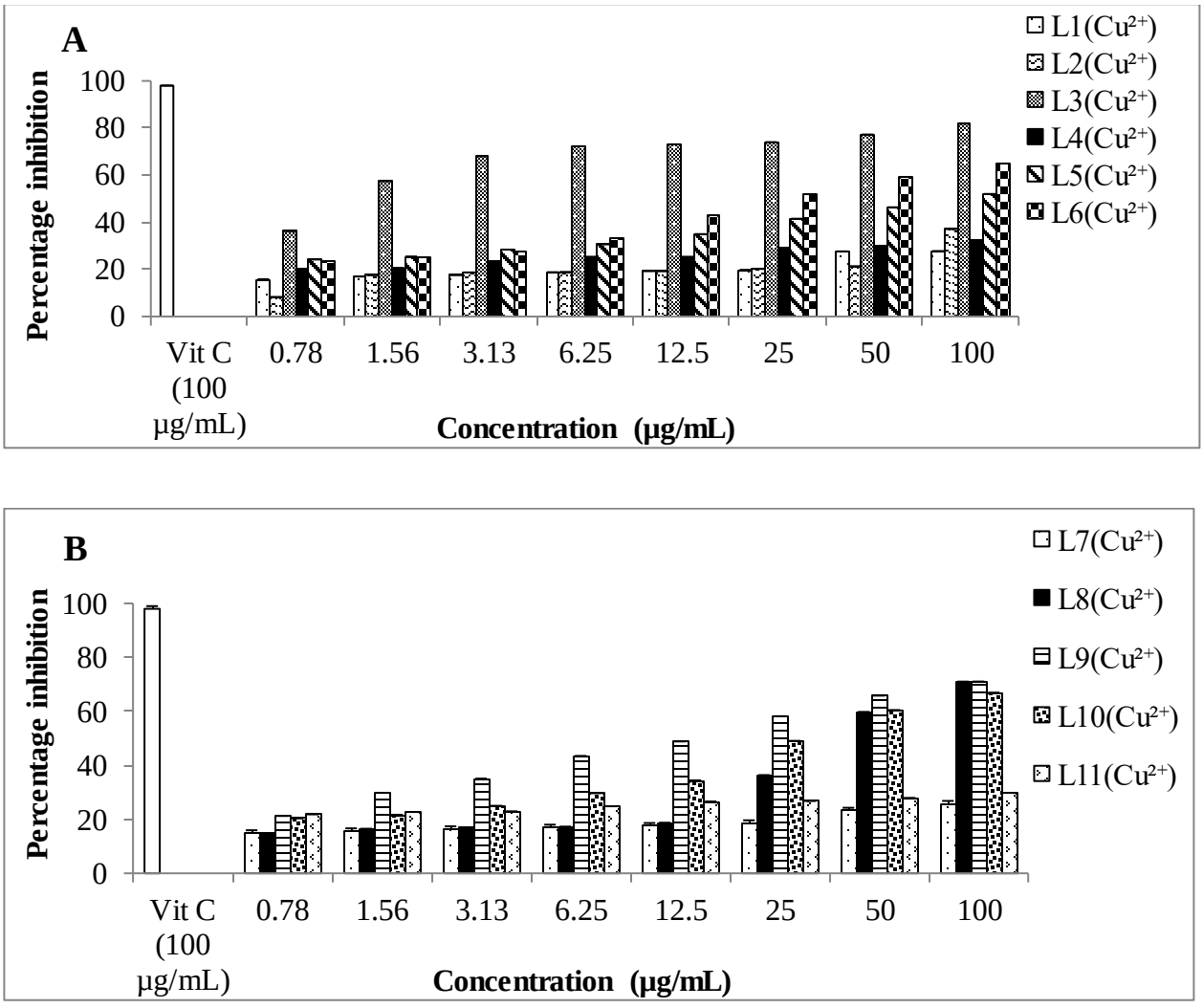

Figure 6. DPPH free radical scavenging activity of copper (II) complexes for L1-L6 (A) and L7-L11 (B) presented as a mean of replicas where n=3. Vitamin C was used as a standard control and error bars are based on SEM.

Table 26 summarizes IC_{50} values of copper (II) metal complexes. The IC_{50} values ranged between 1.36 – 85.81 µg/mL. However, the IC_{50} values for copper (II) metal complexes of L1, L2, L4, L7, and L11 were greater than 100 µg/mL, which is the highest concentration tested in this study.

Table 26. The least concentration of copper (II) complexes required to scavenge 50% DPPH free radicals.

Metal complex	IC_{50} (µg/mL) ± SEM
L1(Cu^{2+})	> 100
L2(Cu^{2+})	> 100
L3(Cu^{2+})	1.36 ± 0.40
L4(Cu^{2+})	> 100
L5(Cu^{2+})	85.81 ± 3.80
L6(Cu^{2+})	31.49 ± 1.30
L7(Cu^{2+})	> 100
L8(Cu^{2+})	38.30 ± 1.70
L9(Cu^{2+})	12.25 ± 3.30
L10(Cu^{2+})	25.49 ± 1.90
L11(Cu^{2+})	> 100
Vitamin C	1.96 ± 0.60

The results obtained from the DPPH antioxidant assay revealed that the ligands analysed in the present study showed an increase in antioxidant activity after forming complexes with Cu^{2+} and Ni^{2+} metal ions. The ligand that demonstrated the best antioxidant activity was L4, with an IC_{50} value of 2.11 ± 0.30 µg/mL. Amongst nickel (II) metal complexes, L4(Ni^{2+}) exhibited the best antioxidant activity (IC_{50} = 1.33 ± 0.30 µg/mL). However, for copper (II) complexes, L3(Cu^{2+}) displayed the best antioxidant activity with an IC_{50} value of 1.36 ± 0.40 µg/mL. Briefly, it is

evident from the IC_{50} values that in the present study, most nickel (II) metal complexes are able to scavenge 50% of DPPH free radicals at lower concentrations. This then implies that nickel (II) metal complexes demonstrated significant antioxidant activity in comparison to the non-chelated/free ligands as well as copper (II) metal complexes tested in this study.

4.6.3 Ferric reducing power of ligands and metal complexes

Most ligands and metal complexes showed an ability to donate electrons to reduce Fe^{3+} into Fe^{2+} which is indicated by the concentration-dependent increase in the absorbance values. In addition, the colour of the test solutions changed to various shades of green and blue, depending on the reducing power of each ligand/metal complex.

The ferric reducing power of the ligands is given in **Figure 7A and B**. The results show that L5 had the highest ferric reducing power with an absorbance of 0.26 ± 0.02 at the highest concentration tested (25 µg/mL), while L1 demonstrated the least ferric reducing power with an absorbance of 0.08 ± 0.01 at that concentration. The standard gallic acid (GA) produced an absorbance of 0.44 ± 0.06 at 25 µg/mL.

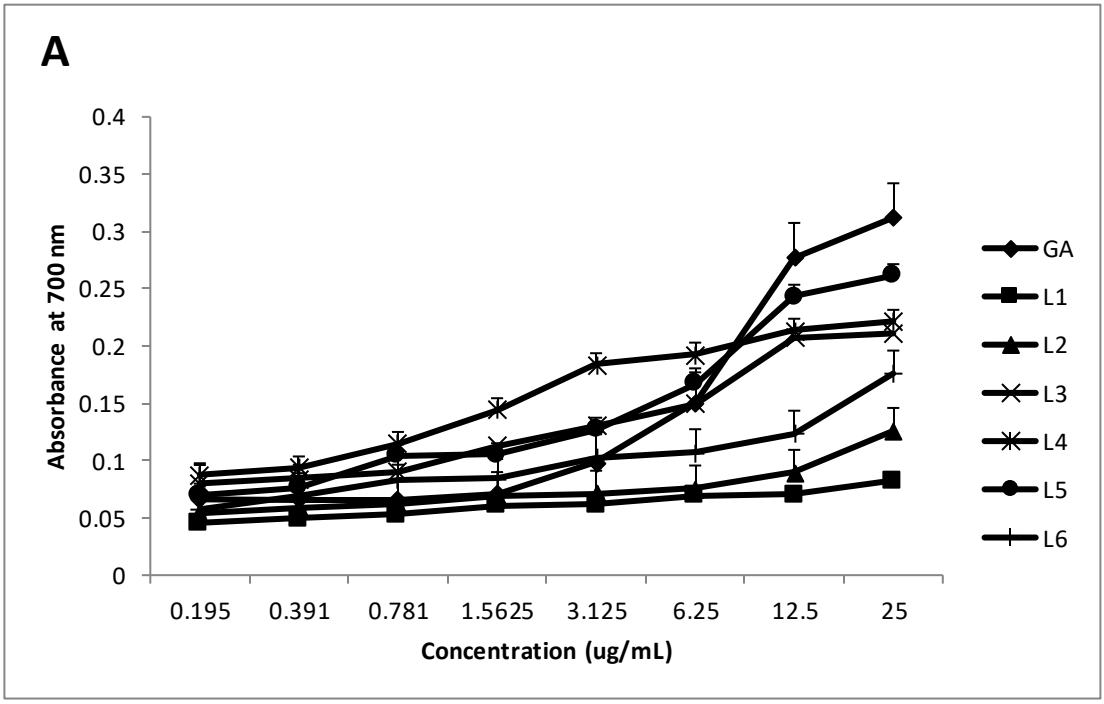

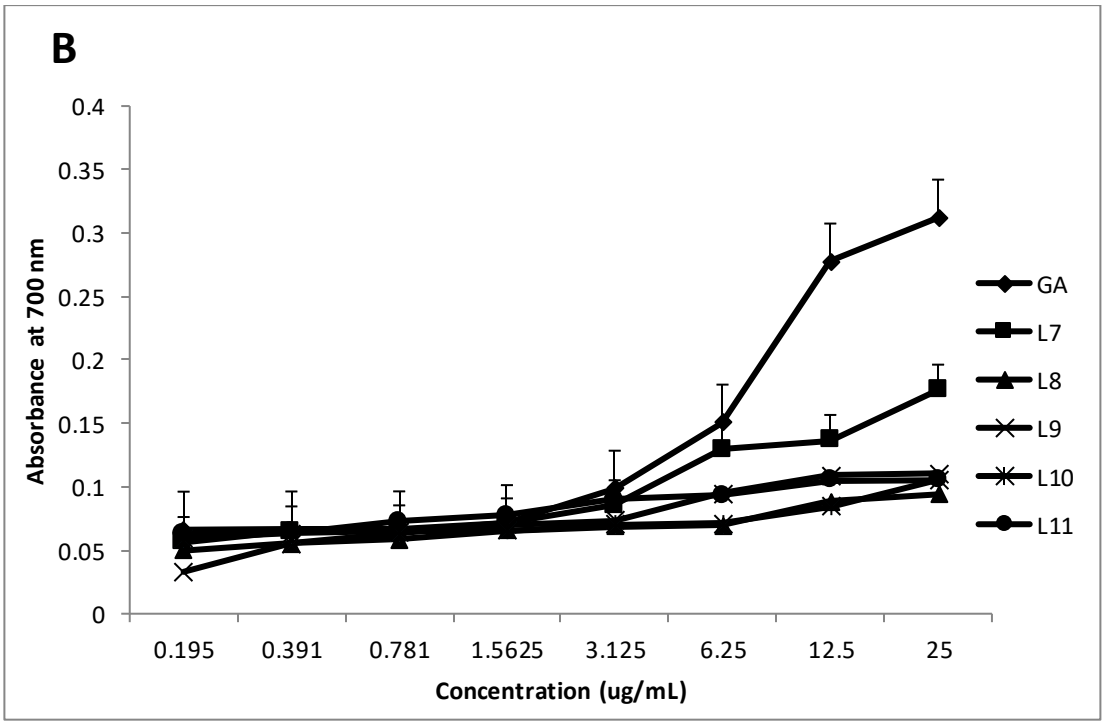

Figure 7. Ferric reducing power of L1-L6 (A) and L7-L11 (B) at concentrations of 0.195-25 µg/mL, where n=3. Standard gallic acid (GA) was used as the positive control.

The ferric reducing power of nickel (II) metal complexes is shown in **Figure 8A and B**. L3(Ni^{2+}) and L4(Ni^{2+}) significantly reduced ferric ions ($p > 0.05$), both with an absorbance value of 0.58 ± 0.02 at the highest concentration tested (25 µg/mL). The absorbance values of L3(Ni^{2+}) and L4(Ni^{2+}) was even greater than that of the standard gallic acid (0.44 ± 0.01). The lowest ferric reducing power was demonstrated by L9(Ni^{2+}) with an absorbance of 0.01 ± 0.02.

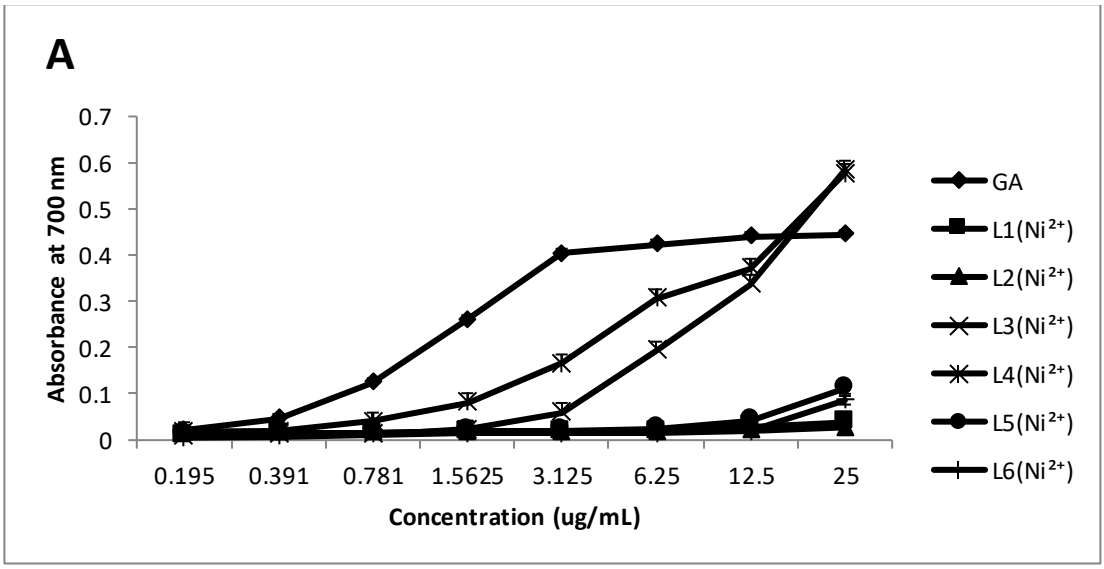

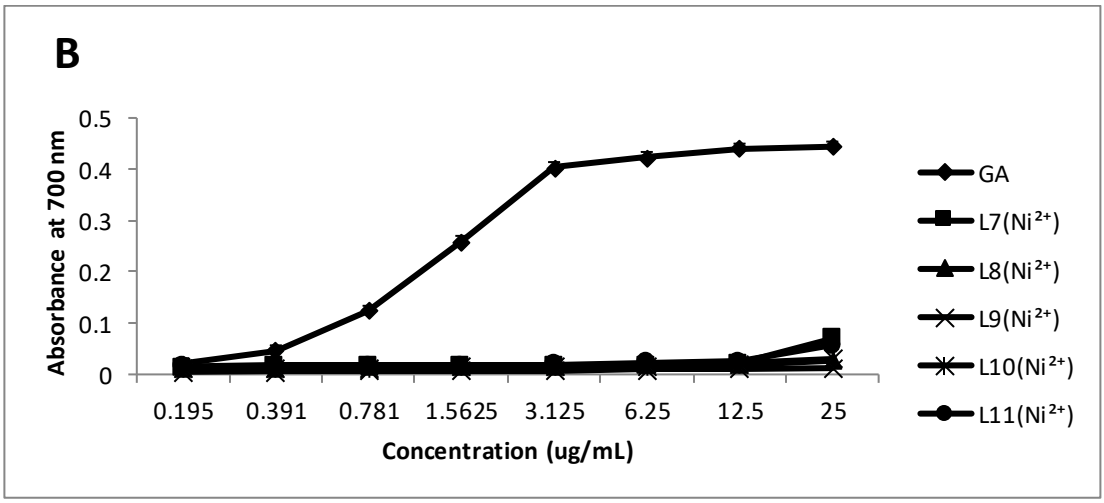

Figure 8. Ferric reducing power of nickel (II) complexes for L1-L6 (A) and L7-L11 (B). The data represents a mean of replicas where n=3. Standard gallic acid (GA) was used as the positive control.

The ferric reducing power of copper (II) complexes is presented in **Figure 9A and B**. L3(Cu^{2+}) significantly demonstrated the greatest ferric reducing power ($p > 0.05$) as this metal complex produced an absorbance of 1.60 ± 0.04 at the highest concentration tested (25 µg/mL). Frankly, the ferric reducing power of L3(Cu^{2+}) was greater than that of the standard gallic acid (GA) which was recorded as 0.44 ± 0.01 at 25 µg/mL. On the other hand, L2(Cu^{2+}) displayed the least ferric reducing power both with an absorbance of 0.02 ± 0.03 at 25 µg/mL.

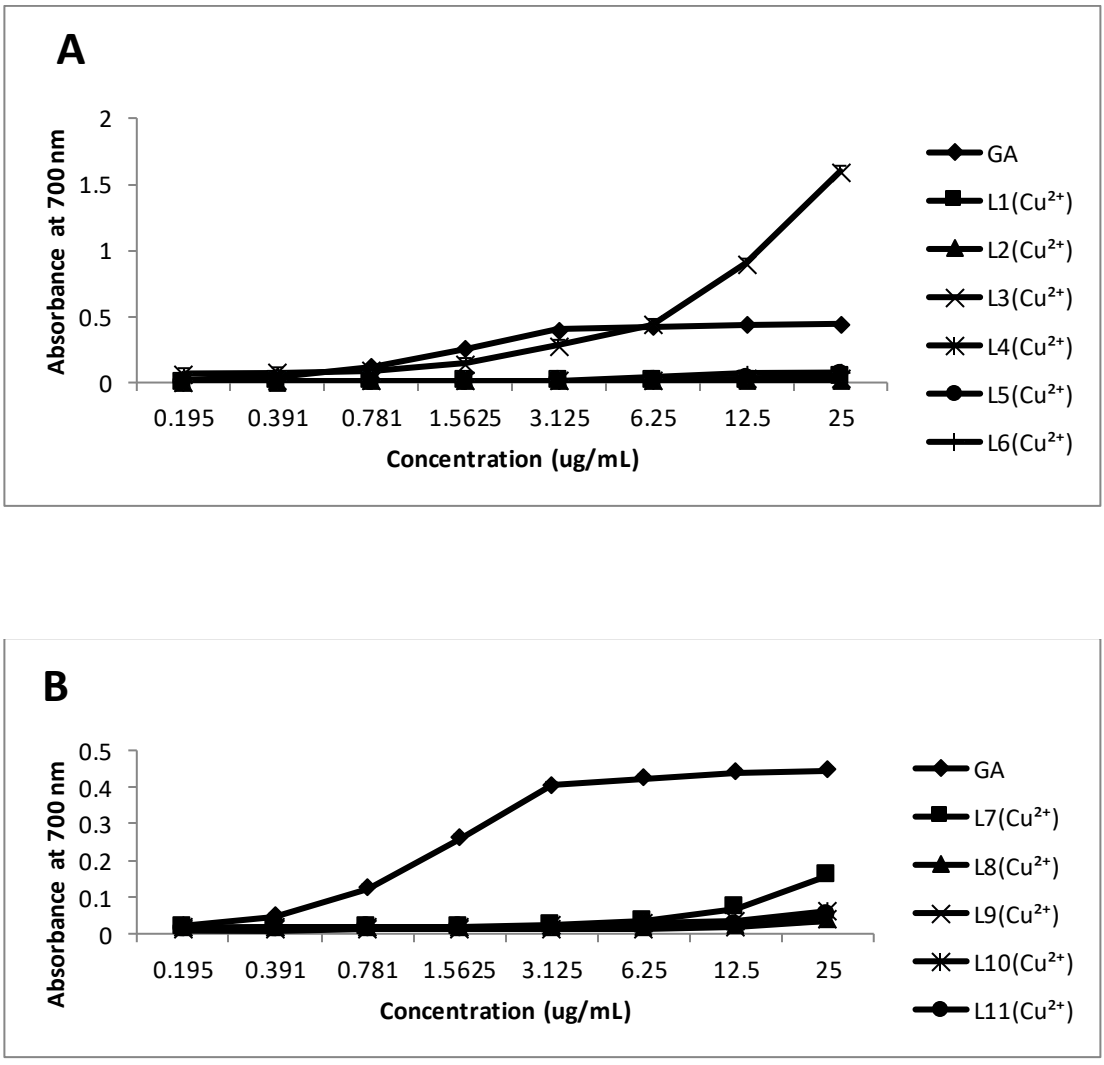

Figure 9. Ferric reducing power of copper (II) complexes for L1-L6 (A) and L7-L11 (B). The data represents a mean of replicas where n=3. Standard gallic acid (GA) was used as the positive control.

The ferric reducing power data indicates that L5 exhibited the best ferric reducing power amongst the ligands analysed in this study. On the other hand, L3(Ni^{2+}) and L4(Ni^{2+}) were the best ferric reducers amongst the nickel (II) metal complexes while L3(Cu^{2+}) demonstrated the best ferric reducing power as compared to other copper (II) metal complexes tested in this study. In a word, the present study revealed that L3(Cu^{2+}) produced higher absorbance values, making this metal complex the best ferric reducer as compared to both free ligands and nickel (II) metal complexes.

Overall, the antioxidant activity results generated in the present study are an indication that some ligands such as L3 and L4 turned out as better electron donors upon complexation with Ni^{2+} and Cu^{2+} metal ions. However, some ligands such as L5, L6, and L7 exhibited better antioxidant activity as free ligands as the activity of these ligands declined when chelated to Ni^{2+} and Cu^{2+} metal ions.

4.7 Cytotoxic activity of ligands and metal complexes against HeLa cells

In the present study, selected ligands and metal complexes that demonstrated the best antibacterial and antioxidant activity were tested for cytotoxicity using the MTT assay, against HeLa cell line. Auranofin, a known cytotoxic compound was used as a positive control. The percentage cell viability of HeLa cells reduced with an increase in concentration of compounds, and cytotoxicity data after treating HeLa cells with ligands and metal complexes for 48 h is presented in **Figure 10** as percentages. It is evident that L3, L3(Cu^{2+}), and L4(Ni^{2+}) demonstrated the lowest toxicity against HeLa cells, as these compounds did not exhibit cell viability ≤ 50 % even at the highest concentration tested. It is evident from the IC_{50} values summarized in **Table 27** that, L6 was highly toxic to HeLa cells, as indicated by a lower IC_{50} of 4.12 ± 0.60 µg/mL compared to other compounds tested in this study. The IC_{50} for the standard Auranofin was 5.04 ± 0.60 µg/mL.

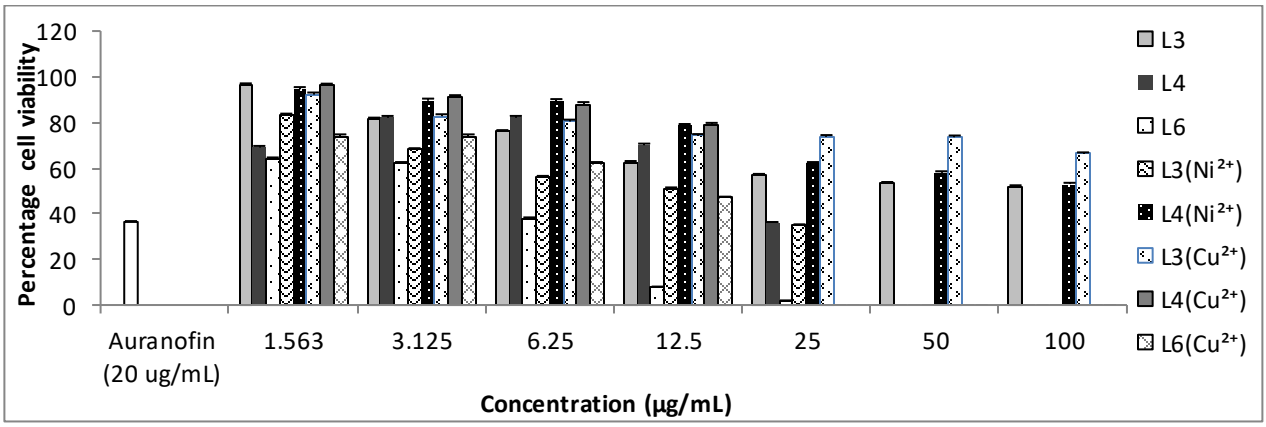

Figure 10. Percent viability of HeLa cells, after treatment for 48 h with selected ligands and metal complexes. The data represents replicas were n=3 and error bars represents mean ± SEM. Untreated cells were used as a negative control and were considered to be 100% viable. Auranofin was used as a positive control (IC_{50} = 5.04 µg/mL).

The IC_{50} values for the ligands and metal complexes analysed for cytotoxic activity in the present study are presented in **Table 27**. IC_{50} values ranged between 4.12 - 16.80 µg/mL. However, the IC_{50} values for L3, L4(Ni^{2+}), and L3(Cu^{2+}) was found to be greater than 100 µg/mL, which was the highest concentration tested in this study.

Table 27. The least concentrations of ligands and metal complexes required to exhibit cytotoxic activity against 50% of HeLa cells.

Ligand/metal complex	**IC_{50} value (µg/mL)**
L3	> 100
L4	15.32 ± 0.80
L6	4.12 ± 0.60
L3(Ni^{2+})	13.6 ± 0.80
L4(Ni^{2+})	> 100
L3(Cu^{2+})	> 100
L4(Cu^{2+})	16.8 ± 0.60
L6(Cu^{2+})	10.2 ± 0.60
Auranofin	5.04 ± 0.60

CHAPTER 5

DISCUSSION

The present study synthesized Schiff base ligands and their Ni (II) and Cu (II) metal complexes to analyse them for biological applications by determining the antibacterial, antioxidant and cytotoxic activity of the synthesized compounds. Structural confirmation of the synthesized compounds was carried out using ^{1}H NMR and FTIR techniques.

^{1}H NMR data of the free ligands confirmed the presence of different proton environments. This was evident from the generated spectra whereby peaks resonated at different chemical shifts and protons were found to be in the expected regions. Ligands and Metal complexes were subjected to FTIR spectroscopy analysis. The synthesized metal complexes exhibited azomethine bands in a lower frequency range as compared to spectral bands of free ligands. In a previous study by Awolope *et al* (192), similar bands were observed, thereby confirming metal chelation with ligands via the azomethine nitrogen. The absence of phenolic bands in the spectra of metal complexes, is an indication that metal ions of Ni^{2+} and Cu^{2+} bonded to the phenolic oxygen (139). The involvement of azomethine nitrogen and phenolic oxygen in coordination further suggests that the synthesized ligands are bidentate since they donated two pairs of electrons to a metal ion (193), which is in agreement with the stoichiometry that was used to synthesize the metal complexes in this study.

In the present study, the synthesized Schiff base ligands and metal complexes demonstrated the ability to inhibit the bacterial growth of *E. coli, N. gonorrhoea, S. aureus and S. mutans*. However, metal complexes displayed better antibacterial activity as compared to free ligands, which is explainable by Tweedy's chelation theory that, upon chelation, the polarity of metal ions is reduced thus enhancing

lipophilicity (36). Lipophilicity allows for metal ions to easily penetrate the lipid bilayer into bacterial cells (194), resulting in a disruption of normal cellular functions such as protein and nucleic acid synthesis (195), hence inhibiting bacterial growth. Furthermore, metal complexes interfere with the respiration process of bacterial cells, which leads to the inhibition of protein synthesis thus further restricting bacterial growth (196). The antibacterial results from the present study are in agreement with a study by Elaaraj *et al* (196), which reported an improved antibacterial activity of metal complexes of Ni^{2+}, Co^{2+}, Cu^{2+} and Zn^{2+} as compared to free ligands. The present study observed a similar trend whereby metal complexes of Ni^{2+} and Cu^{2+} exhibited better antibacterial activity compared to free ligands. However, the results in the present study demonstrated that metal complexes of Cu (II) exhibited higher antibacterial activity compared to Ni (II) metal complexes. This could be attributed to the fact that copper oxidizes DNA more frequently than other bivalent metal ions (197), hence better bacterial growth inhibition. A study by Aljahdali *et al* (198) produced similar antibacterial results, where by metal complexes of Cu (II) showed better antibacterial activity compared to Ni (II) metal complexes.

In this study, L 9, L10, and L11 displayed a broad-spectrum antibacterial activity, since these ligands inhibited the growth of all the bacteria species that were considered. The structures of L9, L10 and L11 have a sulfonic acid moiety, hence the broad spectrum of antibacterial activity since previous studies reported good antimicrobial activity expressed by sulfonic acid-derivatives (199). In fact, a study by Katugampala *et al* (200), revealed that sulfonated compounds do possess antimicrobial activity against most bacteria and fungi.

The antioxidant activity results obtained from this study indicate that the synthesized ligands and metal complexes serve as free radical scavengers or inhibitors. Antioxidant results in the present study also revealed an enhanced antioxidant activity of ligands upon chelation with Cu^{2+} and Ni^{2+} metal ions. According to Elaaraj *et al* (196), the formation of metal complexes results in an electron withdrawal effect of the metal ion, which leads to the release of hydrogen ions which in turn reduces free radicals. In a similar study by Hasi *et al* (201), metal complexes did indeed demonstrate better antioxidant activity as compared to free ligands. The antioxidant results obtained here are further supported by studies conducted by Sumalatha *et al* (202) and Ammar *et al* (203), which revealed that ligands were better free radical inhibitors upon chelation with metal ions including those of Cu(II) and Ni(II).

From the antioxidant activity results of metal complexes generated from this study, it is evident that overall, nickel metal complexes exhibited the best antioxidant activity as compared to copper metal complexes. The differences between antioxidant activity of Nickel and copper metal complexes is supported by Meshram *et al* (204) and Cho *et al* (205), who revealed that Nickel is a stronger reducing agent compared to copper, and has a greater tendency to loose electrons. Despite an enhanced antioxidant activity of metal complexes as compared to free ligand, L5, L6, and L7 exhibited better antioxidant activity as free ligands, as the activity of these ligands declined when chelated to Ni^{2+} and Cu^{2+} metal ions. According to Ugwu and Conradie (120), substituting hydrogen or groups on ligands has an effect on the electron donating or withdrawing properties. Formation of metal complexes in this study also involved substitution of phenolic proton, which must have hindered the electron donating ability of metal complexes of L5, L6, and L7 thereby limiting their

antioxidant activity. In a similar study by Swiderski *et al* (138), the resultant metal complexes which were synthesized by means of substitution reactions, exhibited lower antioxidant activity than the free ligands. The present study noted that, L3, L4, and L6 as well as their metal complexes demonstrated significant antibacterial and antioxidant activity. A distinctive feature of L3, L4, and L6 is the presence of a hydrazine moiety, which is known as a good reducing agent and antimicrobial agent (206,207), and could be attributed to the antioxidant and antibacterial activities observed for these ligands and their metal complexes.

In the present study, L1 and L2 as well as their metal complexes did not show antibacterial activity against the test bacteria. Molecular mass, a determinant of a compound's biological activity (208) could be the reason why these compounds did not demonstrate any antibacterial activity. According to literature reports by Aljahdali *et al* (198), large molecular masses limit the diffusion and penetration of ligands into bacterial cells. L1 and L2 had large masses of 351.41 and 301.12 g/mol respectively, which possibly limits the diffusion and penetration of the ligands into bacterial cells (198). In addition, ligands reportedly have improved biological activity when there is the presence of additional functional groups in their structures (209,210). L1 and L2 lacked additional functional groups compared to the other ligands investigated in this study, which possibly could be another reason why L1 and L2 did not demonstrate any antibacterial activity.

Cytotoxicity studies revealed that selected ligands and metal complexes exhibited a moderate cytotoxic effect on HeLa cells, which is evident from the IC_{50} values obtained. In fact, L3, L4(Ni^{2+}), and L3(Cu^{2+}) did not display % cell viability $\leq$ 50% even at the highest concentration tested, indicating preliminary safety profiles of the tested compounds (116,117). In this study, L6 displayed the greatest cytotoxic

activity against HeLa cells. The observed cytotoxicity of the selected ligands and metal complexes could be attributed to the presence of a hydrazine moiety in the structure of these compounds (206,207). This is further supported by study findings of Kandile *et al* (211), which revealed that compounds containing a hydrazine moiety displayed cytotoxicity against HeLa cells.

The present study, being the first to report on the antibacterial, antioxidant and cytotoxic activities of the synthesized ligands and their corresponding metal complexes has generated results that will contribute towards the discovery of novel compounds with biological activities. Antimicrobial resistance remains a global health threat as most microbes including bacteria no longer sufficiently respond to antimicrobials, rendering most of the existing antimicrobial agents ineffective (212,213). Most of the ligands and metal complexes in this study exhibited antibacterial activity, and thus the findings contribute to the on-going search for novel and effective antibacterial agents. Currently, most synthetic antioxidants are associated with safety concerns (4,214). The ligands and metal complexes that demonstrated antioxidant activity in this study could be potentially considered in the formulation of synthetic antioxidants, thus the antioxidant results generated from this study encourages the discovery of safer and better antioxidants. Selected ligands and metal complexes that exhibited cytotoxicity against HeLa cells suggest the possible use of these compounds as chemotherapeutic agents.

The findings from this study are evidence that the synthesized Schiff base ligands and corresponding metal complexes are promising sources of antibacterial, antioxidant, and cytotoxicity agents. In addition, this study not only contributes valuable insights into the biological activities of the synthesized compounds but

serves as a stepping stone for future investigations in discovering antibacterial, antioxidant and cytotoxic agents derived from Schiff base compounds.

CHAPTER 6

CONCLUSION

In this study, Schiff base ligands and their corresponding Cu (II) and Ni (II) complexes were synthesized. The ^{1}H NMR and FTIR spectroscopic data were successfully used to confirm the formation of ligands and metal complexes, respectively. The tested ligands and metal complexes demonstrated significant antibacterial activity against majority of the tested bacteria strains (*E. coli, S. aureus, S. mutans and N. gonorrhoea*), with an increase in the potential of ligands after coordination with Cu (II) and Ni (II). Metal complexes of Cu (II) exhibited the best antibacterial activity. Results from the antioxidant studies indicate significant free radical inhibition, with Ni (II) complexes exhibiting the best antioxidant activity. The ligands and metal complexes tested in this study showed moderate cytotoxicity against HeLa cell line, with L6 having the greatest cytotoxic activity.

Overall, the results generated in this study provide valuable insight that could potentially make notable contributions towards the development of novel antibacterial, antioxidant and anticancer agents.

CHAPTER 7

RECOMMENDATIONS

Further studies should include chelation of ligands with other bivalent metal ions, such as Zn^{2+} and Co^{2+}. The antiviral and antifungal activity of the ligands and metal complexes were not conducted in this study. It is also advisable to screen the ligands and their metal complexes for antiviral and antifungal activity, to determine whether the compounds have activity against different microorganisms other than bacteria.

Anti - HIV activity studies are ideal for analysing the antiviral activity of the ligands and metal complexes because of the on-going drug resistance emergence of the virus against available antiretroviral drugs. Anti-HIV studies should be done by means of assays such as the Reverse-transcriptase assay. Fungi such as *Candida albicans* are causative agents of common infections such as candidiasis and are sometimes difficult to treat as the fungi have developed resistance against some of the treatment. An analysis of the antifungal activity of the ligands as well as the metal complexes in this study could be a starting point in discovering better antifungal agents. Future studies may include non-cancerous cells such as Vero cell lines to evaluate the effects of the ligands and metal complexes on non-cancerous cells and determine specificity to cancer.

REFERENCES

1. Sen Karaman D, Ercan UK, Bakay E, Topalouglu N, Rosenholm JM. Evolving technologies and strategies for combating antibacterial resistance in the advent of the postantibiotic era. Adv Funct Mater. 2020;30(15):1908783.

2. Kumar S, Devi J, Ghule VD. Synthesis, spectral analysis, DFT-assisted studies, in vitro antioxidant and antimicrobial activity of transition metal complexes of hydrazone ligands derived from 4-nitrocinnemaldehyde. Res Chem Intermed. 2022;48(8):3497–525.

3. Ivanov A V, Bartosch B, Isaguliants MG, others. Oxidative stress in infection and consequent disease. Vol. 2017, Oxidative Medicine and Cellular Longevity. Hindawi; 2017.

4. Poljsak B, Suput D, Milisav I, others. Achieving the balance between ROS and antioxidants: when to use the synthetic antioxidants. Oxid Med Cell Longev. 2013;2013.

5. Martinelli E, Granato D, Azevedo L, Goncalves JE, Lorenzo JM, Munekata PES, et al. Current perspectives in cell-based approaches towards the definition of the antioxidant activity in food. Trends Food Sci Technol. 2021;116:232–43.

6. Kunwar A, Priyadarsini KI. Free radicals, oxidative stress and importance of antioxidants in human health. J Med Allied Sci. 2011;1(2).

7. Stoia M, Oancea S. Low-molecular-weight synthetic antioxidants: classification, pharmacological profile, effectiveness and trends. Antioxidants. 2022;11(4):638.

8. Uniyal S, Kumar N, Joshi BC. An Overview on Free Radicals and Role of Antioxidants in the Management of Cancer (Brief Review). Orient J Chem. 2024;40(1).

9. Upadhyay A. Cancer: An unknown territory; rethinking before going ahead. Genes Dis. 2021;8(5):655–61.

10. Brown JS, Amend SR, Austin RH, Gatenby RA, Hammarlund EU, Pienta KJ. Updating the definition of cancer. Mol Cancer Res. 2023;21(11):1142–7.

11. Abood RA, Abdahmed KA, Mazyed SS. Epidemiology of different types of cancers reported in Basra, Iraq. Sultan Qaboos Univ Med J. 2020;20(3):e295.

12. Sung H, Ferlay J, Siegel RL, Laversanne M, Soerjomataram I, Jemal A, et al. Global cancer statistics 2020: GLOBOCAN estimates of incidence and mortality worldwide for 36 cancers in 185 countries. CA Cancer J Clin. 2021;71(3):209–49.

13. Blackadar CB. Historical review of the causes of cancer. World J Clin Oncol. 2016;7(1):54.

14. Fuchs-Tarlovsky V. Role of antioxidants in cancer therapy. Nutrition. 2013;29(1):15–21.

15. Gacche RN, Gacche RN. Do antioxidants really help cancer patients? The puzzle of benefits and perils. Diet Res Cancer. 2021;131–46.

16. Hassanpour SH, Dehghani M. Review of cancer from perspective of molecular. J cancer Res Pract. 2017;4(4):127–9.

17. Gurunathan S, Qasim M, Kang M-H, Kim J-H. Role and therapeutic potential

of melatonin in various type of cancers. Onco Targets Ther. 2021;2019–52.

18. Huang J, Deng Y, Boakye D, Tin MS, Lok V, Zhang L, et al. Global distribution, risk factors, and recent trends for cervical cancer: A worldwide country-level analysis. Gynecol Oncol. 2022;164(1):85–92.

19. Cohen PA, Jhingran A, Oaknin A, Denny L. Cervical cancer. Lancet. 2019;393(10167):169–82.

20. Khoury R, Sauter S, Butsch Kovacic M, Nelson AS, Myers KC, Mehta PA, et al. Risk of human papillomavirus infection in cancer-prone individuals: what we know. Viruses. 2018;10(1):47.

21. Abbas Z, Rehman S. An overview of cancer treatment modalities. Neoplasm. 2018;1:139–57.

22. Wang J-J, Lei K-F, Han F. Tumor microenvironment: recent advances in various cancer treatments. Eur Rev Med Pharmacol Sci. 2018;22(12).

23. Altun I, Sonkaya A. The most common side effects experienced by patients were receiving first cycle of chemotherapy. Iran J Public Health. 2018;47(8):1218–9.

24. Olver I, Carey M, Boyes A, Hall A, Noble N, Bryant J, et al. The timeliness of patients reporting the side effects of chemotherapy. Support care cancer. 2018;26:3579–86.

25. Satheeshkumar PS, Mohan MP. Association and risk factors of healthcare-associated infection and burden of illness among chemotherapy-induced ulcerative mucositis patients. Clin Oral Investig. 2021;1–10.

26. Da Silva R, Casella T. Healthcare-associated infections in patients who are immunosuppressed due to chemotherapy treatment: a narrative review. J Infect Dev Ctries. 2022;16(12):1784–95.

27. Taplitz RA, Kennedy EB, Bow EJ, Crews J, Gleason C, Hawley DK, et al. Antimicrobial prophylaxis for adult patients with cancer-related immunosuppression: ASCO and IDSA clinical practice guideline update. J Clin Oncol. 2018;36(30):3043–54.

28. Singh K, Bhori M, Kasu YA, Bhat G, Marar T. Antioxidants as precision weapons in war against cancer chemotherapy induced toxicity--Exploring the armoury of obscurity. Saudi Pharm J. 2018;26(2):177–90.

29. Poprac P, Jomova K, Simunkova M, Kollar V, Rhodes CJ, Valko M. Targeting free radicals in oxidative stress-related human diseases. Trends Pharmacol Sci. 2017;38(7):592–607.

30. Kazakova OB, Lopatina T V, Baikova IP, Zileeva ZR, Vakhitova Y V, Suponitsky KY. Synthesis, evaluation of cytotoxicity, and antimicrobial activity of A-azepano-and A-seco-3-amino-C28-aminolupanes. Med Chem Res. 2020;29:1507–19.

31. Gould S, Templin M V. Off target toxicities and links with physicochemical properties of medicinal products, including antibiotics, oligonucleotides, lipid nanoparticles (with cationic and/or anionic charges). Data review suggests an emerging pattern. Toxicol Lett. 2023;384:14–29.

32. Bácskay I, Nemes D, Fenyvesi F, Váradi J, Vasvári G, Fehér P, et al. Role of cytotoxicity experiments in pharmaceutical development. InTech: London,

UK; 2018.

33. Lyapun IN, Andryukov BG, Bynina MP. HeLa cell culture: Immortal heritage of henrietta lacks. Mol Genet Microbiol Virol. 2019;34(4):195–200.

34. Hongbao M. Hela cells and immortality. Cancer Biol. 2017;3(7):71–8.

35. Ali MR, Marella A, Alam MT, Naz R, Akhter M, Shaquiquzzaman M, et al. Review of biological activities of hydrazones. Indones J Pharm. 2012;23(4):193–202.

36. Aly SA, Fathalla SK. Preparation, characterization of some transition metal complexes of hydrazone derivatives and their antibacterial and antioxidant activities. Arab J Chem. 2020;13(2):3735–50.

37. Ayyannan G, Mohanraj M, Gopiraman M, Uthayamalar R, Raja G, Bhuvanesh N, et al. New Palladium (II) complexes with ONO chelated hydrazone ligand: Synthesis, characterization, DNA/BSA interaction, antioxidant and cytotoxicity. Inorganica Chim Acta. 2020;512:119868.

38. Kajal A, Bala S, Sharma N, Kamboj S, Saini V. Therapeutic potential of hydrazones as anti-inflammatory agents. Int J Med Chem. 2014;2014.

39. Badgujar JR, More DH, Meshram JS. Synthesis, antimicrobial and antioxidant activity of pyrazole based sulfonamide derivatives. Indian J Microbiol. 2018;58:93–9.

40. Abbasi Z, Salehi M, Khaleghian A, Kubicki M. In vitro cytotoxic activity of a novel Schiff base ligand derived from 2-hydroxy-1-naphthaldehyde and its mononuclear metal complexes. J Mol Struct. 2018;1173:213–20.

41. Iftikhar B, Javed K, Khan MSU, Akhter Z, Mirza B, Mckee V. Synthesis, characterization and biological assay of Salicylaldehyde Schiff base Cu (II) complexes and their precursors. J Mol Struct. 2018;1155:337–48.

42. Yildiz M, Tan E, Demir NI, Yildirim N, Ünver H, Kiraz A, et al. Synthesis and spectral, antimicrobial, anion sensing, and DNA binding properties of Schiff base podands and their metal complexes. Russ J Gen Chem. 2015;85:2149–62.

43. El-Gammal OA, Mohamed FS, Rezk GN, El-Bindary AA. Structural characterization and biological activity of a new metal complexes based of Schiff base. J Mol Liq. 2021;330:115522.

44. Kani AI, Na'aliya J, Haruna A, others. Antioxidant Evaluation of Co (II) and Zn (II) Complexes with Schiff base derived from 2-hydroxy-1-naphthaldehyde and p-methoxyaniline. Int J Biol Phys Chem Stud. 2020;2(2):1–10.

45. Kratky M, Dzurkova M, Janousek J, Konecna K, Trejtnar F, Stolavrikova J, et al. Sulfadiazine salicylaldehyde-based Schiff bases: Synthesis, antimicrobial activity and cytotoxicity. Molecules. 2017;22(9):1573.

46. Andiappan K, Sanmugam A, Deivanayagam E, Karuppasamy K, Kim H-S, Vikraman D. In vitro cytotoxicity activity of novel Schiff base ligand--lanthanide complexes. Sci Rep. 2018;8(1):3054.

47. Szklarzewicz J, Jurowska A, Hodorowicz M, Grybos R, Kruczała K, Głuch-Lutwin M, et al. Vanadium complexes with salicylaldehyde-based Schiff base ligands—structure, properties and biological activity. J Coord Chem. 2020;73(6):986–1008.

48. Hashmi S, Khan S, Shafiq Z, Taslimi P, Ishaq M, Sadeghian N, et al. Probing 4-(diethylamino)-salicylaldehyde-based thiosemicarbazones as multi-target directed ligands against cholinesterases, carbonic anhydrases and $α$-glycosidase enzymes. Bioorg Chem. 2021;107:104554.

49. Sevgi F, Bagkesici U, Kursunlu AN, Guler E. Fe (III), Co (II), Ni (II), Cu (II) and Zn (II) complexes of schiff bases based-on glycine and phenylalanine: Synthesis, magnetic/thermal properties and antimicrobial activity. J Mol Struct. 2018;1154:256–60.

50. Czaplewski L, Bax R, Clokie M, Dawson M, Fairhead H, Fischetti VA, et al. Alternatives to antibiotics—a pipeline portfolio review. Lancet Infect Dis. 2016;16(2):239–51.

51. Kong Q, Yang Y. Recent advances in antibacterial agents. Bioorg Med Chem Lett. 2021;35:127799.

52. Belete TM. Novel targets to develop new antibacterial agents and novel alternatives to antibacterial agents. Hum Microbiome J. 2019;11:100052.

53. Abushaheen MA, Fatani AJ, Alosaimi M, Mansy W, George M, Acharya S, et al. Antimicrobial resistance, mechanisms and its clinical significance. Disease-a-Month. 2020;66(6):100971.

54. Kapoor G, Saigal S, Elongavan A. Action and resistance mechanisms of antibiotics: A guide for clinicians. J Anaesthesiol Clin Pharmacol. 2017;33(3):300.

55. Anderson R, Groundwater PW, Todd A, Worsley A. Antibacterial agents: chemistry, mode of action, mechanisms of resistance and clinical applications.

John Wiley & Sons; 2012.

56. Divya K, Pinto GM, Pinto AF. Application of metal complexes of Schiff bases as an antimicrobial drug: a review of recent works. Int J Curr Pharm Res. 2017;9(3):27–30.

57. Mohamed MS, Elamin KM, Alenazy R, Mohamed Eltayib E, Timan Idriss M, Alhudaib NAA, et al. Synthesis, Antimicrobial, and Anticancer Activities of Novel Nitrofuran Derivatives. J Chem. 2023;2023.

58. Mohapatra RK, Das PK, Pradhan MK, Maihub AA, El-ajaily MM. Biological aspects of Schiff base--metal complexes derived from benzaldehydes: an overview. J Iran Chem Soc. 2018;15:2193–227.

59. Donnenberg M. Escherichia coli: pathotypes and principles of pathogenesis. Academic Press; 2013.

60. Allocati N, Masulli M, Alexeyev MF, Di Ilio C. Escherichia coli in Europe: an overview. Int J Environ Res Public Health. 2013;10(12):6235–54.

61. Vihta K-D, Stoesser N, Llewelyn MJ, Quan TP, Davies T, Fawcett NJ, et al. Trends over time in Escherichia coli bloodstream infections, urinary tract infections, and antibiotic susceptibilities in Oxfordshire, UK, 1998--2016: a study of electronic health records. Lancet Infect Dis. 2018;18(10):1138–49.

62. Manning SD. Escherichia coli infections. Infobase Publishing; 2010.

63. Johnson TJ, Logue CM, Johnson JR, Kuskowski MA, Sherwood JS, Barnes HJ, et al. Associations between multidrug resistance, plasmid content, and virulence potential among extraintestinal pathogenic and commensal

Escherichia coli from humans and poultry. Foodborne Pathog Dis. 2012;9(1):37–46.

64. Quillin SJ, Seifert HS. Neisseria gonorrhoeae host adaptation and pathogenesis. Nat Rev Microbiol. 2018;16(4):226–40.

65. Aitolo GL, Adeyemi OS, Afolabi BL, Owolabi AO. Neisseria gonorrhoeae antimicrobial resistance: past to present to future. Curr Microbiol. 2021;78:867–78.

66. Unemo M, Shafer WM. Antimicrobial resistance in Neisseria gonorrhoeae in the 21st century: past, evolution, and future. Clin Microbiol Rev. 2014;27(3):587–613.

67. Organization WH, others. Global action plan to control the spread and impact of antimicrobial resistance in Neisseria gonorrhoeae. 2012;

68. Tacconelli E. Global Priority List of Antibiotic-Resistant Bacteria to Guide Research, Discovery, and Development. 2017;

69. Suay-Garc'\ia B, Pérez-Gracia MT. Future prospects for Neisseria gonorrhoeae treatment. Antibiotics. 2018;7(2):49.

70. David MZ, Daum RS. Treatment of Staphylococcus aureus infections. Staphylococcus aureus Microbiol Pathol Immunol Ther Prophyl. 2017;325–83.

71. Sikorska H, Smoragiewicz W. Role of probiotics in the prevention and treatment of meticillin-resistant Staphylococcus aureus infections. Int J Antimicrob Agents. 2013;42(6):475–81.

72. Ford CA, Hurford IM, Cassat JE. Antivirulence strategies for the treatment of Staphylococcus aureus infections: a mini review. Front Microbiol. 2021;11:632706.

73. Guo Y, Song G, Sun M, Wang J, Wang Y. Prevalence and therapies of antibiotic-resistance in Staphylococcus aureus. Front Cell Infect Microbiol. 2020;10:107.

74. Haaber J, Penadés JR, Ingmer H. Transfer of antibiotic resistance in Staphylococcus aureus. Trends Microbiol. 2017;25(11):893–905.

75. Monaco M, de Araujo F, Cruciani M, Coccia EM, Pantosti A. Worldwide epidemiology and antibiotic resistance of Staphylococcus aureus. Staphylococcus aureus Microbiol Pathol Immunol Ther Prophyl. 2017;21–56.

76. Lemos JA, Palmer SR, Zeng L, Wen ZT, Kajfasz JK, Freires IA, et al. The biology of Streptococcus mutans. Microbiol Spectr. 2019;7(1):10–1128.

77. Matsumoto-Nakano M. Role of Streptococcus mutans surface proteins for biofilm formation. Jpn Dent Sci Rev 54: 22--29. 2018.

78. Cui T, Luo W, Xu L, Yang B, Zhao W, Cang H. Progress of antimicrobial discovery against the major cariogenic pathogen Streptococcus mutans. Curr Issues Mol Biol. 2019;32(1):601–44.

79. Avilés-Reyes A, Miller JH, Lemos JA, Abranches J. Collagen-binding proteins of Streptococcus mutans and related streptococci. Mol Oral Microbiol 32: 89--106. 2017.

80. Al-Shami IZ, Al-Hamzi MA, Al-Shamahy HA, Majeed A. Efficacy of some

Antibiotics against Streptococcus Mutans Associated with Tooth decay in Children and their Mothers. On J Dent Oral Heal. 2019;2(1).

81. Salehi B, Martorell M, Arbiser JL, Sureda A, Martins N, Maurya PK, et al. Antioxidants: positive or negative actors? Biomolecules. 2018;8(4):124.

82. Gulcin \.Ilhami. Antioxidants and antioxidant methods: An updated overview. Arch Toxicol. 2020;94(3):651–715.

83. Han H, Yilmaz H, Gulcin I. Antioxidant activity of flaxseed (Linum usitatissimum L.) shell and analysis of its polyphenol contents by LC-MS/MS. 2018;

84. Bulut N, Kocyigit UM, Gecibesler IH, Dastan T, Karci H, Taslimi P, et al. Synthesis of some novel pyridine compounds containing bis-1, 2, 4-triazole/thiosemicarbazide moiety and investigation of their antioxidant properties, carbonic anhydrase, and acetylcholinesterase enzymes inhibition profiles. J Biochem Mol Toxicol. 2018;32(1):e22006.

85. Anraku M, Gebicki JM, Iohara D, Tomida H, Uekama K, Maruyama T, et al. Antioxidant activities of chitosans and its derivatives in in vitro and in vivo studies. Carbohydr Polym. 2018;199:141–9.

86. Jasril J, Ikhtiarudin I, Nurulita Y, Nurisma N. Microwave-assisted synthesis and antioxidant activity of an imine,(E)-1-(3-bromobenzylidene)-2-phenylhydrazine. In: AIP Conference Proceedings. 2020.

87. Halliwell B. The antioxidant paradox: less paradoxical now? Br J Clin Pharmacol. 2013;75(3):637–44.

88. Sindhi V, Gupta V, Sharma K, Bhatnagar S, Kumari R, Dhaka N. Potential applications of antioxidants--A review. J Pharm Res. 2013;7(9):828–35.

89. Pasupuleti VR, Arigela CS, Gan SH, Salam SKN, Krishnan KT, Rahman NA, et al. A review on oxidative stress, diabetic complications, and the roles of honey polyphenols. Oxid Med Cell Longev. 2020;2020.

90. Cakmak KC, Gulcin I. Anticholinergic and antioxidant activities of usnic acid-an activity-structure insight. Toxicol reports. 2019;6:1273–80.

91. Wollinger A, Perrin E, Chahboun J, Jeannot V, Touraud D, Kunz W. Antioxidant activity of hydro distillation water residues from Rosmarinus officinalis L. leaves determined by DPPH assays. Comptes Rendus Chim. 2016;19(6):754–65.

92. Wang S, He G, Chen M, Zuo T, Xu W, Liu X, et al. The role of antioxidant enzymes in the ovaries. Oxid Med Cell Longev. 2017;2017.

93. El-Missiry MA. Antioxidant enzyme. BoD--Books on Demand; 2012.

94. Pisoschi AM, Pop A. The role of antioxidants in the chemistry of oxidative stress: A review. Eur J Med Chem. 2015;97:55–74.

95. Carocho M, Morales P, Ferreira ICFR. Antioxidants: Reviewing the chemistry, food applications, legislation and role as preservatives. Trends Food Sci Technol. 2018;71:107–20.

96. Shah SS, Shah D, Khan I, Ahmad S, Ali U, Rahman A. Synthesis and antioxidant activities of Schiff bases and their complexes: An updated review. Biointerface Res Appl Chem. 2020;10(6):6936–63.

97. Xu X, Liu A, Hu S, Ares I, Martinez-Larranaga M-R, Wang X, et al. Synthetic phenolic antioxidants: Metabolism, hazards and mechanism of action. Food Chem. 2021;353:129488.

98. Papillomavirus H. and Cervical Cancer. World Heal Organ Fact Sheet, World Heal Organ. 2019;24.

99. Arbyn M, Weiderpass E, Bruni L, de Sanjosé S, Saraiya M, Ferlay J, et al. Estimates of incidence and mortality of cervical cancer in 2018: a worldwide analysis. Lancet Glob Heal. 2020;8(2):e191–203.

100. Zhang S, Xu H, Zhang L, Qiao Y. Cervical cancer: Epidemiology, risk factors and screening. Chinese J Cancer Res. 2020;32(6):720.

101. Small Jr W, Bacon MA, Bajaj A, Chuang LT, Fisher BJ, Harkenrider MM, et al. Cervical cancer: a global health crisis. Cancer. 2017;123(13):2404–12.

102. Ma X, Yang M. The correlation between high-risk HPV infection and precancerous lesions and cervical cancer. Am J Transl Res. 2021;13(9):10830.

103. Burmeister CA, Khan SF, Schäfer G, Mbatani N, Adams T, Moodley J, et al. Cervical cancer therapies: Current challenges and future perspectives. Tumour Virus Res. 2022;13:200238.

104. Brown A, Kumar S, Tchounwou PB. Cisplatin-based chemotherapy of human cancers. J Cancer Sci Ther. 2019;11(4).

105. Federico C, Sun J, Muz B, Alhallak K, Cosper PF, Muhammad N, et al. Localized delivery of cisplatin to cervical cancer improves its therapeutic efficacy and minimizes its side effect profile. Int J Radiat Oncol Biol Phys.

2021;109(5):1483–94.

106. Romani AMP. Cisplatin in cancer treatment. Biochem Pharmacol. 2022;206:115323.

107. Wen X, Liu S, Sheng J, Cui M. Recent advances in the contribution of noncoding RNAs to cisplatin resistance in cervical cancer. PeerJ. 2020;8:e9234.

108. Bhattacharjee R, Dey T, Kumar L, Kar S, Sarkar R, Ghorai M, et al. Cellular landscaping of cisplatin resistance in cervical cancer. Biomed Pharmacother. 2022;153:113345.

109. Niles AL, Moravec RA, Riss TL. In vitro viability and cytotoxicity testing and same-well multi-parametric combinations for high throughput screening. Curr Chem Genomics. 2009;3:33.

110. Smits VAJ, Gillespie DA. Cancer therapy: targeting the poison within. Cell Cycle. 2014;13(15):2330–3.

111. Saboowala HK. What HeLa Cells aka Immortal Cells Are and Why They Are Important. An Example of Racism in Medicine. Dr. Hakim Saboowala; 2022.

112. Rutledge S. What HeLa Cells Are You Using? Authorea Prepr. 2023;

113. Varsha DS, Nirmala GS, Santhekadur PK. Our Shero HeLa and Her Immortal Life: The Story Behind the Famous HeLa Cells. Resonance. 2022;27(10):1731–6.

114. Team AR. Hela Cells and their Applications.

115. Mirabelli P, Coppola L, Salvatore M. Cancer cell lines are useful model

systems for medical research. Cancers (Basel). 2019;11(8):1098.

116. Yun X, Tang M, Yang Z, Wilksch JJ, Xiu P, Gao H, et al. Interrogation of drug effects on HeLa cells by exploiting new AFM mechanical biomarkers. RSC Adv. 2017;7(69):43764–71.

117. Tatalick LM, Gerard CJ, Takeya R, Price DN, Thorne BA, Wyatt LM, et al. Safety characterization of HeLa-based cell substrates used in the manufacture of a recombinant adeno-associated virus-HIV vaccine. Vaccine. 2005;23(20):2628–38.

118. Raczuk E, Dmochowska B, Samaszko-Fiertek J, Madaj J. Different Schiff bases—structure, importance and classification. Molecules. 2022;27(3):787.

119. Liu X, Hamon J-R. Recent developments in penta-, hexa-and heptadentate Schiff base ligands and their metal complexes. Coord Chem Rev. 2019;389:94–118.

120. Ebosie NP, Ogwuegbu MOC, Onyedika GO, Onwumere FC. Biological and analytical applications of Schiff base metal complexes derived from salicylidene-4-aminoantipyrine and its derivatives: A review. J Iran Chem Soc. 2021;18(12):3145–75.

121. Xavier A, Srividhya N. Synthesis and study of Schiff base ligands. IOSR J Appl Chem. 2014;7(11):6–15.

122. Ugwu DI, Conradie J. Metal complexes derived from bidentate ligands: Synthesis, catalytic and biological applications. Inorganica Chim Acta. 2023;553:121518.

123. Arora T, Devi J, Boora A, Taxak B, Rani S. Synthesis and characterization of hydrazones and their transition metal complexes: antimicrobial, antituberculosis and antioxidant activity. Res Chem Intermed. 2023;1–25.

124. Kumar N, Asija S, Deswal Y, Saroya S, Kumar A. Development of new tridentate ligands bearing hydrazone motif and their diorganotin (IV) complexes: Synthesis, spectral, antimicrobial and molecular docking studies. Res Chem Intermed. 2022;48(12):5133–54.

125. Hameed A, Al-Rashida M, Uroos M, Abid Ali S, Khan KM. Schiff bases in medicinal chemistry: a patent review (2010-2015). Expert Opin Ther Pat. 2017;27(1):63–79.

126. Fekri R, Salehi M, Asadi A, Kubicki M. Synthesis, characterization, anticancer and antibacterial evaluation of Schiff base ligands derived from hydrazone and their transition metal complexes. Inorganica Chim Acta. 2019;484:245–54.

127. Shakdofa MME, Shtaiwi MH, Morsy N, Abdel-rassel T. Metal complexes of hydrazones and their biological, analytical and catalytic applications: A review. Main Gr Chem. 2014;13(3):187–218.

128. Qi J, Luo Y, Zhou Q, Su G, Zhang X, Nie X, et al. Synthesis, structure and anticancer studies of Cu(Ⅱ) and Ni(Ⅱ) complexes based on 2-hydroxy-1-naphthaldehyde-4-aminoantipyrine Schiff-base. J Mol Struct. 2022;1255:132458.

129. E\uglence-Bak\ir S. New nickel (II) complexes containing N2O2 donor thiosemicarbazones: Synthesis, characterization and antioxidant properties. J

Mol Struct. 2021;1246:131121.

130. Vetlenyi E, Rácz G. The physiological function of copper, the etiological role of copper excess and deficiency. Orv Hetil. 2020;161(35):1488–96.

131. Wang P, Yuan Y, Xu K, Zhong H, Yang Y, Jin S, et al. Biological applications of copper-containing materials. Bioact Mater. 2021;6(4):916–27.

132. Collins JF. Chapter 7-Copper: Basic Physiological and Nutritional Aspects. Molecular, Genetic, and Nutritional Aspects of Major and Trace Minerals. Academic Press; 2017.

133. Ingle AP, Paralikar P, Shende S, Gupta I, Biswas JK, da Silva Martins LH, et al. Copper in medicine: Perspectives and toxicity. Biomed Appl Met. 2018;95–112.

134. Zdrojewicz Z, Popowicz E, Winiarski J. Nickel-role in human organism and toxic effects. Pol Merkur Lek Organ Pol Tow Lek. 2016;41(242):115–8.

135. Poonkothai M, Vijayavathi BS. Nickel as an essential element and a toxicant. Int J Environ Sci. 2012;1(4):285–8.

136. Wang J, Zhang L, Jiang H, Chen K, Liu H. Application of Nickel (II) Complexes to the Efficient Synthesis of $α$-or $β$-Amino Acids. Chimia (Aarau). 2011;65(12):919.

137. Rodrigues RC, Pereira HS, Senra RL, Ribon A de OB, de Oliveira Mendes TA. Understanding the emerging potential of synthetic biology for food science: achievements, applications and safety considerations. Food Chem Adv. 2023;100476.

138. Swiderski G, Jablonska-Trypuc A, Kalinowska M, Swisłocka R, Karpowicz D, Magnuszewska M, et al. Spectroscopic, theoretical and antioxidant study of 3d-transition metals (Co (II), Ni (II), Cu (II), Zn (II)) complexes with cichoric acid. Materials (Basel). 2020;13(14):3102.

139. Devi J, Kumar B, Taxak B. Recent advancements of organotin (IV) complexes derived from hydrazone and thiosemicarbazone ligands as potential anticancer agents. Inorg Chem Commun. 2022;139:109208.

140. Majid SA, Mir JM, Jan G, Shalla AH. Schiff base complexes, cancer cell lines, and anticancer evaluation: a review. J Coord Chem. 2022;75(15-16):2018–38.

141. Kirubavathy SJ, Velmurugan R, Karvembu R, Bhuvanesh NSP, Enoch IVM V, Selvakumar PM, et al. Structural and molecular docking studies of biologically active mercaptopyrimidine Schiff bases. J Mol Struct. 2017;1127:345–54.

142. Mukhtar SS, Hassan AS, Morsy NM, Hafez TS, Hassaneen HM, Saleh FM. Overview on synthesis, reactions, applications, and biological activities of Schiff bases. Egypt J Chem. 2021;64(11):6541–54.

143. Ozdemir UO, Aktan E, Ilbiz F, Gunduzalp AB, Ozbek N, Sari M, et al. Characterization, antibacterial, anticarbonic anhydrase II isoenzyme, anticancer, electrochemical and computational studies of sulfonic acid hydrazide derivative and its Cu (II) complex. Inorganica Chim Acta. 2014;423:194–203.

144. Kratky M, Vinsova J, Volkova M, Buchta V, Trejtnar F, Stolavrikova J.

Antimicrobial activity of sulfonamides containing 5-chloro-2-hydroxybenzaldehyde and 5-chloro-2-hydroxybenzoic acid scaffold. Eur J Med Chem. 2012;50:433–40.

145. Moussa Z, Al-Mamary M, Al-Juhani S, Ahmed SA. Preparation and biological assessment of some aromatic hydrazones derived from hydrazides of phenolic acids and aromatic aldehydes. Heliyon. 2020;6(9).

146. Mahmood AA. Green synthesis of Schiff bases: a review study. Iraqi J Pharm. 2022;18(2):180–93.

147. Qin W, Long S, Panunzio M, Biondi S. Schiff bases: A short survey on an evergreen chemistry tool. Molecules. 2013;18(10):12264–89.

148. Mighani H. Schiff Base polymers: synthesis and characterization. J Polym Res. 2020;27:1–18.

149. Berhanu AL, Mohiuddin I, Malik AK, Aulakh JS, Kumar V, Kim K-H, et al. A review of the applications of Schiff bases as optical chemical sensors. TrAC Trends Anal Chem. 2019;116:74–91.

150. Colak N, Gunduzalp AB, Altiner S, Sahin ZS. Synthesis, characterization and theoretical calculations of Schiff base containing thiophene ring system. Gazi Univ J Sci. 2017;30(3):255–65.

151. Jawoor SS, Patil SA, Kumbar M, Ramawadgi PB. Green synthesis of nano sized transition metal complexes containing heterocyclic Schiff base: structural and morphology characterization and bioactivity study. J Mol Struct. 2018;1164:378–85.

152. Mondal S, Mandal SM, Mondal TK, Sinha C. Spectroscopic characterization, antimicrobial activity, DFT computation and docking studies of sulfonamide Schiff bases. J Mol Struct. 2017;1127:557–67.

153. Yadav P, Sarkar A, Kumar A. Synthesis and biological activities of schiff bases and their derivatives: a review of recent work. J Basic Appl Eng Res. 2019;6(1):62–5.

154. Sinthuja SA, Shaji YC, Rose GL. Synthesis, characterization and evaluation of biological properties of transition metal chelates with Schiff base ligands derived from glutaraldehyde with L-leucine. Int J Sci Res Sci Technol. 2018;4(2):587–93.

155. Saheb V, Sheikhshoaie I. A new Schiff base compound N, N′-(2, 2-dimetylpropane)-bis (dihydroxylacetophenone): Synthesis, experimental and theoretical studies on its crystal structure, FTIR, UV--visible, 1H NMR and 13C NMR spectra. Spectrochim Acta Part A Mol Biomol Spectrosc. 2011;81(1):144–50.

156. Rankin NJ, Preiss D, Welsh P, Burgess KE V, Nelson SM, Lawlor DA, et al. The emergence of proton nuclear magnetic resonance metabolomics in the cardiovascular arena as viewed from a clinical perspective. Atherosclerosis. 2014;237(1):287–300.

157. Tucureanu V, Matei A, Avram AM. FTIR spectroscopy for carbon family study. Crit Rev Anal Chem. 2016;46(6):502–20.

158. Buzon-Duran L, Capita R, Alonso-Calleja C. Antibiotic susceptibility of methicillin-resistant staphylococci (MRS) of food origin: A comparison of

agar disc diffusion method and a commercially available miniaturized test. Food Microbiol. 2018;72:220–4.

159. Jonasson E, Matuschek E, Kahlmeter G. The EUCAST rapid disc diffusion method for antimicrobial susceptibility testing directly from positive blood culture bottles. J Antimicrob Chemother. 2020;75(4):968–78.

160. Ahmed YM, Mahmoud WH, Omar MM, Mohamed GG. Synthesis, characterization and biological activity of transition metals schiff base complexes derived from 4, 6-Diacetylresorcinol and 1, 8-Naphthalenediamine. J Inorg Organomet Polym Mater. 2021;31:2339–59.

161. Hudzicki J. Kirby-Bauer disk diffusion susceptibility test protocol. Am Soc Microbiol. 2009;15:55–63.

162. Parvekar P, Palaskar J, Metgud S, Maria R, Dutta S. The minimum inhibitory concentration (MIC) and minimum bactericidal concentration (MBC) of silver nanoparticles against Staphylococcus aureus. Biomater Investig Dent. 2020;7(1):105–9.

163. Kowalska-Krochmal B, Dudek-Wicher R. The minimum inhibitory concentration of antibiotics: Methods, interpretation, clinical relevance. Pathogens. 2021;10(2):165.

164. Prieto MA, Curran TP, Gowen A, Vázquez JA. An efficient methodology for quantification of synergy and antagonism in single electron transfer antioxidant assays. Food Res Int. 2015;67:284–98.

165. Hamlaoui I, Bencheraiet R, Bensegueni R, Bencharif M. Experimental and theoretical study on DPPH radical scavenging mechanism of some chalcone

quinoline derivatives. J Mol Struct. 2018;1156:385–9.

166. Abramovic H, Grobin B, Poklar Ulrih N, Cigić B, others. Relevance and standardization of in vitro antioxidant assays: ABTS, DPPH, and Folin--Ciocalteu. J Chem. 2018;2018.

167. Gulcin I, Alwasel SH. DPPH radical scavenging assay. Processes. 2023;11(8):2248.

168. Koksal E, Bursal E, Gulcin I, Korkmaz M, Caglayan C, Goren AC, et al. Antioxidant activity and polyphenol content of Turkish thyme (Thymus vulgaris) monitored by liquid chromatography and tandem mass spectrometry. 2017;

169. Sirivibulkovit K, Nouanthavong S, Sameenoi Y. based DPPH assay for antioxidant activity analysis. Anal Sci. 2018;34(7):795–800.

170. Kedare SB, Singh RP. Genesis and development of DPPH method of antioxidant assay. J Food Sci Technol. 2011;48:412–22.

171. Schaich KM, Tian X, Xie J. Hurdles and pitfalls in measuring antioxidant efficacy: A critical evaluation of ABTS, DPPH, and ORAC assays. J Funct Foods. 2015;14:111–25.

172. Liang N, Kitts DD. Antioxidant property of coffee components: assessment of methods that define mechanisms of action. Molecules. 2014;19(11):19180–208.

173. Shalaby EA, Shanab SMM. Antioxidant compounds, assays of determination and mode of action. African J Pharm Pharmacol. 2013;7(10):528–39.

174. Vasyliev GS, Vorobyova VI, Linyucheva O V. Evaluation of reducing ability and antioxidant activity of fruit pomace extracts by spectrophotometric and electrochemical methods. J Anal Methods Chem. 2020;2020:1–16.

175. Singhal M, Paul A, Singh HP. Synthesis and reducing power assay of methyl semicarbazone derivatives. J Saudi Chem Soc. 2014;18(2):121–7.

176. Riss T, Niles A, Moravec R, Karassina N, Vidugiriene J. Cytotoxicity assays: in vitro methods to measure dead cells. Assay Guid Man [internet]. 2019;

177. Setiawati A, Candrasari DS, Setyajati FDE, Prasetyo VK, Setyaningsih D, Hartini YS. Anticancer drug screening of natural products: In vitro: cytotoxicity assays, techniques, and challenges. Asian Pac J Trop Biomed. 2022;12(7):279–89.

178. Papadimitriou M, Hatzidaki E, Papasotiriou I. Linearity comparison of three colorimetric cytotoxicity assays. J Cancer Ther. 2019;10(7):580–90.

179. Buranaamnuay K. The MTT assay application to measure the viability of spermatozoa: A variety of the assay protocols. Open Vet J. 2021;11(2):251–69.

180. Prabst K, Engelhardt H, Ringgeler S, Hübner H. Basic colorimetric proliferation assays: MTT, WST, and resazurin. Cell viability assays methods Protoc. 2017;1–17.

181. Karakacs D, Ari F, Ulukaya E. The MTT viability assay yields strikingly false-positive viabilities although the cells are killed by some plant extracts. Turkish J Biol. 2017;41(6):919–25.

182. Bahuguna A, Khan I, Bajpai VK, Kang SC. MTT assay to evaluate the cytotoxic potential of a drug. Bangladesh J Pharmacol. 2017;12(2):115–8.

183. Riss TL, Moravec RA, Niles AL, Duellman S, Benink HA, Worzella TJ, et al. Cell viability assays assay guidance manual. Assay Guid Man. 2004;1–23.

184. Kanwal A, Parveen B, Ashraf R, Haider N, Ali KG. A review on synthesis and applications of some selected Schiff bases with their transition metal complexes. J Coord Chem. 2022;75(19-24):2533–56.

185. Santiago PHO, Santiago MB, Martins CHG, Gatto CC. Copper (II) and zinc (II) complexes with Hydrazone: Synthesis, crystal structure, Hirshfeld surface and antibacterial activity. Inorganica Chim Acta. 2020;508:119632.

186. Philip JE, Antony SA, Eeettinilkunnathil SJ, Kurup MRP, Velayudhan MP. Design, synthesis, antimicrobial and antioxidant activity of 3-formyl chromone hydrazone and their metal (II) complexes. Inorganica Chim Acta. 2018;469:87–97.

187. Yousif E, Majeed A, Al-Sammarrae K, Salih N, Salimon J, Abdullah B. Metal complexes of Schiff base: preparation, characterization and antibacterial activity. Arab J Chem. 2017;10:S1639–44.

188. Veiga A, da Graça TT, Rossa LS, Mengarda M, Stofella NCF, Oliveira LJ, et al. Colorimetric microdilution assay: Validation of a standard method for determination of MIC, IC50%, and IC90% of antimicrobial compounds. J Microbiol Methods. 2019;162:50–61.

189. Jafari M, Salehi M, Kubicki M, Arab A, Khaleghian A. DFT studies and antioxidant activity of Schiff base metal complexes of 2-aminopyridine.

Crystal structures of cobalt (II) and zinc (II) complexes. Inorganica Chim Acta. 2017;462:329–35.

190. Liu X, Shan K, Shao X, Shi X, He Y, Liu Z, et al. Nanotoxic effects of silver nanoparticles on normal HEK-293 cells in comparison to cancerous HeLa cell line. Int J Nanomedicine. 2021;753–61.

191. Ghasemi M, Turnbull T, Sebastian S, Kempson I. The MTT assay: utility, limitations, pitfalls, and interpretation in bulk and single-cell analysis. Int J Mol Sci. 2021;22(23):12827.

192. Awolope RO, Ejidike IP, Clayton HS. Schiff base metal complexes as a dual antioxidant and antimicrobial agents. J Appl Pharm Sci. 2023;13(3):132–40.

193. Ugwu DI, Conradie J. Bidentate ligands in self-assembly: synthesis, structure and applications. J Mol Struct. 2023;1293:136275.

194. Slavin YN, Asnis J, Hńfeli UO, Bach H. Metal nanoparticles: understanding the mechanisms behind antibacterial activity. J Nanobiotechnology. 2017;15:1–20.

195. Beyene BB, Mihirteu AM, Ayana MT, Yibeltal AW. Synthesis, characterization and antibacterial activity of metalloporphyrins: Role of central metal ion. Results Chem. 2020;2:100073.

196. Elaaraj I, Raouan SER, Nakkabi A, Es-sounni B, Koraichi I, Fahim M, et al. Synthesis, characterization and antioxidant, antibacterial activity Zn2+, Cu2+, Ni2+ and Co2+, complexes of ligand [2-(thiophen-2-yl)-1-(thiophen-2-ylmethyl)-1H-benzo [d] imidazole]. J Indian Chem Soc. 2022;99(5):100404.

197. Ashraf J, Riaz MA. Biological potential of copper complexes: a review. Turkish J Chem. 2022;46(3):595–623.

198. Aljahdali M, El-Sherif AA. Synthesis, characterization, molecular modeling and biological activity of mixed ligand complexes of Cu (II), Ni (II) and Co (II) based on 1, 10-phenanthroline and novel thiosemicarbazone. Inorganica Chim Acta. 2013;407:58–68.

199. Alyar S, Alyar H, Ozdemir UO, Sahin O, Kaya K, Ozbek N, et al. Synthesis, characterization, antibacterial activity and quantum chemical studies of N'-Acetyl propane sulfonic acid hydrazide. J Mol Struct. 2015;1094:237–45.

200. Katugampala S, Perera IC, Nanayakkara C, Perera T. Synthesis, Characterization, and Antimicrobial Activity of Novel Sulfonated Copper-Triazine Complexes. Bioinorg Chem Appl. 2018;2018(1):2530851.

201. Hasi Q-M, Fan Y, Yao X-Q, Hu D-C, Liu J-C. Synthesis, characterization, antioxidant and antimicrobial activities of a bidentate Schiff base ligand and its metal complexes. Polyhedron. 2016;109:75–80.

202. Sumalatha V, Daravath S, Rambabu A, Ramesh G, others. Antioxidant, antimicrobial, DNA binding and cleavage studies of novel Co (II), Ni (II) and Cu (II) complexes of N, O donor Schiff bases: Synthesis and spectral characterization. J Mol Struct. 2021;1229:129606.

203. Ammar RA, Alaghaz A-NMA, Zayed ME, Al-Bedair LA. Synthesis, spectroscopic, molecular structure, antioxidant, antimicrobial and antitumor behavior of Mn (II), Co (II), Ni (II), Cu (II) and Zn (II) complexes of O2N type tridentate chromone-2-carboxaldehyde Schiff's base ligand. J Mol Struct.

2017;1141:368–81.

204. Meshram P, Abhilash, Pandey BD, Mankhand TR, Deveci H. Comparision of different reductants in leaching of spent lithium ion batteries. Jom. 2016;68:2613–23.

205. Cho P, Mattisson T, Lyngfelt A. Comparison of iron-, nickel-, copper-and manganese-based oxygen carriers for chemical-looping combustion. Fuel. 2004;83(9):1215–25.

206. Le Goff G, Ouazzani J. Natural hydrazine-containing compounds: Biosynthesis, isolation, biological activities and synthesis. Bioorg Med Chem. 2014;22(23):6529–44.

207. Barqi MM, Ashar A, Bhutta ZA, Javed M, Abdellah IM, Eletmany MR. Comprehensive Investigation of the Potential of Hydrazine and its Derivatives for the Synthesis of Various Molecules with Biological Activity. Chem Ind. 2023;4:6.

208. Samsonowicz M, Regulska E. Spectroscopic study of molecular structure, antioxidant activity and biological effects of metal hydroxyflavonol complexes. Spectrochim Acta Part A Mol Biomol Spectrosc. 2017;173:757–71.

209. Arora T, Devi J, Dubey A, Tufail A, Kumar B. Spectroscopic studies, antimicrobial activity, and computational investigations of hydrazone ligands endowed metal chelates. Appl Organomet Chem. 2023;37(9):e7209.

210. Khan T, Dixit S, Ahmad R, Raza S, Azad I, Joshi S, et al. Molecular docking, PASS analysis, bioactivity score prediction, synthesis, characterization and

biological activity evaluation of a functionalized 2-butanone thiosemicarbazone ligand and its complexes. J Chem Biol. 2017;10:91–104.

211. Kandile NG, Mohamed MI, Ismaeel HM. Antiproliferative effects of metal complexes of new isatin hydrazones against HCT116, MCF7 and HELA tumour cell lines. J Enzyme Inhib Med Chem. 2012;27(3):330–8.

212. Werner CG, Sittner W, Wagner FD. Antimicrobial Resistance--The Silent Pandemic. J Integr Heal. 2024;3(4):311–22.

213. Gerhard D. Antimicrobial resistance: The silent pandemic. Sci Mag. 2023;

214. Uzombah TA. The Implications of Replacing Synthetic Antioxidants with. Nat food Addit. 2022;3.

Appendix 1

Ethical clearance certificate and research permit letter

UNAM
UNIVERSITY OF NAMIBIA

ETHICAL CLEARANCE CERTIFICATE

Ethical Clearance Reference Number: SOS-0015 Date: 25 October 2021

This Ethical Clearance Certificate is issued by the University of Namibia Ethics Committee (REC) in accordance with the University of Namibia's Research Ethics Policy and Guidelines. Ethical approval is given in respect of undertakings contained in the Research Project outlined below. This Certificate is issued on the recommendations of the ethical evaluation done by the ethics committee.

Title of Project: IDENTIFICATION OF SELECTED HYDRAZONE COMPOUNDS AS LATENT HIV-1 REACTIVATORS AND THEIR MODES OF ACTION

Student: TEOPOLINA NAWINDA

Student Number: 201148757

Supervisor(s): PROF PETRINA KAPEWANGOLO (UNIVERSITY OF NAMIBIA)

Centre for Research Services

Take note of the following:

1. Any significant changes in the conditions or undertakings outlined in the approved Proposal must be communicated to the ethics committee. An application to make amendments may be necessary.
2. Any breaches of ethical undertakings or practices that have an impact on ethical conduct of the research must be reported to the ethics committee
3. The Principal Researcher must report issues of ethical compliance to the ethics committee (through the Chairperson) at the end of the Project or as may be requested by the ethics committee
4. The ethics committee retains the right to:

i) Withdraw or amend this Ethical Clearance if any unethical practices (as outlined in the Research Ethics Policy) have been detected or suspected,

ii) Request for an ethical compliance report at any point during the course of the research.

The ethics committee wishes you the best in your research.

Dr. Zivayi Chiguvare (Chairperson Ethics Committee)

Prof. Davis Mumbengegwi (Head, Multidisciplinary Research)

CENTRE FOR RESEARCH SERVICES
Office of the Pro-Vice Chancellor: Research, Innovation & Development
University of Namibia, Private Bag 13301, Windhoek, Namibia
340 Mandume Ndemufayo Avenue, Pioneers Park, Office F223 - Fblock, Second Floor
☎ +264 61 206 4673; E-mail:kmbulu@unam.na; URL.: http//www.unam.edu.na

UNAM
UNIVERSITY OF NAMIBIA

RESEARCH PERMISSION LETTER

Date: 11/11/2021

Student Name: TEOPOLINA NAWINDA

Student Number: 201148757

Programme: Doctor of Philosophy in Science

Approved Research Title: IDENTIFICATION OF SELECTED HYDRAZONE COMPOUNDS AS LATENT HIV-1 REACTIVATORS AND THEIR MODES OF ACTION

TO WHOM IT MAY CONCERN

I hereby confirm that the above mentioned student is registered at the University of Namibia for the programme indicated. The proposed study met all the requirements as stipulated in the University guidelines and has been approved by the relevant committees.

The proposal adheres to ethical principles as per attached Ethical Clearance Certificate. Permission is hereby granted to carry out the research as described in the approved proposal.

Best Regards

Dr. AEE Shikongo
Head: Postgraduate Support Services
Tel: +264 61 206 3129
E-mail: aeshikongo@unam.na

CENTRE FOR RESEARCH SERVICES
Office of the Director
2021 -11- 11
University of Namibia
UNAM

Appendix 2

^{1}H NMR spectra for ligands and FTIR spectra for ligands and metal complexes

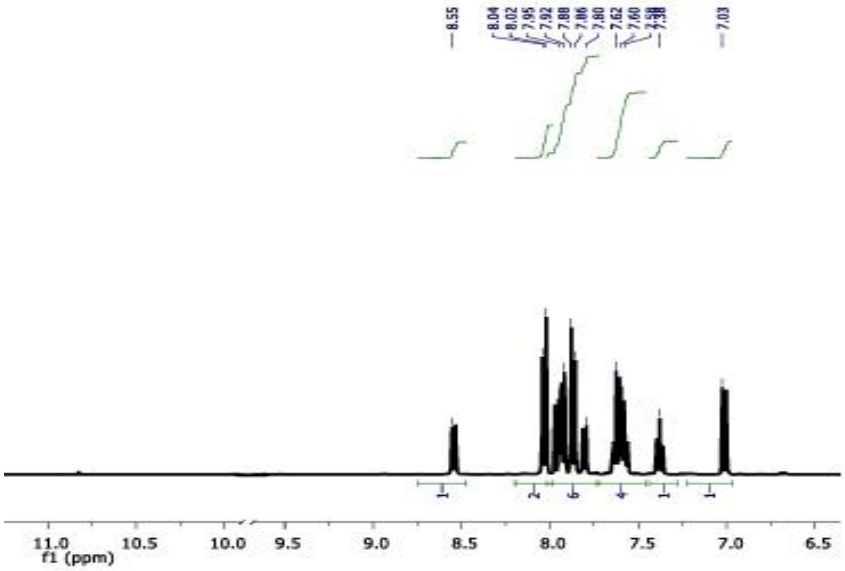

Figure 11. ^{1}H NMR spectrum for L1

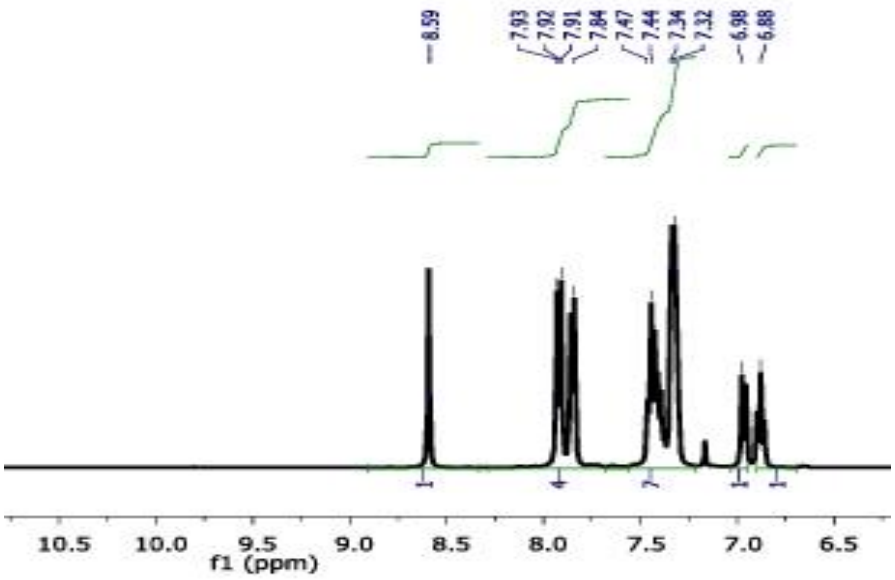

Figure 12. ^{1}H NMR spectrum for L2

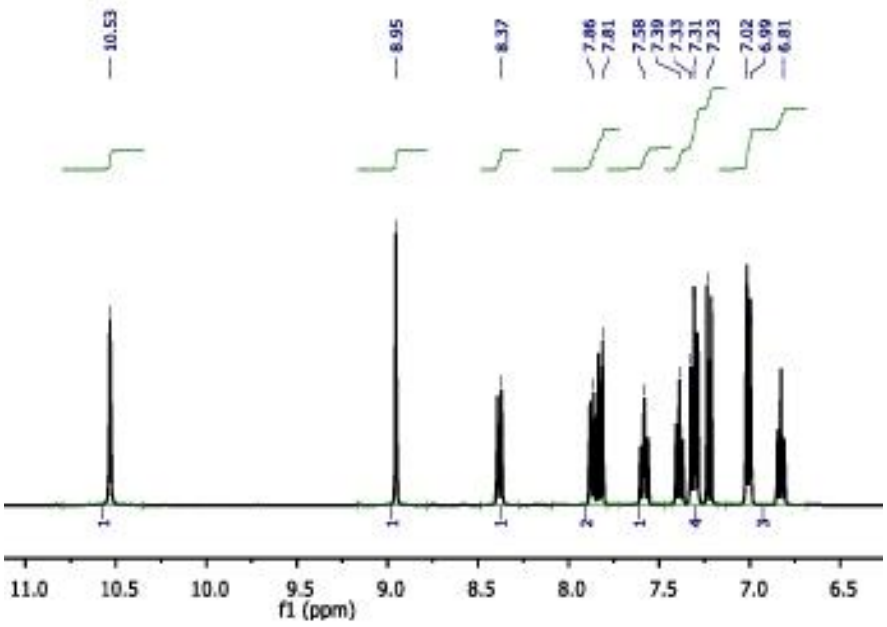

Figure 13. ^{1}H NMR spectrum for L3

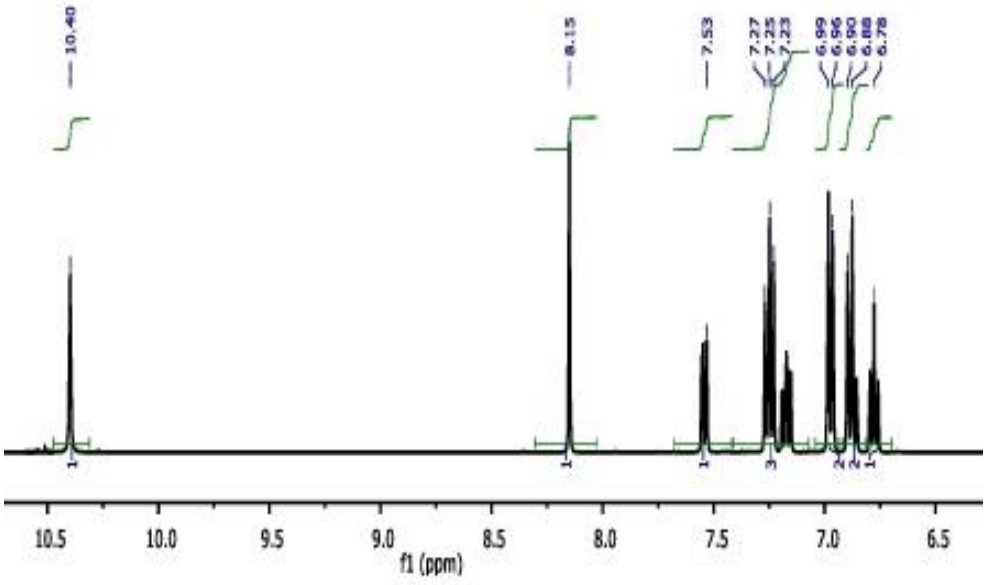

Figure 14. ^{1}H NMR spectrum for L4

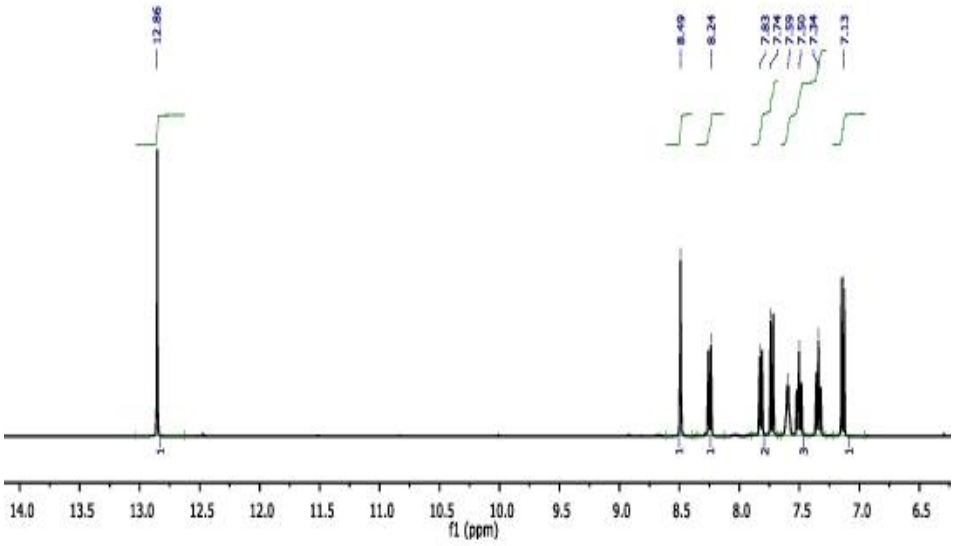

Figure 15. ^{1}H NMR spectrum for L5

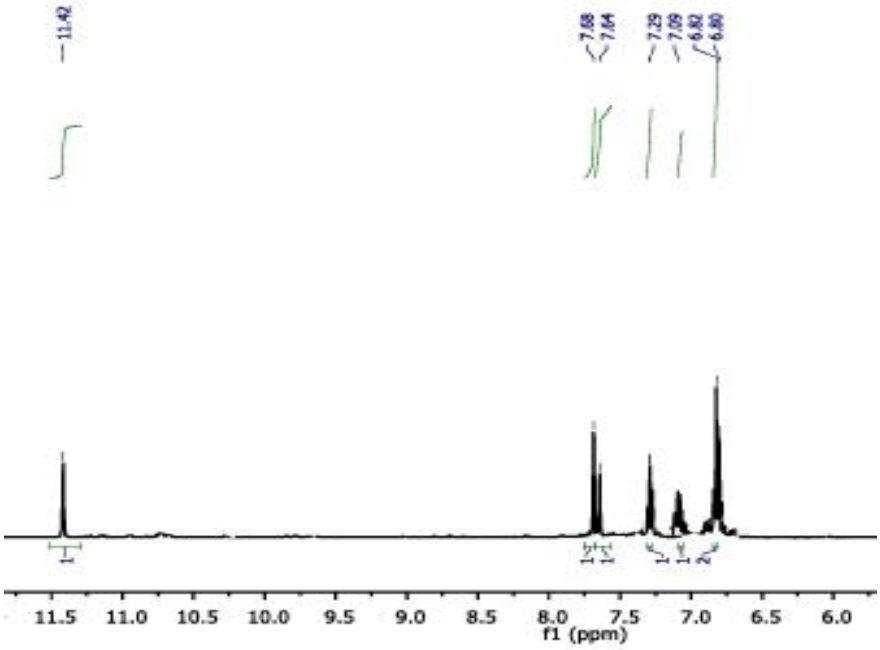

Figure 16. ^{1}H NMR spectrum for L6

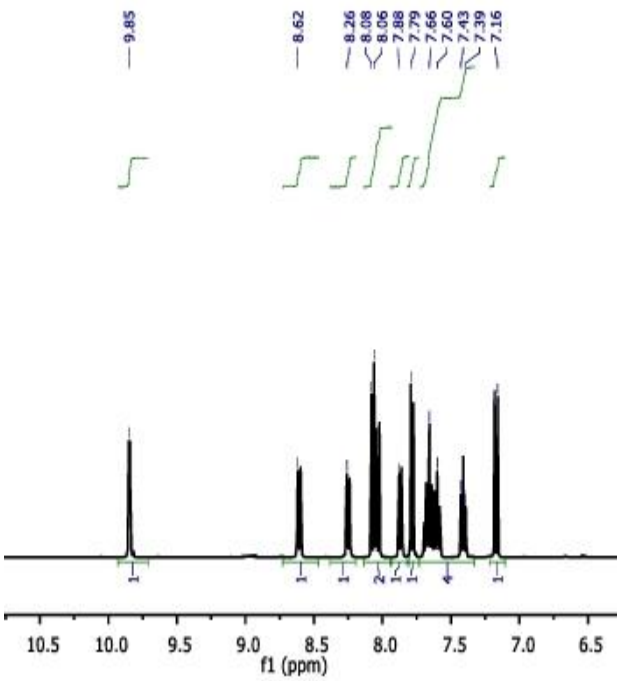

Figure 17. ^{1}H NMR spectrum for L7

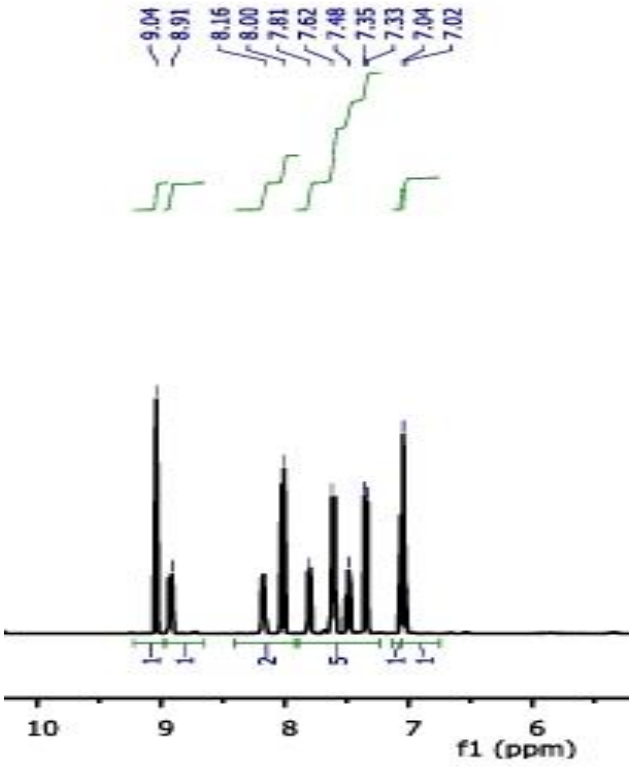

Figure 18. ^{1}H NMR spectrum for L8

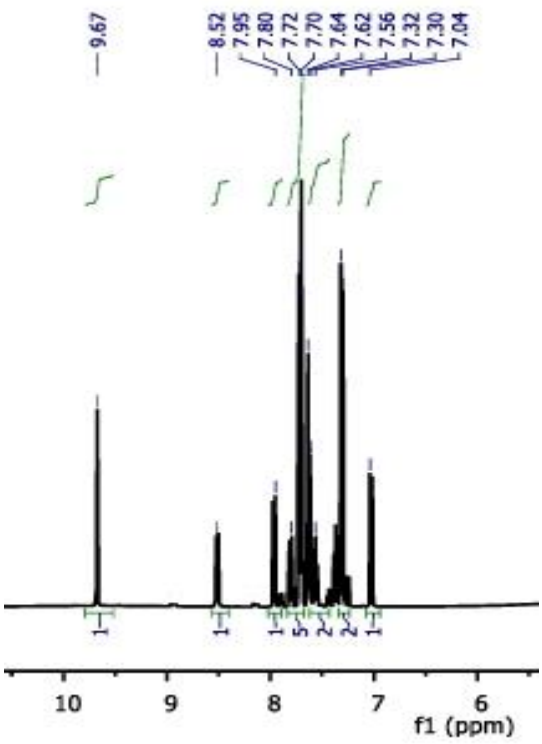

Figure 19. ^{1}H NMR spectrum for L9

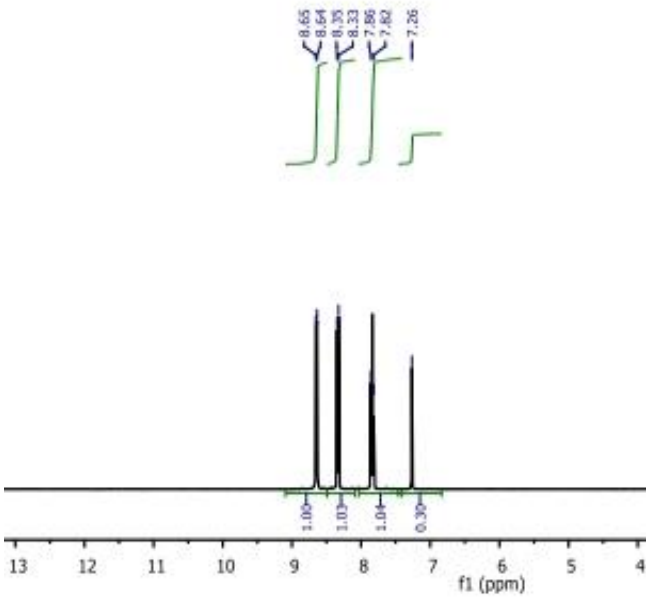

Figure 20. ^{1}H NMR spectrum for L10

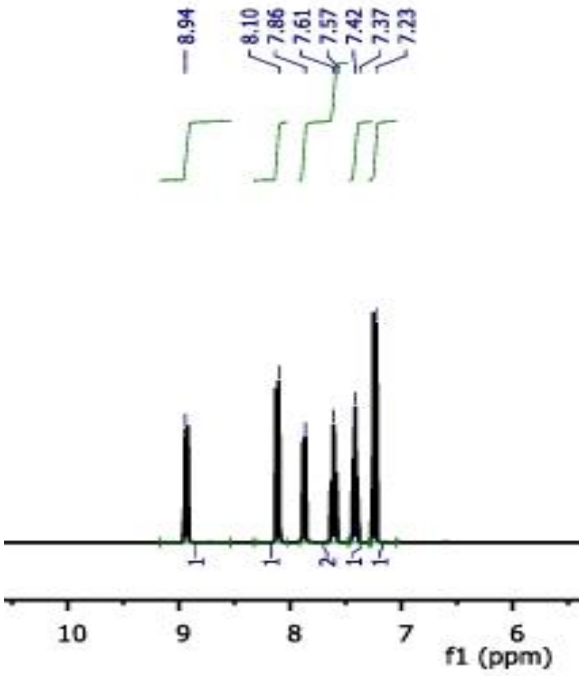

Figure 21. ^{1}H NMR spectrum for L11

FT-IR spectra for ligands and metal complexes

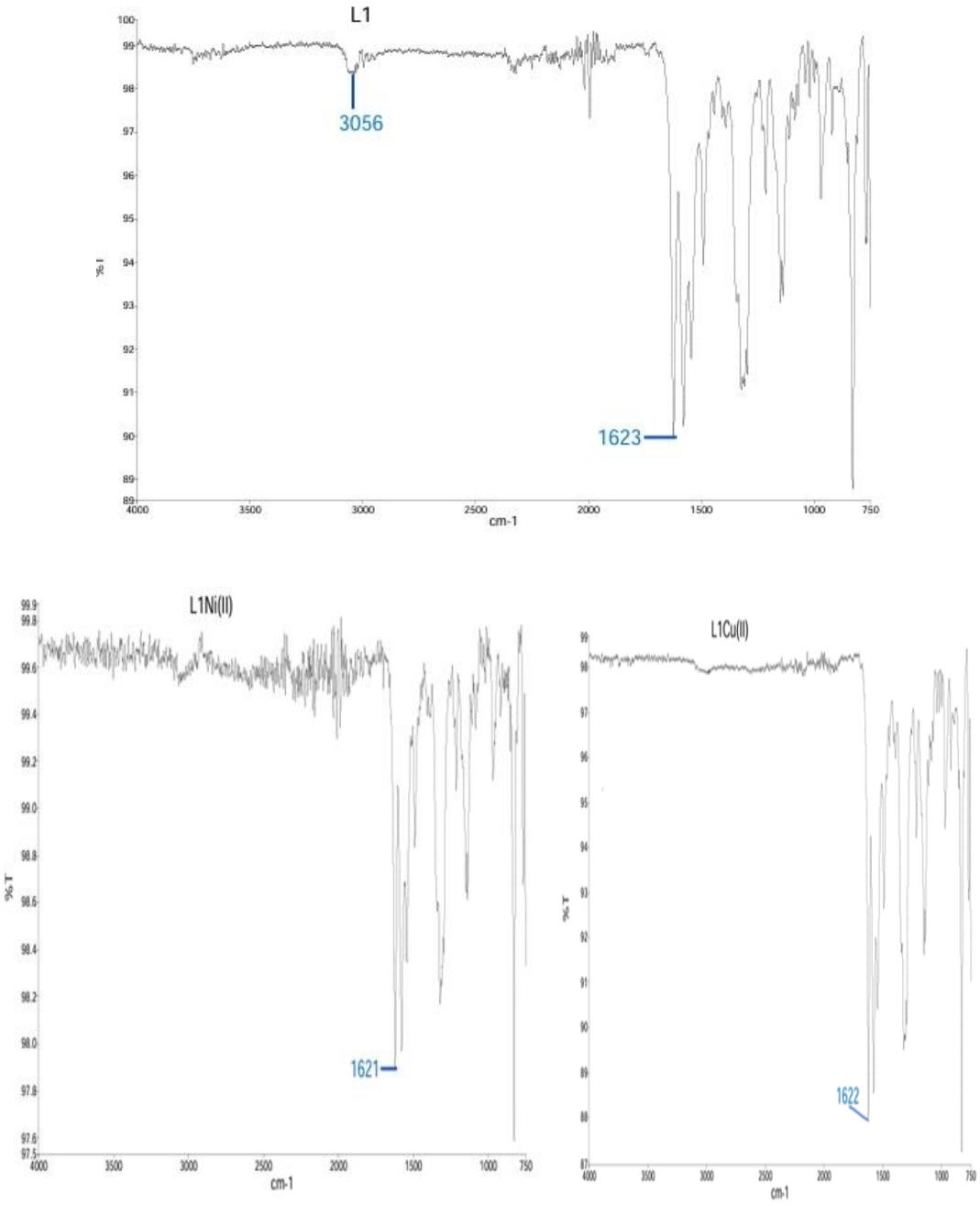

Figure 22. FTIR spectra for L1 and metal complexes

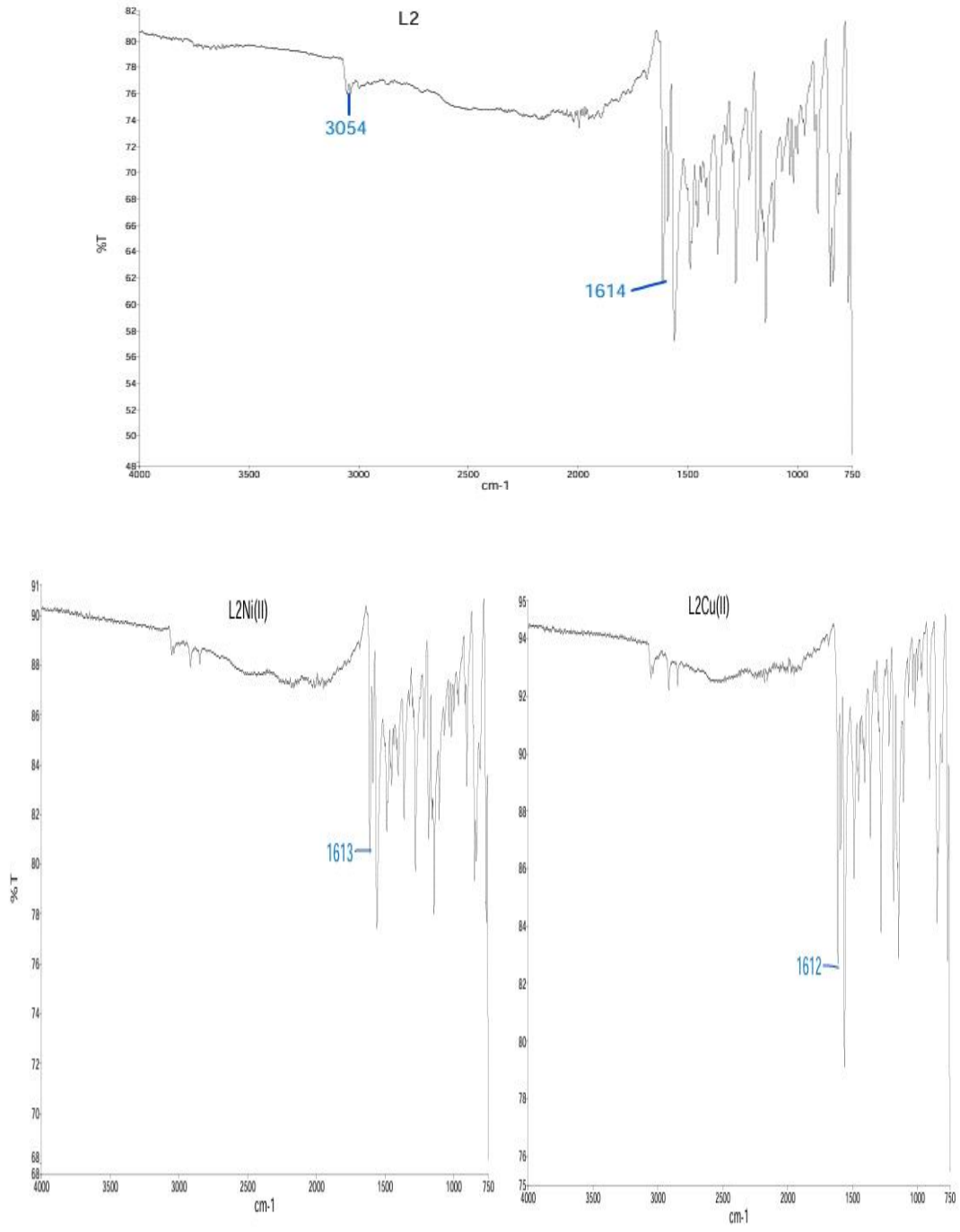

Figure 23. FTIR spectra for L2 and metal complexes

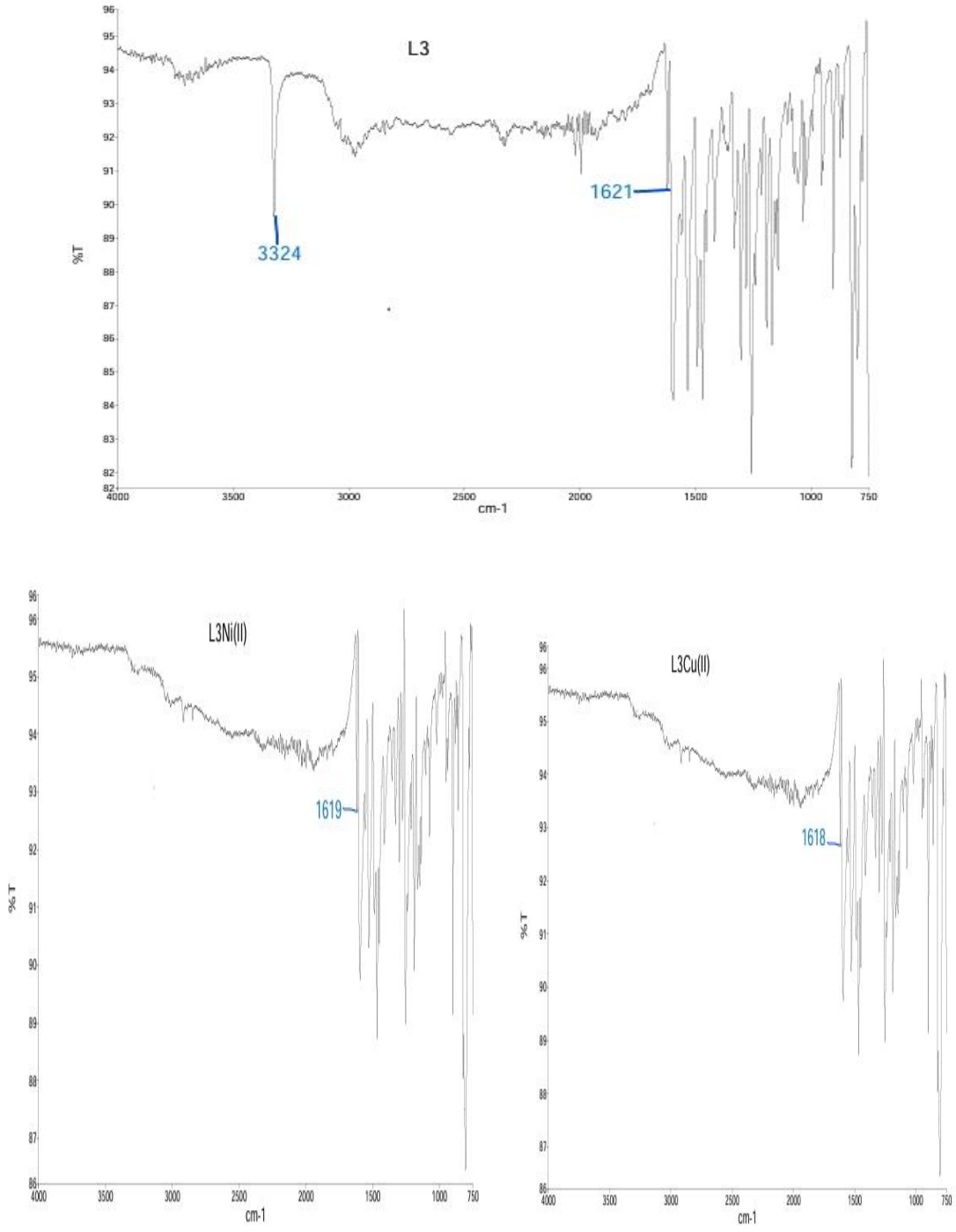

Figure 24. FTIR spectra for L3 and metal complexes

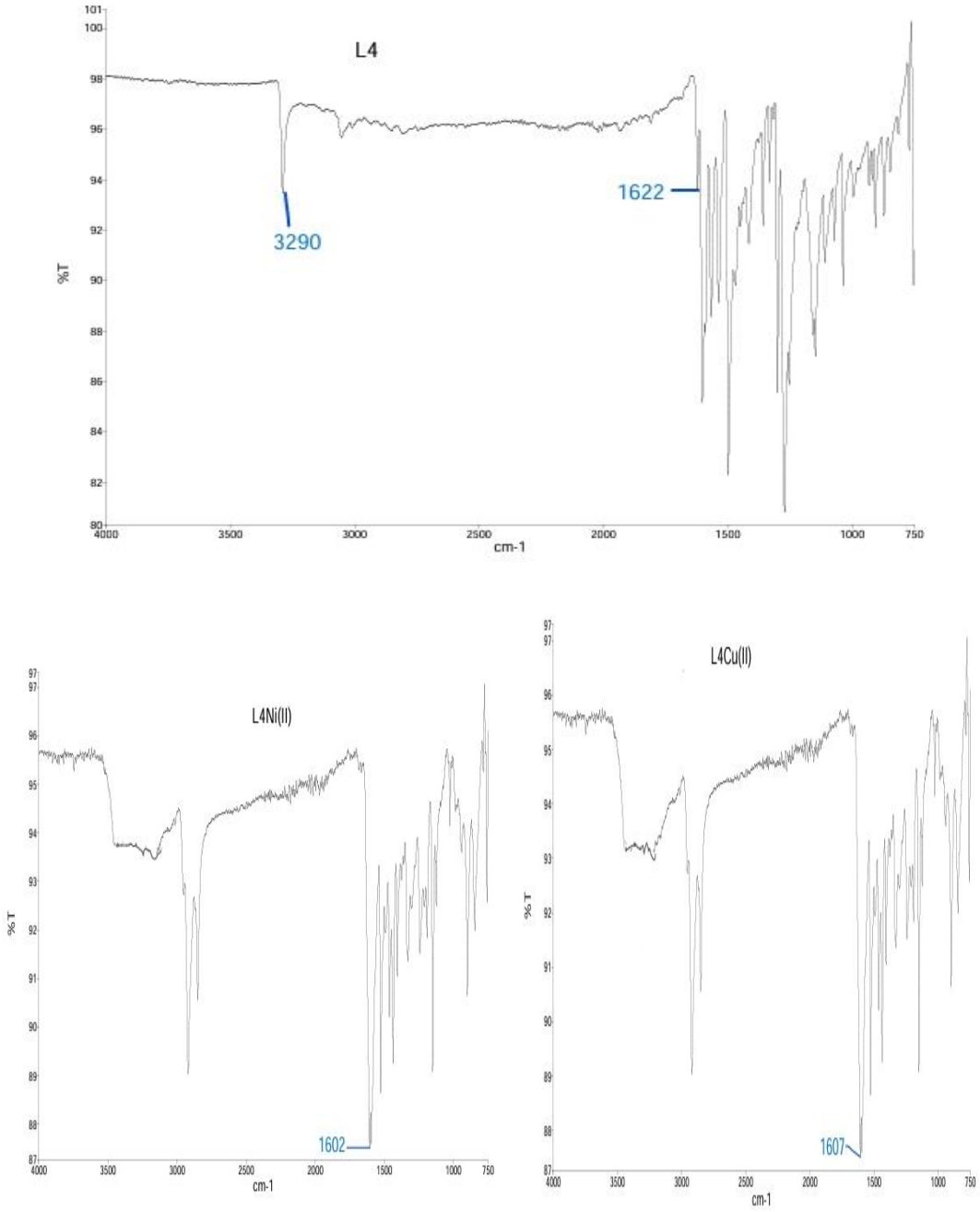

Figure 25. FTIR spectra for L4 and metal complexes

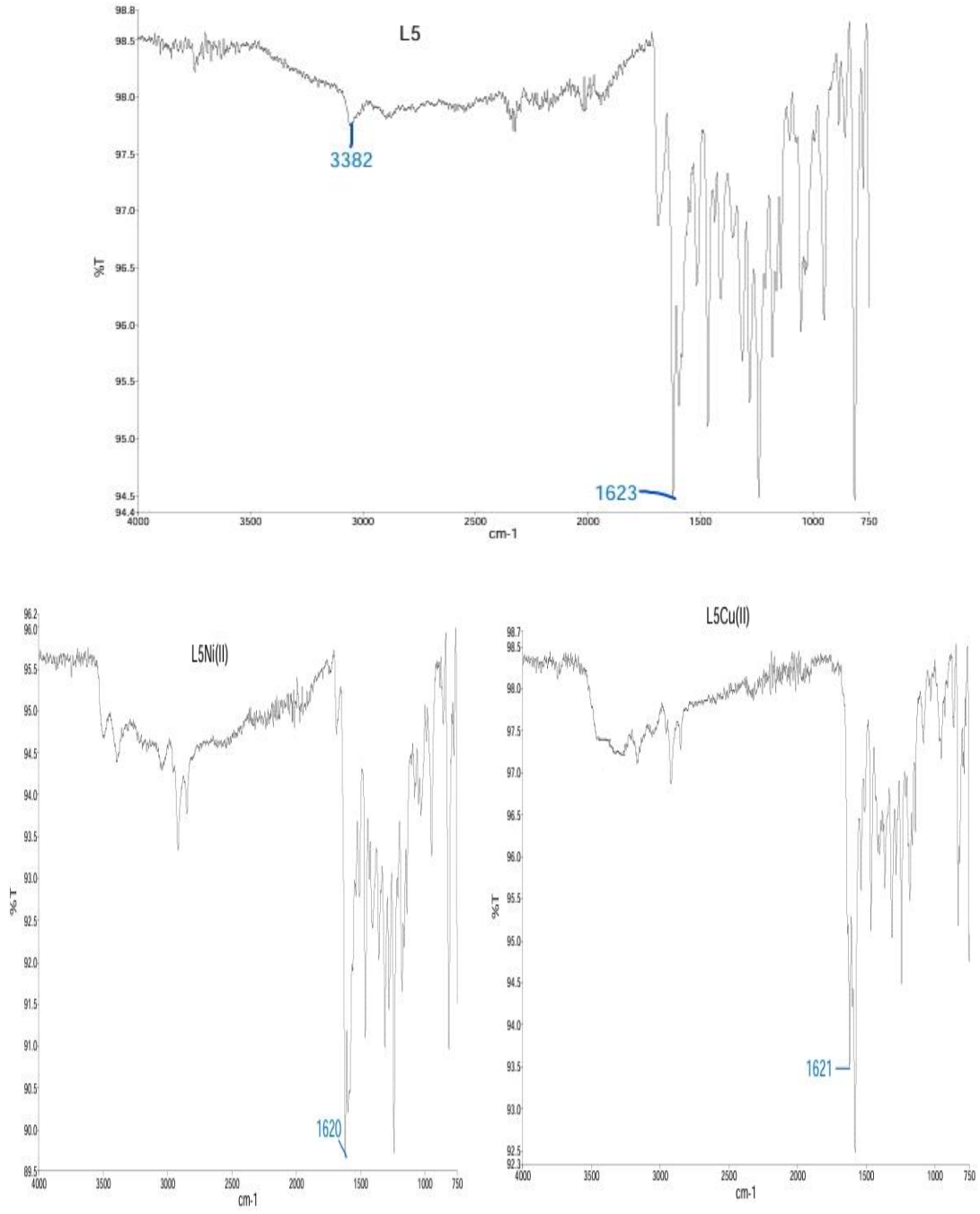

Figure 26. FTIR spectra for L5 and metal complexes

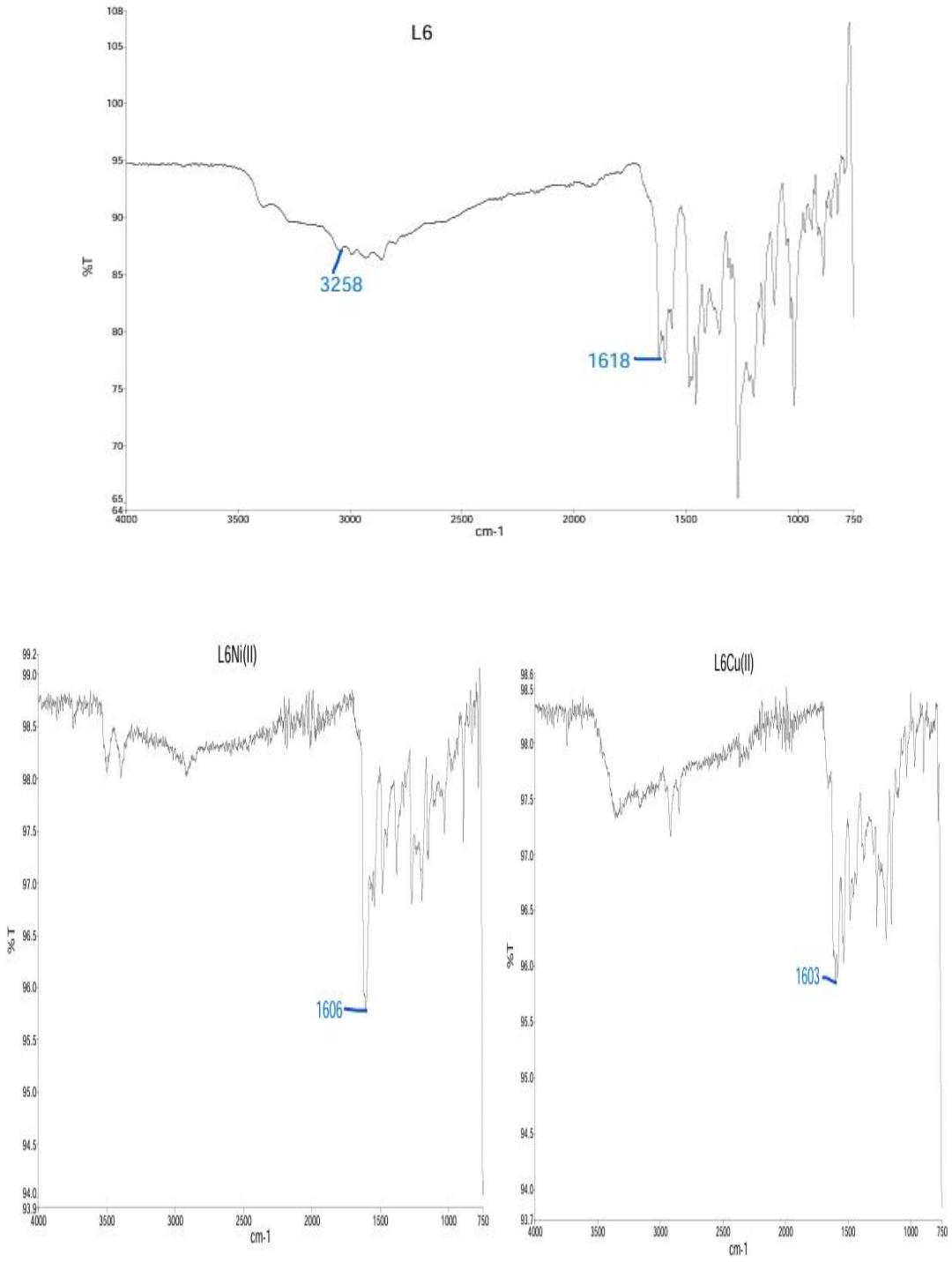

Figure 27. FTIR spectra for L6 and metal complexes

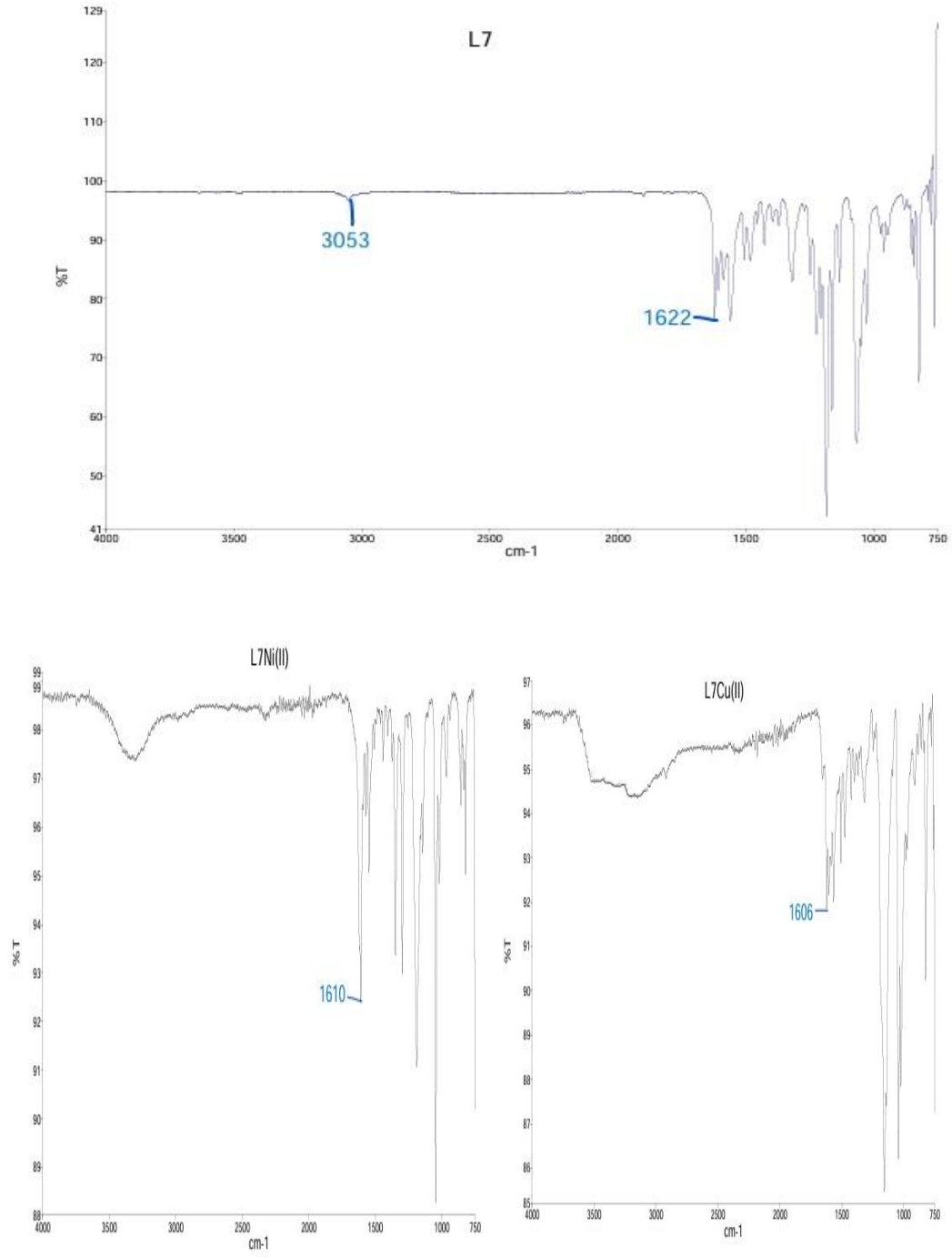

Figure 28. FTIR spectra for L7 and metal complexes

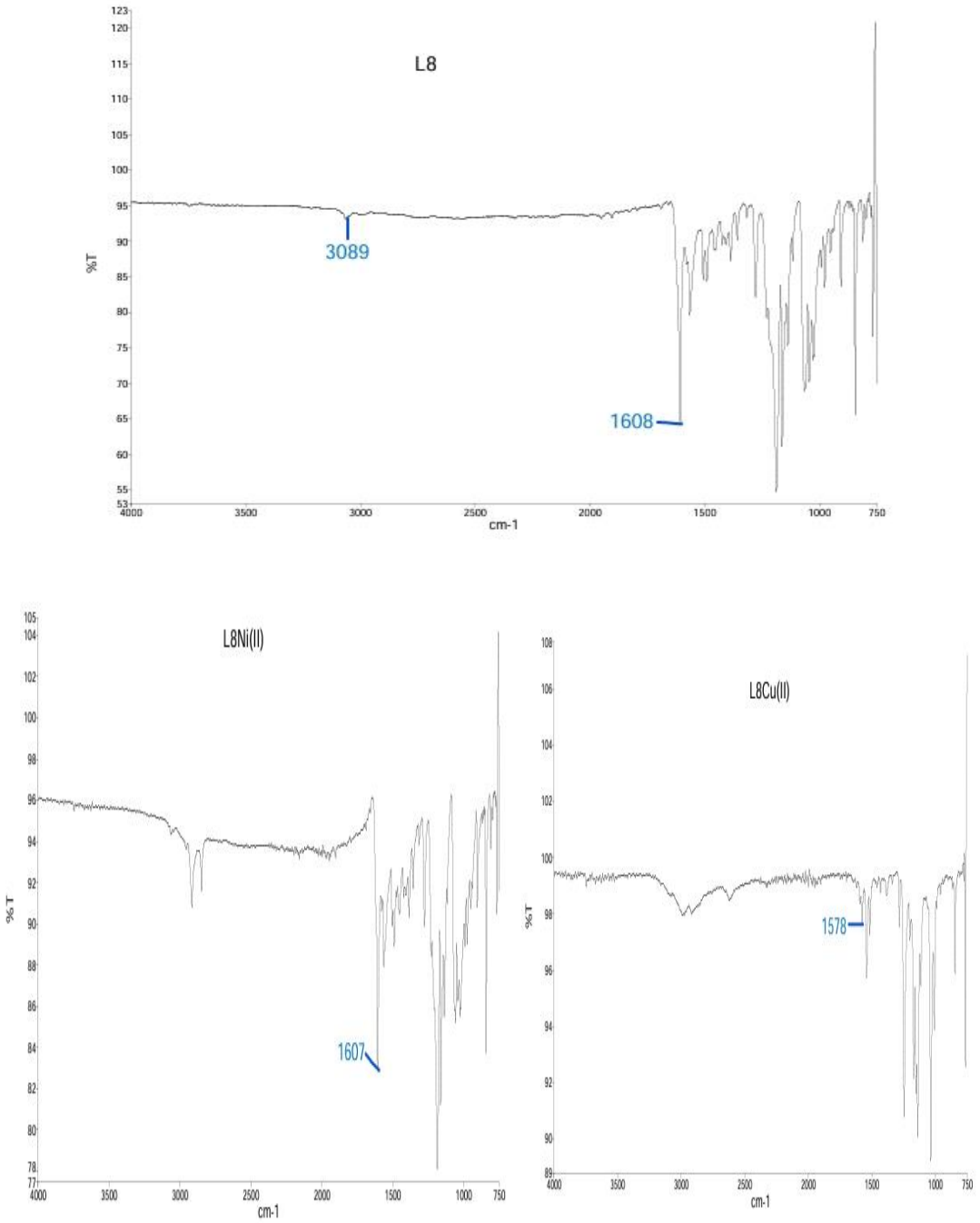

Figure 29. FTIR spectra for L8 and metal complexes

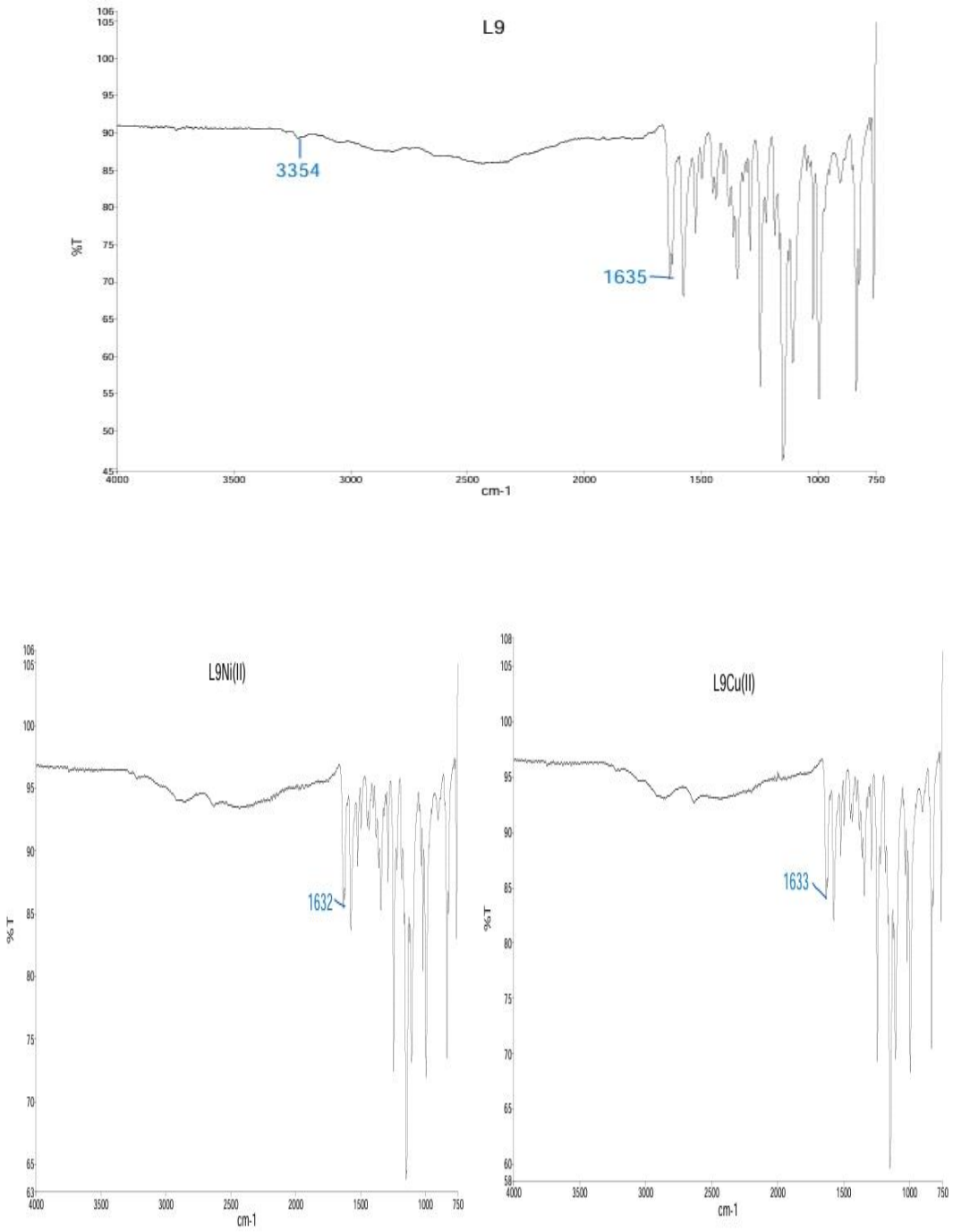

Figure 30. FTIR spectra for L9 and metal complexes

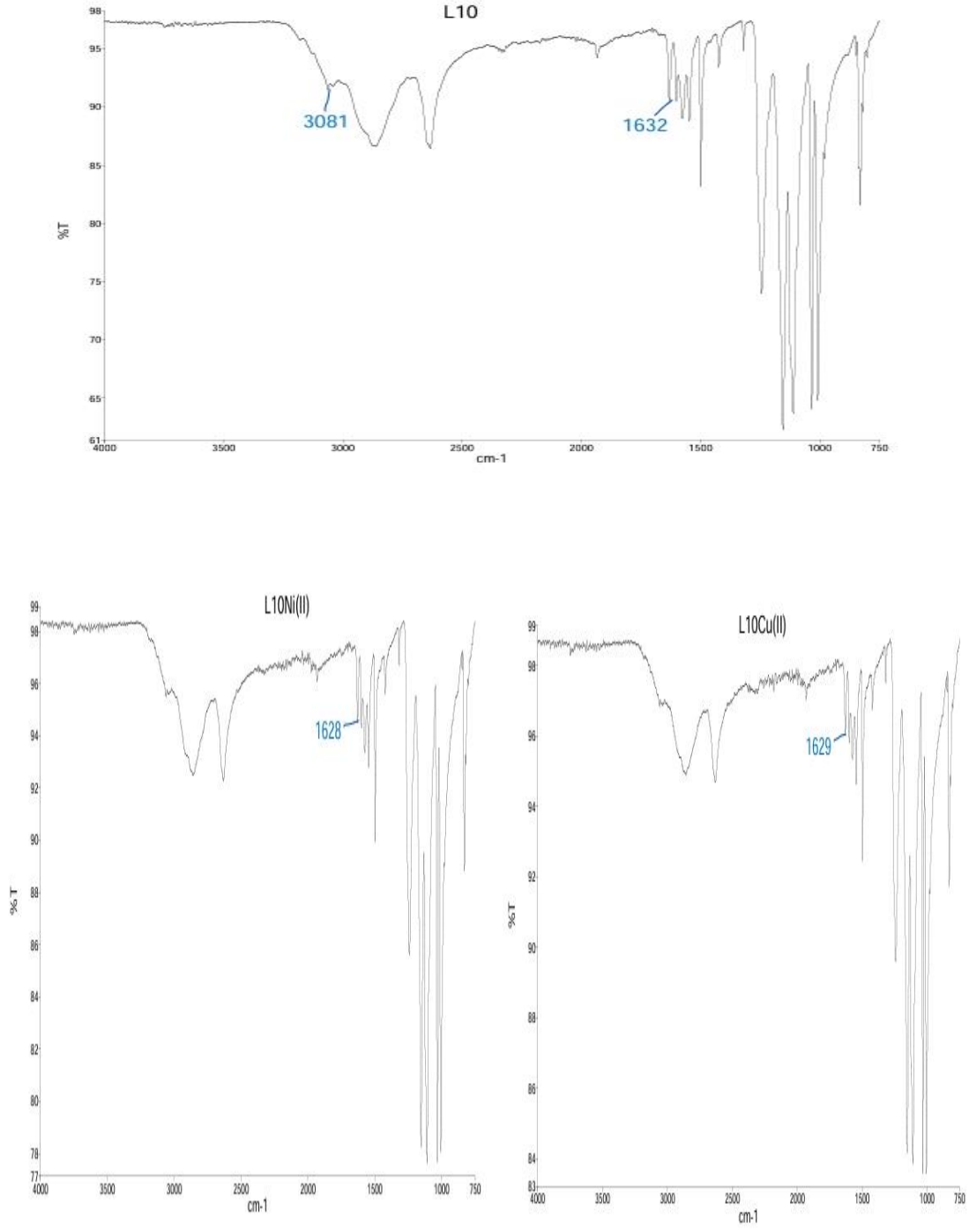

Figure 31. FTIR spectra for L10 and metal complexes

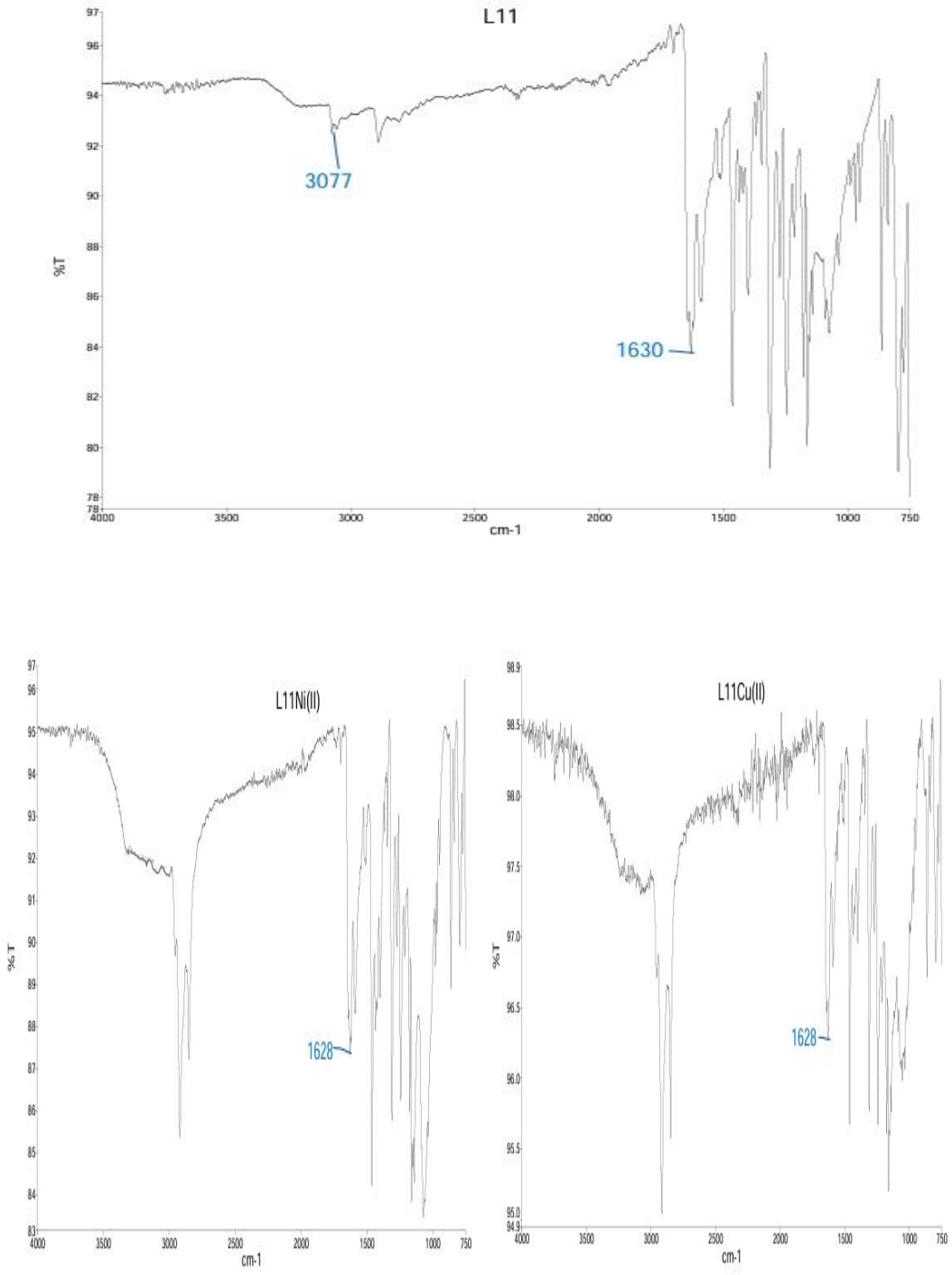

Figure 32. FTIR spectra for L11 and metal complexes

Appendix 3

Supplementary materials

This section contains supplementary materials which support some of the main findings.

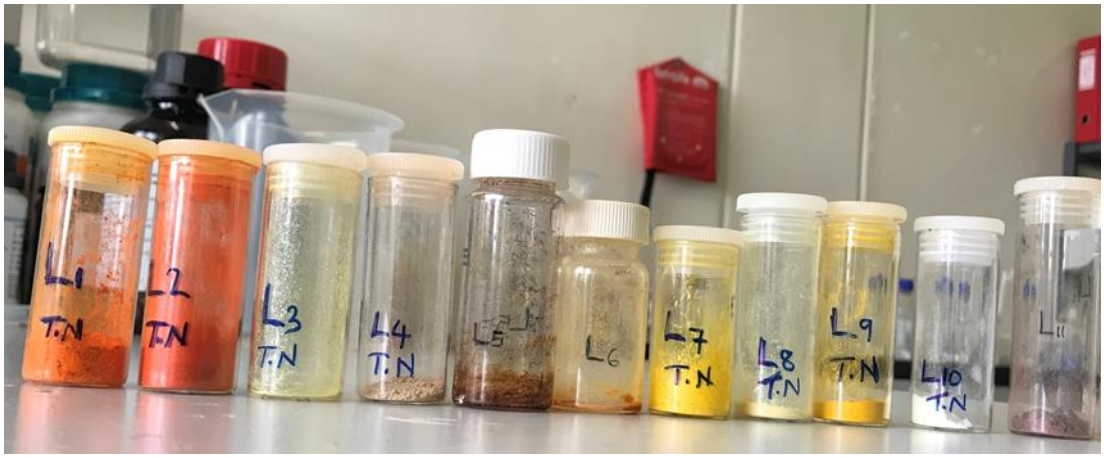

Figure 33. Ligands and metal complexes with varying colours, that were synthesized in the present study. The names of the compounds are indicated on the vials.

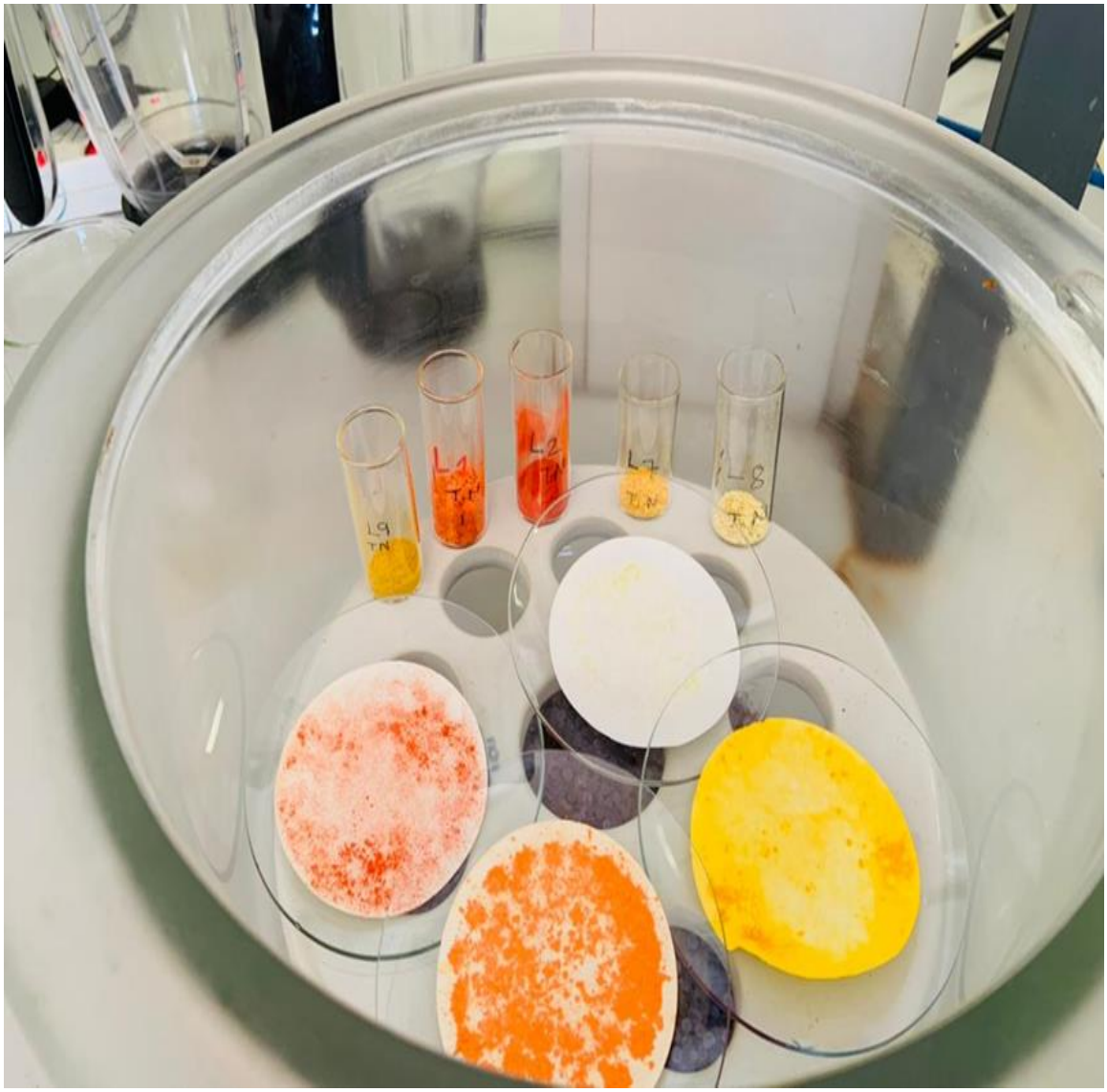

Figure 34. The image shows some of the synthesized compounds drying in a desiccator. Compounds were transferred into pre-weighed vials after drying, for safe keeping. The vials were left open in the desiccator for a few days to allow further drying.

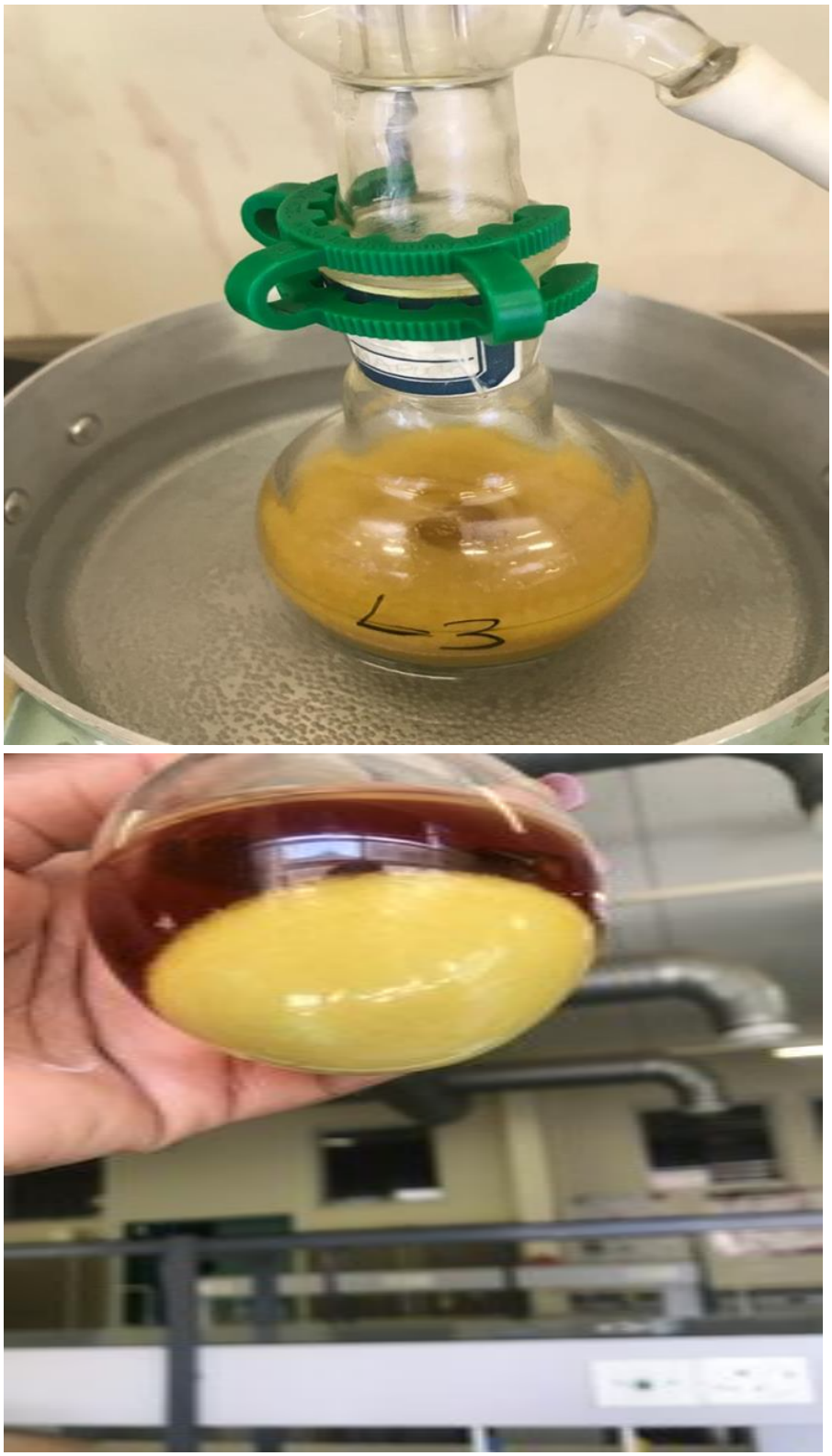

Figure 35. Synthesis of L3 under reflux, yielding a yellow product. L3 was amongst some of the compounds that slowly precipitated out of solution at room temperature, before refluxing.

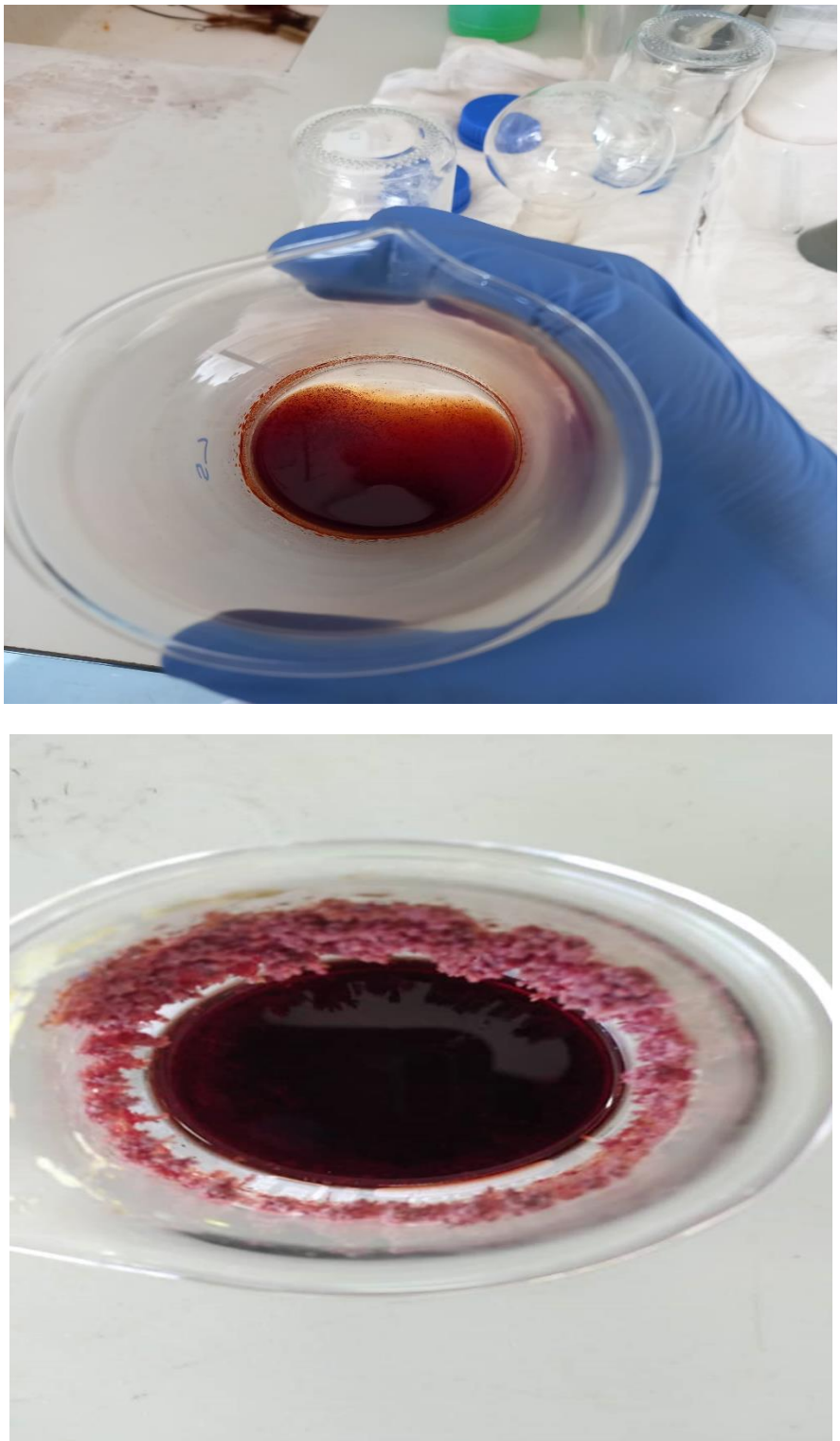

Figure 36. After 4 hours of refluxing, the synthesis of L5 yielded little-to no precipitate. Product formation was only achieved after leaving the reaction mixture in the freezer for 24 hrs. Similar procedures were applied to other compounds that were not formed within the refluxing period.

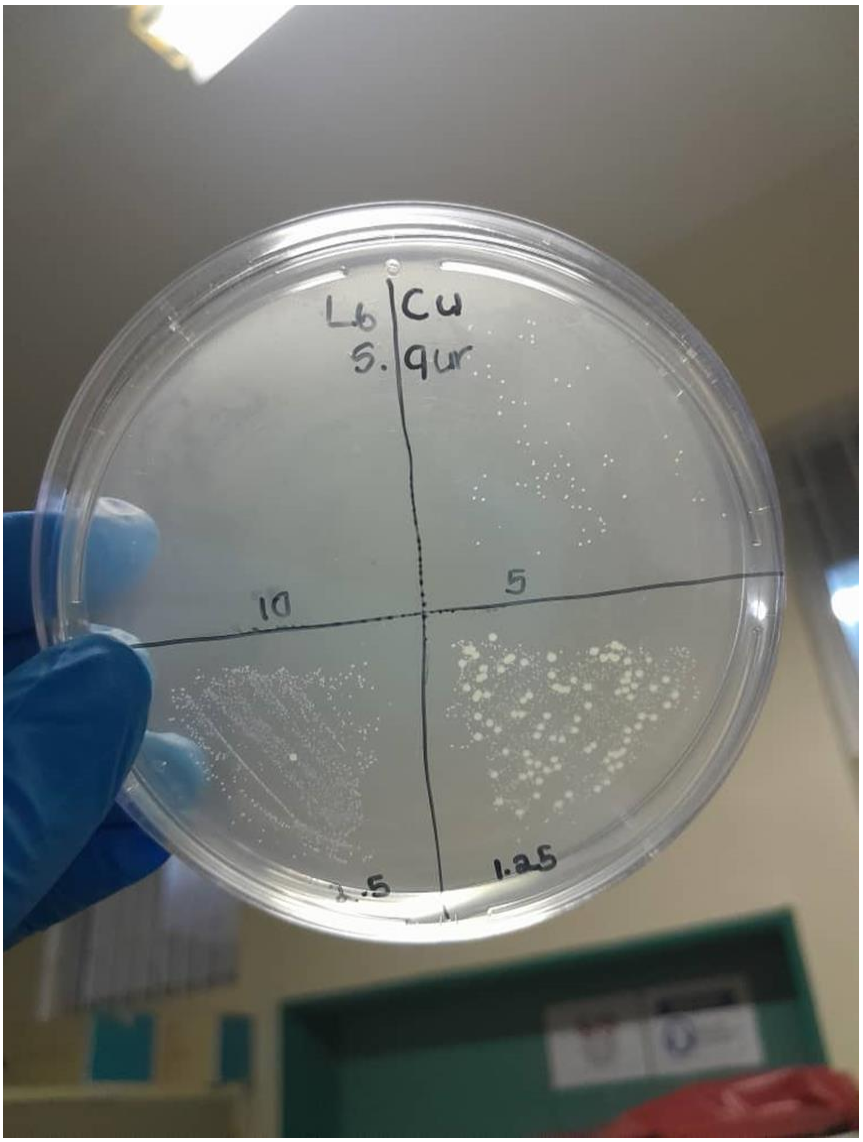

Figure 37. The image shows the minimum inhibitory concentration (MIC) value of L6 Cu (II) against *S. aureus*, which is 10 mg/mL. MIC values were determined as the lowest concentrations of compounds that inhibited visible growth of bacteria.

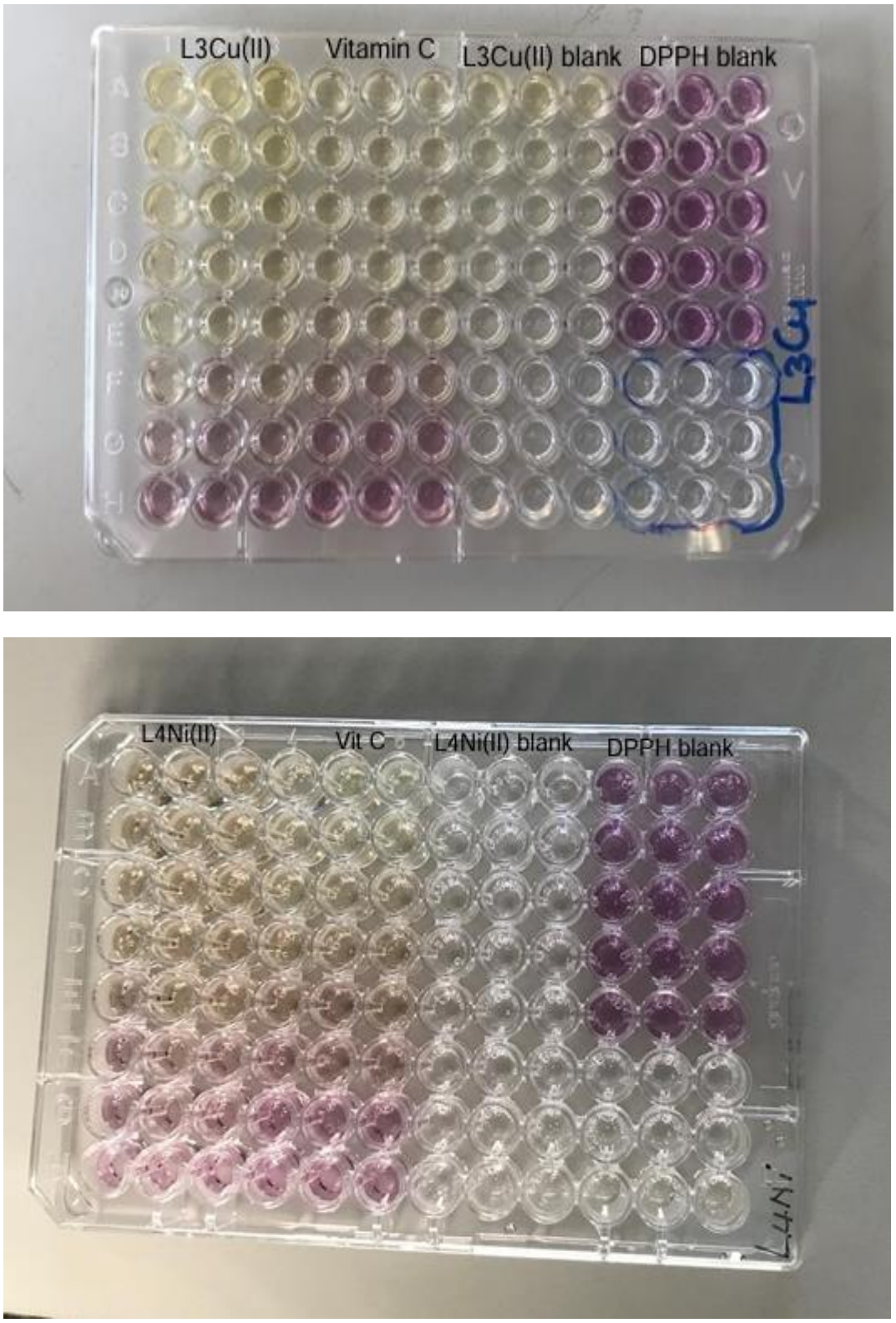

Figure 38. 96-well plates from the DPPH free radical scavenging assay of L3 Cu (II) and L4 Ni (II). Both of these metal complexes bleached DPPH off its violet colour to a pale-yellow colour, similar to the standard vitamin C, signifying very good concentration-dependent electron donating ability to neutralize DPPH free radicals.

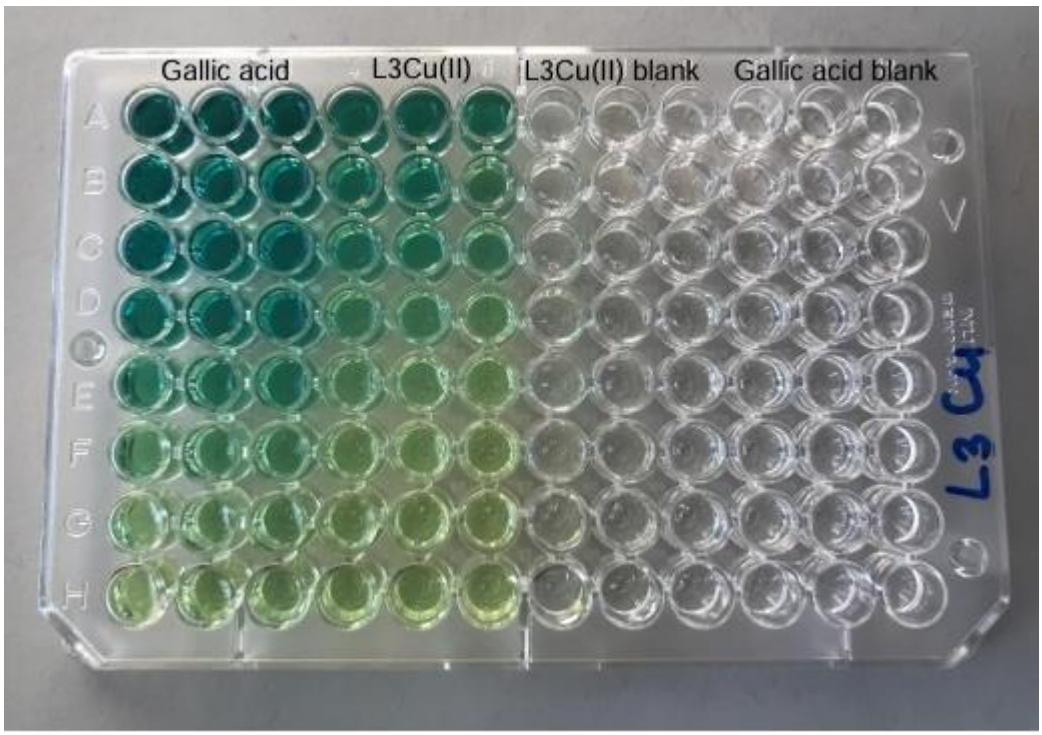

Figure 39. Concentration-dependent ferric reducing power of L3 Cu (II), indicated by the formation of a blue-green colour. Gallic acid was used a positive control.